aerospace

MDPI

Article

Gust Behaviour and Envelope Build-Up Process for Fixed-Wing Multi-Mission Remotely Piloted Aircraft †

Álvaro Gómez-Rodríguez [1,*], Carmelo-Javier Villanueva-Cañizares [2] and Cristina Cuerno-Rejado [1]

[1] Department of Aircraft and Spacecraft, Escuela Técnica Superior de Ingeniería Aeronáutica y del Espacio, Universidad Politécnica de Madrid, Plaza del Cardenal Cisneros, 3, 28040 Madrid, Spain; cristina.cuerno@upm.es
[2] Independent Researcher, 42005 Soria, Spain; c.villanuevac@alumnos.upm.es
* Correspondence: alvaro.gomez.rodriguez@upm.es
† This work is an extended version of the research sent for publication in the Proceedings of the 15th EASN International Conference on "Innovation in Aviation & Space Towards Sustainability Today & Tomorrow", Madrid, Spain, 14–17 October 2025.

Abstract

The study of aircraft gust behaviour is essential in aerodynamic and structural design and analysis, as well as in airworthiness certification. The particularities of fixed-wing Remotely Piloted Aircraft (RPA) demand a specific study of gust effects on these vehicles and their implications in RPA design and operation. The research presented here addresses the investigation of gust behaviour of RPA within the frame of conceptual design through three complementary approaches, which are respectively based on the assessment of gust and manoeuvring envelopes of RPA, the modelisation of multi-mission flight profiles of RPA towards the evaluation of the variations in gust load factor along the mission, and the analysis of the interaction of RPA conceptual design parameters with gust behaviour. These approaches are applied to various case studies, providing several key insights into the gust behaviour characteristics of RPA. These include the assessment of the operational conditions in which gust-induced stall may occur and the way in which they interact with typical mission conditions of RPA, the evaluation of the impact of mission parameters in RPA gust response along with the capability of identifying the most critical gust load factor condition for the set of considered design missions, and the ways in which undesirable gust effects may be mitigated in the conceptual design stage through the change in overall RPA design parameters.

Keywords: Remotely Piloted Aircraft (RPA); Unmanned Aerial Vehicle (UAV); multi-mission Remotely Piloted Aircraft; RPA conceptual design; RPA certification; RPA airworthiness; gust; gust envelope; flight envelope

Check for updates

Academic Editor:
Andreas Strohmayer

Received: 27 February 2026
Revised: 24 April 2026
Accepted: 29 April 2026
Published: 2 May 2026

Copyright: © 2026 by the authors. Licensee MDPI, Basel, Switzerland. This article is an open access article distributed under the terms and conditions of the Creative Commons Attribution (CC BY) license.

1. Introduction

The study of the effects caused by atmospheric gusts and turbulence on aircraft has been the subject of a substantial amount of research since the early years of aviation [1,2] and it has remained a significant field of study over the years, as seen for example in [3–5], in which the authors have sought to analyse various aspects related to aircraft response when subjected to these atmospheric effects. This topic nowadays continues to be the focus of several research efforts in both the fields of manned aviation [6,7] and of remotely piloted aircraft [8–10].

One of the main reasons behind the ongoing interest in this subject is the potential hazard that atmospheric gusts can constitute to flight safety. An aircraft encountering moderate to severe gusts or turbulence may undergo significant aerodynamic load variations and accelerations, resulting in a potentially unsafe scenario as presented in [4,5], which shows that gust encounters represent a relevant proportion of incidents and accidents in manned aviation. Considering this, requirements related to aircraft behaviour when subject to atmospheric gusts and turbulence constitute a fundamental set of specifications within aviation airworthiness regulations [4], as seen for example in the standards published by both the Federal Aviation Administration (FAA) and the European Union Aviation Safety Agency (EASA), with distinct specifications being found depending on the aircraft type. The works presented in [4,5,11] provide a detailed background on historical and current developments on the regulatory requirements related to aeroplane gust behaviour.

A particular topic that has raised substantial interest within the area of study of aeroplane gust behaviour is the interaction between design and operational variables and the response of the aircraft when subject to atmospheric turbulence and gusts [4,5]. The impact that the aforementioned variables can have in aeroplane gust behaviour along with the regulatory demands placed on the performance of the aircraft when withstanding gusts are two aspects that substantiate the need of considering gust-related aeroplane behaviour requirements within the design continuum even from the early stages of development, such as in the conceptual design phase [4,12–14]. As highlighted in previous research works, methodologies used in the conceptual design stage should be compatible with rapid calculation approaches that require few input variables, since at this point in the design process many aspects of the aircraft concept have yet to be defined [14,15].

An example of the way in which gust considerations may be integrated in the fixed-wing aircraft conceptual design stage is through the flight envelope (also called V—n diagram, with V representing airspeed and n representing load factor) [13,14]. This envelope summarises the set of conditions derived from the combination of manoeuvring and vertical gust cases that the aeroplane must be able to withstand. These conditions are evaluated in this diagram in terms of vertical acceleration, and thus of the loads that the aeroplane must bear along the space contained in the envelope. Other aspects, such as the changes in aeroplane attitude when withstanding gusts, as well as the roll, pitch, and yaw dynamics effects, fall outside the conditions evaluated within this envelope. In any case, obtaining this diagram is a crucial step in the initial stages of aeroplane design, as it provides key information on the set of flight conditions that must be accomplished, and it serves later on within the design continuum as a fundamental tool for structural design [12–14]. Overall, and considering the impact of gust behaviour requirements in aeroplane design and airworthiness, the development of gust analysis methodologies that are compatible with the needs of the conceptual design stage and which are also grounded in the requirements of the applicable regulations constitutes a key area of work in the intersection of the fields of fixed-wing aircraft design, gust analysis, and airworthiness regulations.

The latest decades have seen an unprecedented growth in the research, development, and deployment of Remotely Piloted Aircraft (RPA). These aircraft have demonstrated a noteworthy versatility to carry out missions of very diverse types [16,17]. Moreover, it is common for the same air vehicle to be able to perform distinct kinds of operations, usually by swapping its payload, giving a single platform significant multi-mission flexibility [17,18], with each sortie potentially having remarkably different characteristics in terms of payload mass, fuel mass, mission altitude, and speed, among other aspects. Many operations that leverage the potential of RPA show substantial differences to those that are usual in manned aircraft, with the design of both types of air vehicles themselves also differing significantly [17,19].

Considering the information presented above, RPA are expected to show significantly different gust behaviour when compared to conventional manned aircraft, which is one of the starting premises of the research presented in this paper. In recent times, this notion has motivated a substantial amount of research efforts dedicated to studying the particularities of RPA gust behaviour. Upon conducting an overview of the recent scientific literature, three main research areas have been identified:

1. RPA gust physics: investigations in this area seek to characterise the atmospheric turbulent structures that may be encountered by RPA, as well as the fluid dynamic interactions of these atmospheric effects with the aerodynamics of RPA [8,20–22]. Special emphasis is placed on the operational scenarios and environments in which RPA may fly but which are not common to the usual operating conditions of manned aircraft. These include, among others, flight at very low altitudes and operations close to the terrain [20,21] and obstacles [8], even during cruise. Topics covered in this area include the collection of in situ wind measurements [20,21], the measurement of unsteady aerodynamic behaviour of RPA in wind tunnels [23], and the flight test of small RPA prototypes in windy conditions [24–26].
2. Impact of gusts in RPA operations: instead of emphasising fluid dynamic considerations as in the previous line of work, here the focus is set on the analysis of the ways in which gust and turbulence encounters may affect RPA performance and the outcome of their operation. There are various gust effects that may be studied depending on the scope and objectives of each research. These include the analysis of gust time response [25], the response of the aircraft in terms of its acceleration when encountering gusts [26,27], and the trajectory deviations produced by gust encounters [9,26].
3. Fixed-wing RPA certification flight envelope modelling: due to the significance of the flight envelope in relation to aircraft design and airworthiness, there is a remarkable amount of work in the development and application of analysis approaches based on gust modelling and flight envelope estimation for fixed-wing RPA. Within this area, the work presented in [28] used an approved EASA policy at the time to perform gust load factor calculations on various existing RPA through the adaptation of manned aircraft airworthiness codes. The research presented in [29] emphasises the relevance of the V—n diagram and estimates it for a light RPA, albeit no regulatory requirements nor gust conditions used for its construction are specified. More recently, the authors of [27,30] have applied FAA Part-23 and EASA Certification Specifications (CS) CS-23 to obtain the flight envelope for specific RPA designs, and in the case of the investigations presented in [10,31], RPA airworthiness codes are used instead.

Despite the significant research interest in the study of gust effects on RPA, there are still many substantial gaps in the analysis and quantification of various particularities and issues related to RPA gust behaviour when compared to that of manned aircraft. Overall, the way in which RPA design, mission-related considerations, and airworthiness requirements all intersect has not been studied in detail in previous works within the state-of-the-art. This can lead to: (1) the design of RPA which are not compliant with gust response requirements found in the applicable airworthiness standards of RPA, (2) the lack of consideration of the impact that the envisioned missions of RPA might have on their gust behaviour, and (3) the lack of feedback of RPA gust response in the selection of the values of overall design parameters of the aircraft, among other noteworthy shortcomings. A list of outstanding gaps in the current literature within the above context is provided below.

- A lack of RPA design compliance with RPA-specific airworthiness codes: as commented beforehand, many previous works, such as [27–30], do not refer to the specific requirements found in RPA regulations to develop their design and analysis approaches, using instead manned aviation codes in either a direct or an adapted

manner. This leads to a disconnect between the design of RPA and the airworthiness requirements that are applicable to them.

- A lack of additional and systematic guidance in the flight envelope build-up process: airworthiness regulations show different levels of detail in their requirements depending on the code that is being considered. For instance, requirements for aircraft such as normal category aeroplanes or RPA are usually less prescriptive in nature and leave more room for interpretation. Certain authors in the field of manned aeroplane design prefer to complement the specifications of the stipulations of the codes with additional guidance to propose envelope build-up procedures that are more systematic and repeatable [14]. However, in the field of RPA, there is room for improvement in the availability of detailed methodologies for V—n diagram estimation that are adapted to the peculiarities and needs of RPA conceptual design.
- The disconnection between RPA operational requirements and flight envelope build-up process: as it will be expounded in detail later on within this paper, the certification design airspeeds used as references for estimating the flight envelope should be related to the operational characteristics of RPA. In a typical design process, mission requirements are among the most important initial specifications. Thus, there should be a link between the mission airspeed requirements and the selected certification airspeeds. However, the way in which certification design airspeeds are derived from the target mission airspeeds is a part of the analysis and design process that is left unexplored in current works on RPA envelope modelling such as in [10,31]. This is a particularly significant issue for multi-mission RPA, in which the selection of certification speeds is not as straightforward due to their operational variability.
- A lack of analysis of the impact of RPA airworthiness regulations on their design and operation: one of the main advantages of design–airworthiness integration is that, since regulatory requirements are considered from the beginning of the development process, the final aircraft concept has a higher change in complying with the required specifications, mitigating the need for complex and costly additional design modifications and iterations. Despite this, and save for the works focusing on flight envelope modelling, very few research efforts in this area consider regulatory stipulations. Therefore, any feedback that airworthiness considerations might have on the design and operation of RPA is mostly neglected in the present research landscape.
- A lack of consideration of RPA multi-mission characteristics in gust analysis: previous works are mainly focused on the impact of gusts on RPA performance when considering a single mission type or operational scenario, such as in [9,25]. When accounting for the analysis of multi-mission RPA, it is key to model various potential missions to study how the gust response characteristics vary among distinct sorties to identify the most critical operating conditions. This is also the case in the current RPA envelope modelling studies, which usually only present a single envelope for a specified flight condition and do not consider potential mission variability in certification airspeed derivation, as seen for example in [10,31].
- A lack of feedback of RPA gust behaviour in the selection of key design parameters: in most previous works, the evaluation of RPA gust characteristics has no clear and explicit feedback on the design characteristics of these aircraft. In early design phases, there is room for modifying certain design parameters to mitigate certain undesirable gust effects. However, even in those works that consider the design of specific RPA [29,30], there is no feedback from the gust-related analytical results to potential design decisions that may be applied to improve the gust behaviour of these aircraft.

The context of the scientific research area of RPA gust analysis as commented in the literature overview along with the aforementioned gaps found in current methodologies

constitute the backdrop against which the research problem that the research presented in this paper seeks to address may be formulated. In particular, the overall objective of this investigation is to advance the development, proposal, and application of novel methodologies for fixed-wing RPA gust analysis in the context of conceptual design, considering the simultaneous intersection of design, airworthiness and operational considerations, while seeking to address the above-mentioned research gaps. As the problem statement covers a broad scope, the set of specific research questions underpinning the new scientific understanding sought in this investigation, along with the methodologies applied to answer them, are expounded below.

- How can the regulatory stipulations related to the flight envelope build-up process be complemented to arrive at a systematic and repeatable methodology that addresses the points that are left open to interpretation in the codes? Can the envelope build-up process be adapted to the typical data scarcity encountered in the literature for current fixed-wing RPA designs as well as in the initial design stages? From a quantitative standpoint, what are the main interactions between the manoeuvring and gust loading conditions defined in the flight envelope and which of them have the most significant impact on aircraft sizing? What potential undesirable gust effects may be identified through the V—n diagram of RPA? What are the main differences that can be seen between RPA flight envelopes and those for manned aircraft? How do the particular characteristics of fixed-wing RPA influence their resulting envelopes? What are the predominant load conditions and limitations seen in these envelopes? These questions shall be addressed through the proposal of a systematic and repeatable envelope build-up process, which not only adheres to the code's requirements, but integrates novel additions to tailor it to the specific issues and gaps related to RPA conceptual design that were discussed beforehand.
- From a quantitative standpoint, how do variations in RPA mission-related parameters, such as wing loading, airspeed, and flight altitude impact the gust load factor and thus the accelerations that the aircraft must withstand? What impact does the cruise procedure have on gust response? Can a rapid calculation approach be defined for the estimation of the load factor for multi-mission RPA covering operations with distinct flight profiles? In a set of different RPA missions, which is the most critical point in terms of the gust load factor? The gust load factor is a crucial indicator related to the acceleration of gust response. The above-mentioned questions shall be answered through the combination of gust models and fixed-wing RPA integral performance modelling in the context of the conceptual design stage while considering various potential cruise procedures.
- What is the linkage of fixed-wing RPA gust response and their main conceptual design parameters influencing gust behaviour? What sensitivity does gust response have to different design parameters? In what ways might these parameters be modified in the context of the conceptual design stage to improve potential undesirable gust effects? These questions address the aforementioned design–airworthiness integration gaps, and they shall be answered through a sensitivity analysis that applies simplified gust models that are compatible with the needs of the conceptual design stage, as well as through the quantification of the gust behaviour variations when applying changes to the selected design parameters.

Attending to the gap analysis conducted beforehand, there is still room for improvement in addressing the aforementioned questions. Some of these are based on intuitive premises, such as the fact that the singular characteristics of RPA impact the shape of their envelopes or that the mission-related operational variables have an effect on the accelerations due to gust. Starting from these premises, the original contributions and

new knowledge that this article seeks to contribute to the current state-of-the-art lie in the application of analysis approaches in the context of RPA conceptual design that provide a systematic and more detailed answer to the above questions. These approaches will allow to quantify the regions of the envelope where gust-induced stall occurs as well as the differences in gust behaviour when modifying design parameters, among other aspects.

Considering the information presented above, this article uses three complementary approaches for the study of gust behaviour of fixed-wing RPA with the purpose of giving the answer to the problem statement and research questions above. The approaches are as follows:

1. A systematic and repeatable methodology for the build-up of flight envelopes of fixed-wing RPA attending to the requirements of both civil and military RPA-specific airworthiness codes, incorporating novel additional guidance for the derivation of certification airspeeds covering the potential application to multi-mission RPA.
2. An original methodology for the study of gust load factor variations along specified multi-segment mission profiles of fixed-wing RPA, attending to the gust models prescribed in RPA regulations, which is compatible with two different cruise procedures and with multi-mission RPA. The application of this method shall allow the detection of the most demanding operating scenario in terms of gust loads.
3. An assessment of the impact of conceptual design parameters in fixed-wing RPA on their gust behaviour, the purpose of which is to identify the potential variables that might be modified to mitigate undesirable gust effects and to quantify the changes in gust behaviour upon changing these selected design parameters.

These three approaches are complementary, and each is tailored to answer a set of research questions proposed beforehand. The methodology and results corresponding to each of them shall be expounded in full detail in different sections of the paper, where the novel contributions resulting from their development and application with respect to current works shall also be emphasised. It is noted that the methodologies presented here are not limited to a direct application of RPA airworthiness regulations, with the objective of this work not being to provide an approach for RPA certification, which is a much broader and complex endeavour exceeding the scope of this work. Rather, the main highlight is the adaptation of the regulatory requirements towards their streamlined integration in RPA conceptual design and analysis approaches, as well as their application in the quantification and assessment of particular aspects of fixed-wing gust behaviour as proposed in the research questions. The way in which the proposed methodologies could be integrated within the RPA design continuum is illustrated in Figure 1.

The scope of the research presented here is explicitly delimited attending to the following considerations:

- The focus is set on fixed-wing RPA and on current regulations applicable to them.
- The investigation is centred on medium and large RPA, as these are the ones for which most current airworthiness codes have been developed. The codes are not intended for small RPA since their safety assurance is conducted through other means.
- The scope is focused on propeller-driven RPA and particularly on those with reciprocating engines, as this is the most usual powerplant in these aircraft [18].
- The study is focused on cruise flight of RPA in clean configuration.
- The research is focused on vertical gusts and on the acceleration that they produce on the aircraft, which are the characteristics covered by the flight envelope used in aircraft design and airworthiness analysis. Other gust types such as lateral or composite gusts are not directly covered by the models proposed in this work. There are other aspects of RPA gust response that fall outside the scope of the analyses and research questions proposed here, such as trajectory deviation and the potential roll moments induced by

gusts with intensities that are distributed unevenly through the wingspan. The latter present the risk of overturning the RPA, which is a significant issue particularly in small RPA due to their low wingspan, mass, and inertia moments [22], with the issue being mitigated as the RPA increases in mass and size, as it is the case of the medium and large RPA that fall within the scope of this work. More details on gust modelling are given in the following section.

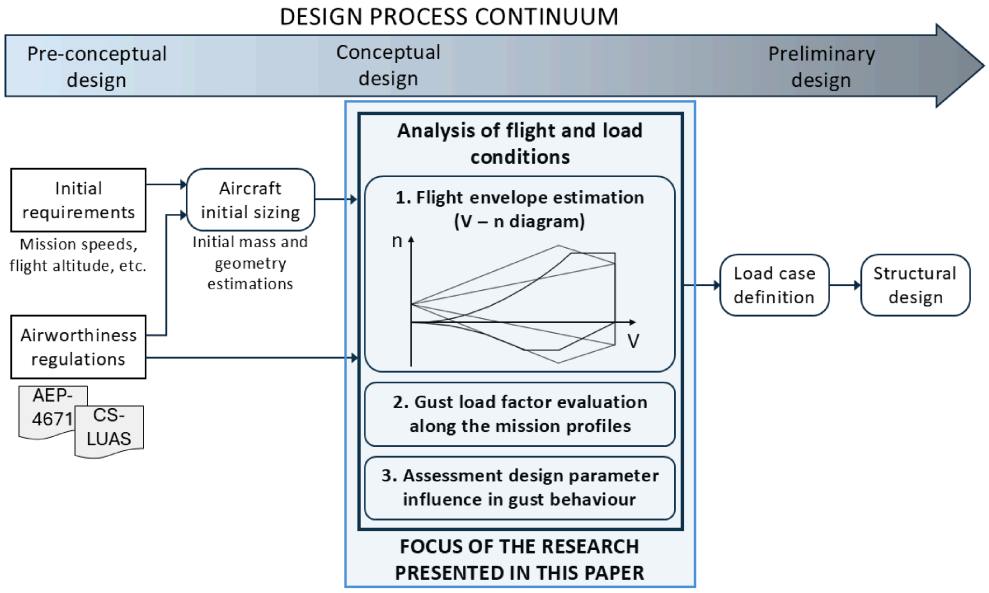


Figure 1. The context of the integration of the proposed methodologies for fixed-wing RPA gust analysis within the aircraft design continuum. AEP: Allied Engineering Publications, LUAS: Light Unmanned Aeroplane Systems.

The organisation of the paper presented hereafter is structured as follows: Section 2 lays out the background of the methodologies proposed in this work, covering the gust model and background regulatory requirements that are common to the three analysis approaches proposed in this research. Section 3 presents the methodology for the flight envelope build-up process. This method is applied to two case studies of RPA, which are accompanied with an analysis of the resulting envelopes. A comparison of these with the envelopes that would result from direct application of the corresponding manned aeroplane requirements is also provided and discussed. Section 4 covers the second methodology for gust behaviour study proposed in this work, which is focused on the analysis of gust load factor variations through the flight profile of the RPA attending to the cruise procedure and wing loading variation. The methodology is accompanied by an application case showcasing its use on a multi-mission RPA. Section 5 contains the third approach, which is based on the quantification of the impact of design parameters on RPA gust behaviours, seeking to more directly reflect the gust–design interaction. The results obtained from these methodologies converge in Section 6, which contains an expanded discussion on the insights provided by the three approaches, exploring in further detail their potential impact on RPA design when attending to the regulatory requirements. Finally, Section 7 presents the overall conclusions of the research.

2. Materials and Methods

This section provides the methodological background underpinning the three approaches for the analysis of RPA gust behaviour proposed in this research. As anticipated in the introduction, attending to the objectives of the research presented here, the design of these approaches shall be done attending to the following criteria:

1. The methodologies shall be based on the requirements and modelling assumptions laid out by current RPA regulations, so that the results obtained when using them are compatible with airworthiness requirements of RPA.
2. The approaches shall be compatible with the needs of rapid sizing and analysis approaches that are usual in the initial RPA design stages.

To comply with the first criterion, it is necessary to select the airworthiness regulations that will be used as a basis for extracting the applicable requirements and models This is crucial for addressing the problem statement and research questions laid out in the introduction, as the integration of airworthiness-related considerations of RPA regulations in the gust analysis approaches is a key point of the objectives of the research and is also one of the main differentiating points and novel aspects of this work with respect to many previous investigations in the state-of-the-art.

Provisions with respect to gust criteria for RPA are given in airworthiness codes for these aircraft. These codes are mainly intended for high-risk operations and certain medium-risk scenarios. These include the Certification Specifications for Light Unmanned Aeroplane Systems (CS-LUAS) [32] and Certification Specifications for Unmanned Aircraft Systems (CS-UAS) [33] published by the Joint Authorities for Rulemaking on Unmanned Systems (JARUS), as well as the Allied Engineering Publications (AEP) AEP-4671 [34] and AEP-83 [35] by the North Atlantic Treaty Organization (NATO).

Each of the aforementioned codes has very different features in terms of their applicability range and the level of detail of their requirements, which are aspects that impact the integration of their specifications into design and analysis methodologies. However, a detailed review and discussion of the characteristics of these codes would fall outside the scope of the current research, the focus of which is instead on the methodologies that can be derived from these specifications for RPA design and analysis. Therefore, the reader is referred to the review presented in [36] for a detailed background and analysis of the characteristics of the codes. Here, instead, a summary of the characteristics of these codes, emphasising those aspects that are more tightly related to this research, is presented in Table 1, with main manned aviation codes also being included for comparison.

Table 1. Summary of characteristics of prospective airworthiness codes for selecting the most appropriate ones for the development of the methodologies proposed in this research.

Code	Applicability		Gust Models	Level of Detail in Requirements		
	Aircraft Type	MTOM [kg]		Overall Code	Design Airspeeds	Gust Conditions
CS-LUAS [32]	Small and medium RPA	<750 kg	Discrete gust	High	High	High
CS-UAS [33]	Small, medium, and large RPA	<8618 kg [d]	Not explicitly stated	Medium	Low	Low
AEP-4671 [34]	Medium and large RPA	150–20,000 kg	Discrete gust	High	High	High
AEP-83 [35]	Small RPA	<150 kg	Discrete gust	Medium-High	Medium	Medium
CS/Part-25 [37,38]	Transport/ large aeroplanes	>8618 kg [e]	Discrete gust and continuous turbulence	High	High	High
CS/Part-23 (legacy) [39,40] [a]	Normal aeroplanes [c]	<8618 kg [e]	Discrete gust	High	High	High
CS/Part-23 (current) [41,42] [a]	Normal aeroplanes	<8618 kg [e]	Not explicitly stated	Medium	Low	Low

Table 1. *Cont.*

Code	Applicability		Gust Models	Level of Detail in Requirements		
	Aircraft Type	MTOM [kg]		Overall Code	Design Airspeeds	Gust Conditions
CS-VLA (legacy) [43] [b]	Light aeroplanes	<750 kg	Discrete gust	High	High	High

MTOM: Maximum Take-Off Mass. [a] The CS/Part-23 codes were changed to follow a performance-based approach in 2017. This change took place in the transition from CS-23 Amendment 4 to 5 and in the transition from Part-23 Amendment 63 to 64. More information on this process and its implications on the regulations can be found in [44]. [b] Currently, requirements for Very Light Aeroplanes (VLAs) are integrated in CS-23. This is effective from Amendment 5 onward. However, the original CS-VLA may still be used as Acceptable Means of Compliance (AMC). [c] Aside from normal category aeroplanes, these regulations included specifications for utility, acrobatic, and commuter categories. [d] The indicated limit is for non-Vertical Take-Off and Landing (VTOL) aircraft, according to the scope of this research. For VTOL aircraft, the limit is <3175 kg. [e] There are further applicability considerations for these codes. For example, Part 25 applies to aeroplanes with either an MTOM above 8618 kg or with a seating capacity of over 19 passengers. More details can be found in the codes.

There are both remarkable similarities and differences among the codes included in Table 1. One of the most relevant features is related to the level of detail of the requirements contained in the codes. Detailed specifications make the task of deriving design and analysis approaches more straightforward, while on the other hand they leave less room for the applicant in selecting the way in which they demonstrate compliance with the specifications, as discussed in [36].

Within the context of this work, to ensure as much as possible that the methodologies developed here have a high level of assurance in complying with the applicable regulations, a higher level of detail in the specifications shall be prioritised. However, as it can be seen in Table 1, there are often differences between the level of detail seen in the requirements of the overall code and that found in particular sections of the specifications. For instance, neither CS-UAS [33] nor NATO AEP-83 [35] give detailed provisions for the build-up process of the manoeuvring and gust envelopes. In contrast, CS-LUAS [32] and AEP-4671 [34] provide a higher level of detail regarding different constraints involved in the flight envelope construction and the related certification design airspeeds. Therefore, the provisions given in these two airworthiness codes fall more in line with the needs of the methodologies to be proposed in this research, since detailed specifications provide a more substantiated basis for the development of systematic and repeatable gust analysis approaches with greater assurance of adhering to the regulatory prescriptions.

Another remarkable characteristic of the codes is the type of gust model prescribed by the regulations for analysing aircraft gust response. While the codes with a lower level of detail do not provide explicit details on the type of model to be used, two different approaches for gust modelling and aircraft response can be observed in the codes whose requirements have a higher level of detail: continuous turbulence and discrete gust. The first one focuses on a stochastic representation of atmospheric turbulence whereas the second models gusts through pre-defined deterministic profiles of vertical air velocity. More details on the background and foundations of each model can be found in [3–5]. Previous research has highlighted that there is no direct link between the aircraft response resulting from the application of both models [4], since both are based on different starting assumptions with respect to turbulent structures. The fact that both formulations are maintained in the regulations is due to each model serving to represent different types of turbulent structures that may be encountered by the aircraft in flight. The discrete model is tailored to represent high-load events of the aircraft upon encountering isolated, high-intensity gust structures (which have been noted to represent most cases of catastrophic gust encounters in manned aeroplanes [5]), whereas the continuous model seeks to represent rough air structures covering broader volumes of the atmosphere and with lower peak

intensities. Therefore, previous research has highlighted the need for continuing to study each of them [4,5].

Whereas the former continuous turbulence approach is only found in CS/Part 25, the discrete gust model is present in all airworthiness codes and is the only gust model specifically prescribed in the RPA certification specifications. This latter model has several advantages in terms of its integration in conceptual design approaches due to its closed-form analytical formulation and compatibility with rapid calculation approaches. Therefore, the discrete gust criterion shall be the one to be used in this research.

Taking into account this assessment of the codes and the objectives of this investigation, the CS-LUAS [32] and AEP-4671 [34] shall be the certification specifications selected as a basis to extract the regulatory requirements on which the methodologies proposed in this research shall be based. Thus, the discrete gust criterion, according to the prescriptions laid out in these codes shall be the model to be used. This selection of codes allows to cover RPA of both medium and large sizes, roughly corresponding to operations in the medium- and high-risk categories, which are the main scope for which these certification codes are intended. This choice of codes also allows compatibility with both civil and military RPA analysis according to the scope of each of these regulations.

Having selected the codes from which the airworthiness requirements related to RPA gust behaviour shall be extracted, the remainder of this section is structured as follows: First, Section 2.1 provides explicit assumptions on the gust model used through the three approaches employed in this paper, which are based on the specific details of the discrete gust criterion prescribed by CS-LUAS [32] and AEP-4671 [34]. This subsection also contains other general modelling assumptions used throughout this work, including stall estimation, lift–curve slope derivation, and wing loading variation along the mission, among others. Then, Section 2.2 provides the applicable requirements in terms of certification design airspeeds. Here, some aspects for which the code does not provide a high level of detail in the requirements are highlighted, as these will be complemented in the methodology for flight envelope built-up proposed in this paper. Finally, Section 2.3 provides a preliminary analysis of the impact of certain key variables on the results of the flight envelope.

2.1. Modelling Assumptions

This subsection provides information on the modelling assumptions used as a basis for the development of the three analytical approaches proposed in this research. These modelling aspects cover many aspects, ranging from the form of the gusts considered in the regulations, moving on to various hypotheses related to aircraft modelling, and also covering gust and stall load factor estimations.

As commented beforehand, both CS-LUAS [32] and AEP-4671 [34] propose a gust model following the discrete gust approach. Subparagraph (c) contained within paragraph 333 of both codes prescribe the same gust shape:

$$U(s) = \frac{U_{de}}{2}\left(1 - \cos\left(\frac{2\pi s}{25 \cdot MGC}\right)\right) \quad (1)$$

where s represents the distance penetrated into the gust, MGC is the aircraft's mean geometric chord, and U_{de} is the derived gust velocity, which is prescribed by the regulations as a function of altitude in the following manner:

- For V_C: 50 fps up to 20,000 ft, with a linear transition towards 25 fps at 50,000 ft.
- For V_D: 25 fps up to 20,000 ft, with a linear transition towards 12.5 fps at 50,000 ft.

where V_C and V_D represent the design cruise and design dive speeds, respectively, the definition of which is also prescribed by the regulations, as it shall be expounded in Section 2.2. The reason for the variation in the gust intensity prescribed by the regulation

as a function of aircraft speed is discussed hereafter. As it will be seen in the mathematical formulation presented in this same subsection, both gust intensity, U, and aircraft speed, V, are two variables that increase the load factor, and thus the acceleration withstood by the aircraft when encountering the gust. V_C, as it will be commented in the following subsection, is selected attending to the RPA's operating requirements. Thereby, and as expounded in [14], flight at speeds above V_C are not expected to represent typical operating conditions and will seldom be flown through the operating life of the aircraft. Therefore, it is considered that the combination of the gust intensity, U_C, with airspeeds above V_C would result in unnecessary structural reinforcement. Thus, the regulation considers a reduction in gust intensity for speeds above V_C, so as to account for the fact that the scenario in which the most intense gusts considered in the code are being encountered with the aircraft operating at airspeeds well above the maximum ones expected in service constitutes a very unlikely scenario that would result in excessively prescriptive structural sizing requirements.

The gust shape in Equation (1) and the gust velocity described above are represented graphically in Figures 2 and 3 respectively.

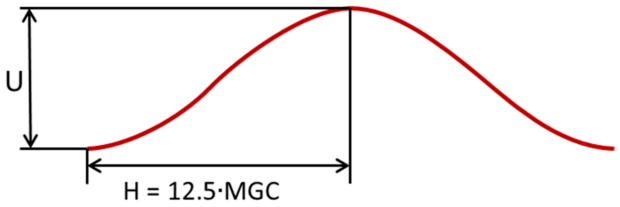


Figure 2. Gust shape considered in the regulations.

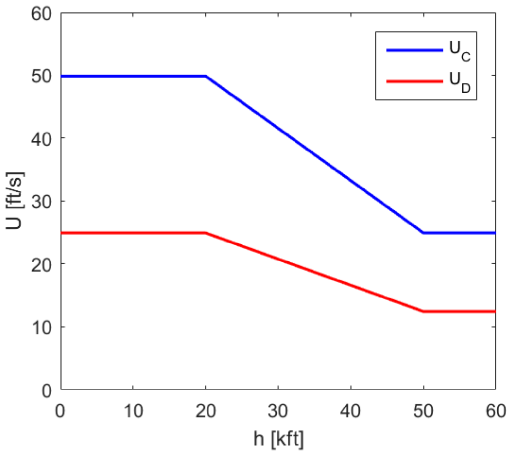


Figure 3. Gust intensity, U, as a function of altitude, h, for the two design speeds V_C and V_D.

It can be seen that the gust shape follows a 1—cosine shape also known as "bell-shaped pulse", through which the aircraft progressively encounters increasing vertical velocities as it penetrates the gust. The distance corresponding to half of the wavelength of this shape is commonly referred to as the gradient [1], which in the case of the considered regulations takes the value of 12.5 times the mean geometric chord. In contrast to other gust shapes such as the sharp-edge gust or the linear ramp gust, this 1—cosine shape is symmetric, finite in length, and has an explicit mathematical definition after the maximum gust intensity is attained, with these being among its advantages when compared to other potential discrete gust shapes, as expounded in further detail in [1,11]. Considering the information presented above, this 1—cosine shape was adopted in the discrete gust models prescribed by airworthiness regulations of both manned and unmanned aircraft and

nowadays remains the one to be used in certification-related gust analyses. Furthermore, it continues to be used in very recent research works such as [6,7,45].

From the perspective of the authors of this work, this type of shape can serve as a useful model in the initial sizing steps of aircraft design to represent isolated, high-intensity gust structures, which, as mentioned beforehand, have been shown to be more likely to result in catastrophic events [5]. Certainly, this model could not adequately represent large volumes of rough air with very high frequencies and short wavelengths of varying intensity, which are more accurately modelled through a power spectral density approach [4,5]. Even though the airworthiness regulations of RPA do not consider such a continuous turbulence model [32–35], it could be used in further design stages to provide an additional layer of safety to the RPA design through the model of different types of turbulent encounters. It is also noted that the gust model considered here, when applied uniformly across the wingspan, does not present the risk of overturning the aircraft. This is an issue that should be accounted for with more involved gust models and once the dynamics of the aircraft are known with a certain level of detail, which is feasible at later design stages when the control surface layout has been defined and the moments of inertia can be estimated, and once the structural sizing of the aircraft has been conducted, which is usually carried out in the preliminary design phase. For the purposes of this work, taking into account its main objectives and scope within the initial steps of conceptual design, it can be argued that the model proposed by the regulations provides an acceptable approximation for initial gust modelling.

Following the description of the gust shape, paragraph 341 of both regulatory codes [32,34] indicates that each RPA must be designed in accordance with the aforementioned gust conditions. Both codes suggest a common model to represent the behaviour of RPA when subjected to the aforementioned discrete gusts. The characteristics of this model are compatible with the needs of the conceptual design stage, during which exact sizing and performance data are not yet available, thus requiring the use of models depending only on general aircraft data and on those parameters capturing the most significant physical effects of the aspects that are being modelled. Thus, this approach shall be the one used throughout this work. According to the model proposed in the codes, the gust-induced load factor is given by the following expression:

$$n_g = 1 \pm \frac{K_g \rho_0 U_{de} V_{EAS} a}{2\left(\frac{W}{S_w}\right)} \tag{2}$$

which depends on the gust alleviation factor:

$$K_g = \frac{0.88\mu_g}{5.3 + \mu_g} \tag{3}$$

and this in turn depends on the mass ratio of the aeroplane:

$$\mu_g = \frac{2\left(\frac{W}{S_w}\right)}{\rho \cdot MGC \cdot a \cdot g} \tag{4}$$

where

- a: slope of the aeroplane's normal force coefficient curve per radian.
- g: acceleration due to gravity.
- MGC: mean geometric chord of the aircraft.
- S_w: wing surface of the aircraft.
- U_{de}: altitude-dependent gust velocity computed as indicated above.

- V_{EAS}: aeroplane Equivalent Airspeed (EAS).
- W: weight of the aircraft.
- ρ_0: density of air at sea level.
- ρ: density of air at the considered altitude.

Even though the regulations considered in this section do not include an explicit reference to the theoretical foundations of the proposed model, the expressions are recognised to be coincident with the studies of Pratt [1,2]. While the current research does not intend to reproduce the original theoretical work underpinning the derivation of the equations expounded beforehand, a summary is provided here on the main hypotheses on which such work is based [1], with these being:

- The aeroplane is modelled as a rigid body. Therefore, this gust model does not consider elastic dynamic effects. Albeit these are accounted for in manned aeroplane gust modelling such as in CS/Part-25, the model accepted by current RPA regulations does not integrate these considerations when covering gust flight envelope requirements.
- The forward speed of the aeroplane is constant.
- The aeroplane is in a steady level flight condition prior to entry into the gust.
- The aeroplane can rise but cannot pitch. Therefore, transient unsteady effects appearing due to the change in aircraft pitch attitude are left outside the scope of this model.
- The lift increments of the fuselage and horizontal tail are considered to be negligible in comparison with the wing lift increment.
- The gust velocity is uniform across the wingspan and is parallel to the vertical axis of the aeroplane at any instant. Therefore, potential roll dynamic effects are not considered in the scope of the V—n diagram as proposed in the airworthiness codes.

The interested reader may turn to references [1,2] for a derivation of the expressions included in this section, which also contain a more detailed substantiation of the associated modelling assumptions. It is noted that both the CS-LUAS and NATO AEP-4671 follow the same gust models used in the gust envelope estimation in the historical CS/Part-23 and CS-VLA regulations for manned aircraft, which prescribe the same modelling assumptions and are also based on Pratt's gust model.

Both manoeuvring and gust envelopes also require considering aircraft stall, since the subset of points falling outside of the stall boundaries represent unattainable flight conditions. Within the context of conceptual design and analysis approaches and in the absence of more complex aerodynamic assumptions, stall can be modelled through Equation (5), which is derived from the vertical force equilibrium equation in manoeuvring flight when a specified value of maximum normal aerodynamic force coefficient, C_{Nmax}, is attained. This approach has been used in previous works in the context of RPA conceptual design [16,46], and, more particularly, in recent research focused on gust and manoeuvring envelope representation for RPA as seen in [10,30]. Furthermore, it is compatible with the RPA requirements laid out by the regulations used in the present research, which state that, in the context of the flight envelope, stall may be modelled through static maximum lift coefficients, as indicated in CS-LUAS.333 (b) and USAR.333 (b).

$$n_s = \frac{\rho_0 C_{Nmax} V_{EAS}^2}{2\frac{W}{S_w}} \tag{5}$$

Negative stall should also be considered, corresponding to the use of C_{Nmin} instead of C_{Nmax}. These expressions correspond to positive and negative parabolas.

The gust and stall modelling assumptions discussed above form the basis of the flight envelope estimation and build-up process. The full set of regulatory stipulations used as reference in this research can be consulted in the original codes [32,34]. These

prescriptions shall be complemented with additional novel considerations as proposed in the methodology to be expounded in Section 3.

Aside from the above-mentioned modelling assumptions, the following additional hypotheses are used through the models used in the approaches employed in this work:

- The atmospheric variables shall be modelled attending to the hypotheses of the International Standard Atmosphere (ISA) considering a standard stay in terms of sea level temperature.
- With respect to aerodynamic derivatives, since the gust response model only considers the vertical motion of the aeroplane as discussed beforehand, aerodynamic derivatives related to angular velocities and accelerations are not involved in the models used here. The aerodynamic coefficients involved in the simplified gust model based on the stipulations of the airworthiness regulations are those seen in Equations (2)–(5), which are the slope of the aeroplane normal force coefficient curve, a (albeit this symbol is used in regulations, this derivative is usually found in the literature as $C_{N\alpha}$), and the maximum normal force coefficient, C_{Nmax}. Where data on the full aircraft aerodynamic coefficients obtained from tests are available, these shall take precedence. In the case that estimations have to be made, and considering that the aircraft used in the case studies of this work fly in the low subsonic flight regime, as is typical of many RPA, the classic wing-lifting-line model accounting for the correction of non-elliptical wings is used for the lift–curve slope, and the full aeroplane normal force coefficient is estimated considering the contribution of the horizontal tail attending to the model proposed in [14]. With respect to C_{Nmax}, where data is not available, the reference values accepted in CS-LUAS [32] shall be used.
- Static aerodynamic coefficients shall be used according to the stipulations of the regulations as commented beforehand.
- Maximum and negative manoeuvring load factors, n_{lim+m} and n_{lim-m}, shall be obtained as a function of Maximum Take-Off Mass (MTOM) according to the prescriptions of the codes found in paragraphs CS-LUAS.337 [32] and USAR.337 [34].
- Wing loading variations during the mission shall be estimated according to integral performance-based modelling using approaches for the estimation of range and endurance typical of aircraft and RPA conceptual design such as those in [14,46]. Variations in wing loading across different missions will be calculated by adding to the aircraft's Operating Empty Mass (OEM) the values of payload mass and fuel mass required to complete the operation while accounting for the fuel consumed throughout the different flight segments. More details on integral performance modelling are given in Section 4.

2.2. Certification Design Airspeeds

Design airspeeds are essential in the description of the aircraft's flight envelope according to airworthiness regulations, since various aspects related to the construction of the envelope and its constraints are given with respect to these reference airspeeds. Thus, these airspeeds have critical implications in the set of flight conditions that the RPA must be able to accomplish according to its flight envelope. This envelope in turn has a direct impact on the design of the aircraft, which is sized so that it can withstand the aforementioned set of flight conditions defined in the V—n diagram. This is the reason for dedicating the present subsection to these concepts. Furthermore, as it will be seen below, the lack of guidance provided by the regulations at certain points leave room for interpretation with respect to the process of selecting the values of these airspeeds. Identifying these gaps is key for the development of the systematic envelope build-up process, which is to be proposed in Section 3. Thus, this section is not limited to enunciating the stipulations of the

airworthiness codes, but it also contains a discussion on their significance, which will form the basis of the novel steps to be proposed in Section 3.

Table 2 compiles an excerpt of the requirements related to the scope of this research contained in both CS-LUAS and AEP-4671 regarding the design airspeeds, V_C and V_D, which are the ones involved in the construction of the gust envelope as seen in the preceding subsection. Furthermore, the applicable provisions related to the never-exceed speed, V_{NE}, have also been included in the table. Even though it is an operating airspeed and not a design airspeed, this has been done due to its relationship with V_D and also due to its significance in the flight envelope build-up process proposed in Section 3 of the paper.

Table 2. Excerpt of regulatory requirements pertaining to main certification airspeeds. The full provisions can be checked in the original codes.

Certification Airspeed	CS-LUAS [32]	AEP-4671 [34]
Design cruising speed V_C	CS-LUAS.335 (a): For V_C, the following apply (1) V_C shall be defined according to RPA operating requirements. (2) At altitudes where an M_D is established, a cruising speed M_C limited by compressibility may be selected.	USAR.335 (a): For V_C, the following apply: (1) V_C shall be defined according to UAS operating requirements. (4) At altitudes where an M_D is established, a cruising speed M_C limited by compressibility may be selected.
Design dive speed V_D	CS-LUAS.335 (b): For V_D the following apply: (1) V_D/M_D may not be less than $1.25 \cdot V_C/M_C$.	USAR.335 (b): For V_D the following apply: (1) V_D/M_D may not be less than $1.25 \cdot V_C/M_C$; however, where credit may be claimed from existing experience and / or high speed flight envelope protection, lesser margin values may be considered.
Never-exceed speed V_{NE}	CS-LUAS.1505 (a): The never-exceed speed V_{NE} must be established so that it is (1) Not less than 0.9 times the minimum value of V_D allowed under CS-LUAS.335; and (2) Not more than the lesser of (i) 0.9 V_D established under CS-LURS.335; or (ii) 0.9 times the maximum speed shown under CS-LURS 251. *	USAR.1505 (a): The never-exceed speed V_{NE} must be established so that it is: (1) Not less than 0.9 times the minimum value of V_D allowed under USAR.335; and (2) Not more than the lesser of: (i) 0.9 V_D established under USAR.335; or (ii) 0.9 times the maximum speed shown under USAR.251. *

* Both CS-LUAS 251 and USAR.251 refer to buffeting conditions, requiring that up until the minimum value of V_D allowed in CS-LUAS 335 or USAR.335, there is no excessive vibration or buffeting that could result in structural damage. It is noted that, here, the text of CS-LUAS seems to refer to CS-LURS, which are the JARUS Certification Specifications for Light Unmanned Rotorcraft Systems. However, a paragraph with this number identification is not found in CS-LURS, so it is assumed here that the original text refers to the own CS-LUAS.

Before going further, some brief comments are presented here on the paragraphs of the regulation included in Table 2. With respect to the differences between both codes, the definition of V_D in AEP-4671 integrates an additional consideration when compared to CS-LUAS, which is that a lower margin between V_C and V_D may be used if it is demonstrated to be safe. This possibility is not included in CS-LUAS. A lower margin between V_C and V_D would result in a narrower envelope and potentially a lighter aircraft sizing. However, in the initial stages of a new RPA design, the most possible scenario is that the means of demonstrating the safety of a lower margin would not be readily available to the designer, since at this stage the level of definition of the RPA concept is still low. In any case, and aside from the aforementioned alternative option given in AEP-4671, the 1.25 factor prescribed by both regulations provides a conservative result that is applicable to both, thus it will be the main option considered in the current research. However, overall, there are only minor differences between paragraphs of both codes referred to these certification airspeeds. The

high degree of similarity between both is advantageous, as it makes the methodologies to be proposed in this paper simultaneously compatible with both codes.

From the requirements compiled in Table 2, the expected interrelationships among the airspeeds included in this assessment may be summed up in the following form:

$$V_C < V_{NE} < V_D. \quad (6)$$

In view of the requirements of the airspeed definitions contained in Table 2, the one that may be considered to be more open is that of V_C, as the regulation only states that the applicant must select it according to RPA operating requirements. This suggests choosing a representative airspeed of the typical operations expected of the RPA for V_C. However, this might not be as straightforward in the case of RPA, which, as commented in the introduction, tend to have a marked multi-mission nature [17,18]. It is therefore possible, particularly if the RPA is designed to conduct missions of very different types, that there will be a set of potential flight airspeeds in distinct conditions. The Guidance Material (GM) of the regulations does not give any additional indications to select this airspeed.

The matter of how to choose the value of V_C is also left relatively open in the historical CS/Part-23 regulations. While this leaves more flexibility for the designer, certain authors prefer to complement the stipulations of the codes with additional guidance so as to propose a methodology that is more systematic and repeatable, while at the same time leaving room for other alternatives should the designer prefer them. This is the case of the envelope build-up process proposed by Gudmundsson [14], which provides a high level of detail in different steps of the process and provides additional criteria to aid the designer in this procedure. When selecting V_C, the author highlights that one of the main implications of this airspeed, as it will be seen further in this text, is that the highest gust load factors that the aircraft must bear are experimented on precisely at this airspeed. Therefore, if a value of V_C that is lower than the usual expected operating speed of the aircraft is selected, the vehicle will have to be slowed down when turbulence is present, which may interfere with the operation. On the other hand, if a value of V_C that is significantly above typical operating airspeeds, and thus closer to the maximum level speed, is selected, then the value of V_D may become exceedingly high, resulting in a heavier airframe [14]. This leads to the notion of selecting a value of V_C around the cruising speed that the aeroplane is capable of, but no higher than the typical values of operation [14]. This substantiated criterion complementing the prescriptions of the regulations aids to set up a more systematic design process, and it will be used as a basis in the envelope build-up process to be proposed later on in this research.

Several differences may be seen in these RPA-specific regulations when compared to those of manned aeroplanes. For instance, the latter tend to have additional provisions and have a higher level of detail, particularly those belonging to the transport category of aeroplanes. Furthermore, it is noted that the design speed for maximum gust intensity, V_B, which needs to be accounted for in commuter and transport aeroplanes, is not prescribed in these RPA regulations. This substantiates the need for performing a particular study on both the envelope build-up process and its application on RPA within these codes. Additional details on the CS/Part-23 design airspeeds are given in Appendix A.

2.3. Impact of RPA Design and Operational Variables on Flight Envelope

Central to the problem of conceptual design and certification is the understanding of which design and mission variables have an impact on the envelope and what the nature of such impact is. The purpose of the present section is to conduct an initial assessment of the effect of the variables involved in Equations (2)–(5) on stall and gust conditions, with

a more detailed quantitative assessment being presented later on from Sections 3–5, as applied to the RPA case studies conducted within them.

Firstly, a summary of the variables of interest is presented in Table 3, which also includes the main factors that may cause changes in their values.

Table 3. Summary of relevant design and operational parameters within the flight envelope.

Variable	Cause of Variation
W/S_W	Varies between flights due to different payload and fuel mass conditions and also along each flight due to fuel consumption.
V_{EAS}	Related to mission requirements. May vary between flights, and, depending on the cruise procedure, it may also change throughout the operation.
ρ	Depends on mission requirements.
U_{de}	Varies with altitude, which depends on mission requirements.
MGC	Depends on wing design.
a	Mainly depends on aerodynamic surface design.
C_{Nmax}	Mainly depends on aerodynamic surface design.

From a mathematical viewpoint, the gust and stall load factor expressions are respectively linear and quadratic in V_{EAS}, and the only degree of freedom in the shape of the expression is the coefficient associated with this velocity. This enables the impact of the variables to be qualified with a pair of complementary verbs. The chosen verbs are "improve" and "worsen", depending on whether the change in the variable makes them less or more prominent in the diagram, respectively. For stall (Equation (5)), a reduction in the quadratic coefficient increases the velocity at which stall occurs for a certain load factor, and therefore a reduction in this coefficient worsens the stall behaviour. Conversely, an increase in this factor improves the stall behaviour. For stall, an increment in the linear coefficient raises the load factor for a given airspeed, which is detrimental for structural sizing. Therefore, an increment in the linear coefficient of the gust curve worsens gust behaviour, and a decrement improves gust behaviour. The systematic application of the aforementioned criteria to the variables of Table 3 yields Table 4.

Table 4. The impact of the increment of design and operational parameters on gust and stall behaviours. The upper arrow next to each variable indicates that the impact is understood for an increment of the corresponding variable. h represents the flight altitude.

Variable	Impact on Stall	Impact on Gust
$\uparrow W/S_W$	Worsen	Improve
$\uparrow\rho$ ($\downarrow$h)	Improve	Improve
$\uparrow U_{de}$	None	Worsen
↑MGC	None	Improve
↑a	None	Worsen
$\uparrow C_{Nmax}$	Improve	None

3. RPA Flight Envelope Build-Up Process and Analysis

This section presents the first gust analysis approach proposed in this paper. This methodology consists of a systematic and repeatable build-up process for estimating the flight envelopes of RPA attending to the prescriptions of the CS-LUAS and AEP-4671 regulations. As commented beforehand, the flight envelope is not only an essential step in airworthiness evaluation but it also provides a significant amount of information within the aircraft design process on the interaction of manoeuvring and gust conditions that the aircraft must be able to achieve. Therefore, among other aspects, it can highlight the airspeed regions in which a gust can induce a stall condition, allowing to study the

operational implications that this might have and whether either gust or manoeuvring conditions are dominant along the different airspeed intervals covered by the envelope. Thus, the possibility of obtaining representative envelopes of RPA with the proposed methodology also opens up the opportunity of using them to study particular aspects of RPA gust behaviour within the frame of RPA conceptual design. Considering the information presented above, the main contributions presented in this section include both the systematic approach to estimate RPA flight envelopes as well as the novel insights derived from its application.

As discussed in the introduction, up until now very few research works have used this representation as an approach for the analysis of gust behaviour of RPA [10,27,30,31]. Of these, only the authors of [10] and of [31] have based their envelope build-up process on RPA regulations, particularly on the military AEP-4671 code. Some specific gaps seen in previous works regarding RPA flight envelope estimation are identified below:

- Only one envelope is obtained in each of the aforementioned works, neglecting the study and quantification of the variations in the shape and in the set of loading conditions represented by it when changing aircraft mass and operating conditions. This is crucial for aircraft sizing, since the structure must be designed to withstand the most critical load cases, which may occur at mass values different from the MTOM.
- The envelope is obtained for a single RPA in each case, missing the chance to make a comparison among envelopes obtained through the same method for distinct types of RPA.
- The process through which the certification design airspeeds are derived starting from RPA available mission data or from initial requirements is not explicitly detailed, complicating the reuse of the methodologies within the context of an RPA design framework. This is particularly relevant for V_C, since, as mentioned in Section 2.2, the regulation does not provide detailed stipulations for its selection.
- A direct comparison between the envelopes obtained through RPA-specific regulations and those obtained through manned aeroplane codes has not yet been conducted. This can be a relevant issue in the realm of Optionally Piloted Vehicles (OPVs), with the same air vehicle potentially having to be designed according to both manned and unmanned regulatory codes, thus having to comply with the most restrictive stipulations resulting from the application of both.
- Moreover, there are still various crucial aspects related to RPA gust behaviour that can be analysed through the flight envelope, and which still remain to be discussed in the literature. These include the study of the flight conditions in which bearing a gust of a certain intensity could cause the RPA to stall, evaluating whether the critical condition in different regions of the envelope is due to gust or manoeuvring requirements, and analysing the particular shapes that the envelope can take for certain RPA types and flight conditions, among others. These aspects have clear design and safety implications that could benefit from a particular analysis.

The methodology for the flight envelope build-up process proposed in this section seeks to address the aforementioned gaps as well as to answer to the research questions laid out in the introduction. It is noted that the methodology proposed here is not limited to a direct application of the models, procedure, and stipulations of the codes, as this would not address the aforementioned gaps and research objectives. In particular, the novel aspects of the procedure proposed here, which will be expounded in full detail throughout this section, are summarised as follows:

- A direct and explicit connection shall be made between the expected mission speeds of the RPA, considering the potential of different airspeeds being defined as in the

case of multi-mission RPA, with the certification airspeeds used in the envelope. This provides additional guidance with respect to the requirements found in the codes.

- The method shall be tailored to account for challenges in conceptual design of RPA. Specifically, the possibility of deriving a representative and conservative envelope from a low volume of starting data is considered.
- The methodology shall be developed accounting for its potential application both to new RPA in their initial conceptual design stages and also to the existing RPA when considering the low number of data items that are usually found in the open literature for already developed RPA.

The methodology presented in this section shall allow to obtain an initial estimation of the flight envelope according to the requirements of both the CS-LUAS [32] and the AEP-4671 [34] codes. The development of the envelope estimation process based on the common prescriptions of both codes constitutes one of the contributions of this methodology, which allows the RPA concept to be developed according to both civil and military standards specific to RPA, enabling their compatibility with dual applications. As discussed above, the method proposed here shall be developed to be compatible with two potential application cases:

1. Obtaining an estimation of the flight envelope of a new RPA within the conceptual design stage.
2. Performing an estimation of the flight envelope of the existing RPA when considering the scarcity of data that is usually present in the open literature. This issue related to RPA data scarcity has been noted by previous researchers [47,48], with a more detailed analysis of the challenges that arise due to this situation being developed in the cited works.

In both cases, a major challenge in the envelope build-up process is the comparative lack of data when compared to that which would be available in later design stages or if more information on existing aircraft were available. Thus, the proposed procedure seeks to obtain reasonable and conservative approximations of the flight envelope within the expected accuracy of conceptual design, which may be refined in later design stages where detailed information on the aerodynamic, propulsive, and performance characteristics of the aircraft as a function of mass and flight altitude are available.

Two application cases of the envelope build-up process proposed here shall be conducted, with a different type of RPA being considered in each. The analysis of these envelopes shall allow to answer various research questions laid out in the introduction as well as the gaps mentioned beforehand. Considering the aforementioned gaps and research questions, one of the purposes of the analysis of the results of these case studies is to compare the resulting shapes of the envelopes with those that are typical of manned aeroplanes. This comparison shall be conducted from two perspectives:

- The shapes of the envelopes obtained for RPA using their regulatory codes, as derived from the methodology proposed in this section, shall be compared to the typical shapes found in manned aeroplanes.
- The envelopes obtained for RPA using their regulatory codes shall be compared to the envelopes that are obtained through the direct application of manned aeroplane regulations to the same RPA.

The comparison with manned aeroplane flight envelopes shall be made considering those resulting from the application of historical CS/Part-23 codes, since they have a high level of specificity in their requirements. Appendix A contains, as a reference, a graphical representation of several types of flight envelopes that may be found in manned aeroplanes certified with these regulations. Furthermore, the envelope corresponding to the normal

category aeroplane with low wing loading, which is the design that is most comparable to RPA, has also been derived quantitatively. The main results from these comparisons as well as their analysis shall be presented in the current section, with Section 6 containing an expanded discussion on the implications and novel insights that may be gained from this assessment.

The content of this section is organised attending to the following schema: Section 3.1 contains an approach for deriving typical flight speed intervals starting from the data elements which are usually available in the aforementioned two application cases. This procedure is compatible with multi-mission RPA which may have distinct kinds of operations and constitutes a preceding step to the certification design airspeed selection process. Section 3.2 covers the envelope build-up process, which is based on the regulatory prescriptions previously expounded in Section 2, but which is complemented with additional guidelines proposed in this research. Then, Section 3.3 covers the two application cases of the envelope build-up process on existing RPA to demonstrate the methodology. Furthermore, Section 3.4 presents the envelopes that would be obtained for the same RPA case studies when directly applying the manned aviation CS/Part-23 regulations as discussed beforehand.

3.1. Derivation of Typical Flight Speed Intervals from Initial Requirements or Available Data

The main purpose of the procedure proposed in this subsection is to propose a repeatable process that connects, in an effective manner, the expected mission speeds of the RPA with the construction of its certification envelope. In particular, the results from the approach proposed here shall provide a novel way to aid the designer in the selection of the certification design airspeeds compiled in Table 2. The approach is also tailored to address the challenge related to the scarce data that is usually available at the onset of the two application cases discussed beforehand.

The approach expounded here is based on the definition of various typical flight speed intervals that represent different kinds of possible operating scenarios of the RPA that is being studied. These ranges of airspeeds shall then be used in the forthcoming subsection to derive, in a repeatable manner, the certification design airspeeds required for the envelope construction. These expected airspeeds shall be defined as intervals instead of single values so as to cover the variability in RPA operations and also to account for uncertainties associated both with the early design stages and with the data that is available in the open literature. The definition of various distinct intervals of typical airspeeds along with their formalisation as ranges of values also seek to make the methodology compatible with multi-mission RPA. Furthermore, these intervals do not only support the selection of the design airspeeds, but they can also be used to check whether the resulting envelope is consistent either with the specifications found in the design missions or with the available data on the RPA, depending on the application case that is being considered. If the envelope is being obtained in the context of an RPA design process, any inconsistencies that may appear could indicate that certain design changes or variations in mission specifications might be needed.

The definition of these typical airspeed intervals is a feasible task at the onset of the conceptual design stage and also when analysing the existing RPA based on the information that is usually available in the open literature. Three different intervals shall be defined to cover RPA missions and operating conditions of diverse nature:

- Low operating mission speeds (V_{ml}): These correspond to the operating conditions and mission target airspeeds in which the aircraft is flying at a low regime, even close to stall. This scenario may be usual in surveillance and intelligence operations, which are very common in RPA [16,17], as well as other high-persistence missions in

which achieving high endurance is key. Low flight speeds typically result in higher endurance flight conditions due to the higher values of lift coefficient, C_L, being closer to those that yield maximum endurance [49]. In the open literature, information related to these kinds of operations usually correspond to loiter speed data.

- Medium operating mission speeds (V_{mm}): These correspond to missions conducted at average to moderate airspeeds. These may potentially include payload delivery operations in which very fast arrival is not a crucial factor, certain area coverage missions where very high endurance is not required, some phases of Search and Rescue (SAR) operations and other types of sorties that are expected to be common operations of the aircraft and not require either flight very close to stall or to the maximum level airspeed of the RPA. If operations conducted at very low or high airspeeds are among the most common ones for the RPA, the present airspeed interval may overlap with the other ones, indicating that these are not only potential missions of the RPA but also part of the most commonly expected sorties. This is also seen in the data found on RPA missions in the open literature, where for example in certain Jane's datasheets, loiter and cruise speed share the same values [50–52]. It is relevant that this V_{mm} interval covers the usual operating conditions expected of the RPA, since it will then be used in the selection of the V_C certification design airspeed.
- High operating mission airspeeds (V_{mh}): These correspond to the high-speed flight regime operation of the RPA, often close to or even reaching its maximum level speed. The present airspeed range need not represent the airspeeds flown in common sorties of the aircraft. Nevertheless, certain operations such as rapid penetration reconnaissance missions or fast payload delivery may be flown in these conditions when the purpose is not as much to maximise efficiency, but rather to conduct the mission rapidly [53]. Thus, this interval may be selected to include within its lower bound airspeeds corresponding to potential high-speed operations and matching in its upper bound the maximum airspeeds that the aircraft can achieve.

The definition of these three distinct intervals allows to cover various possible flight regimes and common missions of RPA. It is noted that, usually, both mission requirements as well as RPA performance data are given in terms of true airspeed (TAS), as it is commonly the case in Jane's Yearbook datasheets [50,51] and RPA manufacturer brochures. This is in contrast to the definition of the certification design airspeeds in EAS that is prescribed in the regulations and that must be used when representing the flight envelope. Therefore, the input TASs need to be converted to EAS format with the expression corresponding to the relationship between both airspeed definitions [14].

$$\rho V_{TAS}^2 = \rho_0 V_{EAS}^2 \rightarrow V_{EAS} = V_{TAS}\sqrt{\rho/\rho_0} = V_{TAS}\sqrt{\sigma} \quad (7)$$

where V_{TAS} corresponds to the true airspeed and σ represents the atmospheric density ratio. Therefore, aside from data on the operating airspeeds of the RPA in its different potential mission scenarios, it is required that the information on the operating altitude is available to enable the calculation of the corresponding EAS values that must be used in the certification design airspeed selection and the envelope build-up process.

Within the two application cases considered in the development of the methodology proposed in this section, different scenarios in terms of quantity and format of available data may be found, each requiring unique considerations. These may be summed up in three possible scenarios, which are illustrated in Figure 4 and discussed briefly below. These correspond to actual scenarios that are encountered when performing the design and analysis of RPA, as substantiated by the references included below, and as it will also be illustrated in the case studies, developed further throughout this paper.

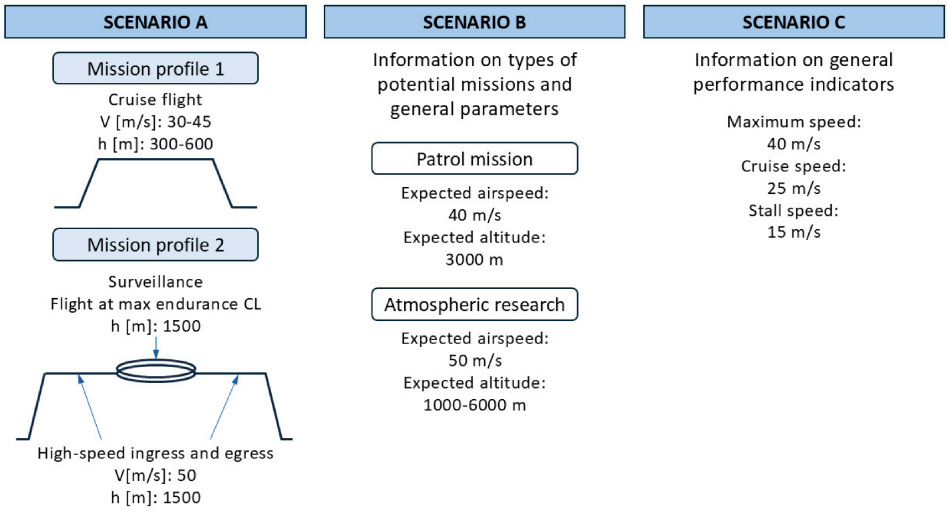


Figure 4. Example scenarios in terms of initial data availability for generating typical flight speed intervals for envelope construction depending on the design's initial specifications and the data found in the literature with respect to existing RPA.

- Scenario A: Flight profiles are available for the main missions of the RPA along with the data on the flight parameters defining each of the segments of the operation. Certain aircraft missions may be defined by various segments, potentially including diverse phases such as ingress, egress, loiter, etc. Each of these segments may be conducted in different flight conditions (for instance, a loiter phase is usually conducted at a low airspeed seeking to maximise endurance) [53]. This scenario may be found, for instance, in the designs developed in [54,55].
- Scenario B: In this case, the data on the features describing each flight segment of the missions conducted by the RPA may not be available, but information is obtainable on the usual types of operation of the RPA, which may be available along with the expected characteristic airspeeds for each of them. This scenario may be found in both application cases, as the design's initial requirements may often be given without specifying mission profiles but still giving data on the expected typical missions [56], and for existing RPA, it is unusual that information on their flight profiles is available in the open literature, but a description on their main missions may be found in certain cases [57].
- Scenario C: No information is available on the characteristics of the different types of missions of the RPA, and only certain overall performance values may be found. This is commonly the case in the second application scenario discussed beforehand, as the information on existing RPA in the literature is often scarce, and only certain indicative values on characteristics such as maximum level speed, cruising speed, loiter speed, and stall speed may be found. These are often not related to specific missions, and in many cases, even when consulting Jane's datasheets, not all the mentioned airspeeds are available [50–52].

There can be intermediate cases between those discussed above. The case studies that will be presented further throughout this paper not only seek to provide the results and discussion on RPA gust behaviour, but also to document the process followed to reach these results. In particular, the results in Section 3.3 shall be obtained starting from scenario C and those of Section 4 shall correspond to scenario A.

As mentioned above, once the data on different usual missions of the RPA has been compiled, it has to be converted to EAS format for the use in the envelope construction. Thus, the information on the corresponding density is needed, requiring additional con-

siderations. Often, RPA operational data is given in the form of Above Ground Level (AGL) height instead of being provided in terms of altitude. Furthermore, as discussed beforehand, the data on RPA airspeeds is usually not given alongside the corresponding weights and altitudes, with an overall operating height or altitude band being found in the open literature instead [50]. In other cases, the only data item is the ceiling. In these cases, and in view of the type of mission and other characteristics of RPA, a representative operating altitude band may be deduced.

To address the aforementioned scenarios and obtain conservative ranges of the typical flight speed intervals in EAS, the following approach may be used. Firstly, an overall height band covering the potential operations of the RPA is defined from the available data on typical AGL height, the envisioned types of operation, etc. If more detailed information is available, a different interval may be defined for each of the airspeed ranges of V_{ml}, V_{mm}, and V_{mh}. Then, four values of EAS are obtained for each of the three airspeed intervals, corresponding to the combinations between the upper and lower boundaries of both the airspeed and altitude ranges of values. From these, the upper and lower bounds are selected, which cover all envisioned operational scenarios for each of the three flight regimes, providing the largest potential interval in EAS. This is a conservative approach since it results in the largest possible airspeed range, thus accounting for the uncertainties associated with the available information. Furthermore, as it will be discussed below, this largest possible EAS interval also results in a conservative estimation of the envelope. This proposed approach may see particular application in scenarios B and C, where data is more limited. The process is illustrated in Figure 5 for the case of V_{ml} and may be applied to each of the three intervals.

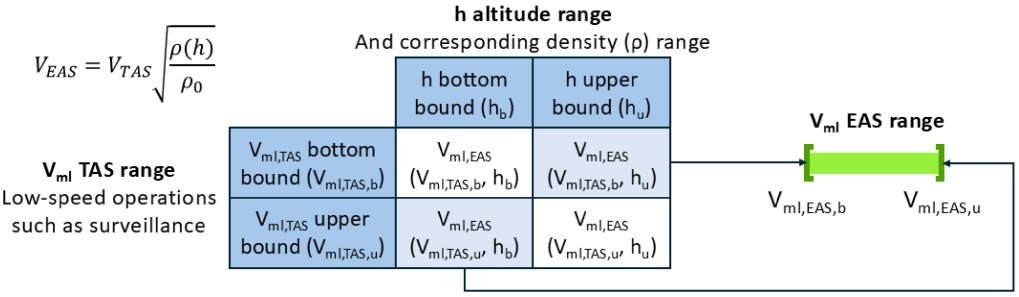


Figure 5. Example of EAS flight speed range derivation process for V_{ml} that may be applied when a direct correspondence between airspeed and altitude data is not available.

It must be highlighted that this is an approximated process, the limitations of which should be underlined. Since the EAS intervals are obtained from the combinations of airspeed and altitude that give the largest possible range of values, these intervals shall probably cover a higher range of airspeeds when compared to the most usual cases of operation of the RPA. This may result in the lower bound of V_{ml} being close to stall and the upper bounds of both V_{mm} and V_{mh} giving a higher design dive speed, V_D, as a result.

Within the context of the design of a new RPA, the first of the effects mentioned above may give the designers the impression that the wing loading should be reduced to give a larger margin from operating conditions to stall, whereas this might not be required due to the conservatism of the results obtained with this approach. The second effect results in an increase in the overall width of the envelope. Since the RPA has to be designed to withstand all manoeuvring and gust cases within the flight envelope, this envelope overestimation can potentially result in the design of an RPA with a larger weight, resulting in a less efficient air vehicle. In spite of this, it is highlighted that, since the method presented in this paper covers the flight envelope estimation within the context of the initial design stages, the higher grade of conservatism resulting from the aforementioned approach may

be addressed in further design stages when a greater knowledge of the RPA that is being developed is available and more detailed analyses may be applied once the design space has been narrowed down after the first iteration.

A further effect resulting from the aforementioned conservative approach for estimating EAS intervals is that, when accounting for the effect of the density interval, overlaps between the three airspeed intervals may appear even if these did not happen in the original TAS value ranges.

3.2. Flight Envelope Build-Up Process

This subsection covers the flight envelope build process that is applied as part of the approach proposed in this section for the analysis of gust behaviour of RPA. This procedure is based on the background, assumptions, equations, and regulatory requirements that were previously expounded in Section 2. These are complemented with novel steps that are mainly based on the three typical flight speed intervals derived through the process proposed in the previous subsection, which shall be used here as a support to the designer in the selection of the certification design airspeeds. The proposed envelope build-up procedure is carried out according to the following steps.

1. Firstly, it is required to define the weight and altitude conditions in which the flight envelope is to be obtained, since these aspects have an impact on several variables involved in the envelope estimation process. The weight of the RPA is involved in the wing loading W/S_w, which influences both the stall restriction (Equation (5)) and the gust load factor lines (Equation (2)). Furthermore, the flight altitude influences air density, ρ, which is involved in the calculation of the mass ratio of the aeroplane, μ_g (Equation (4)), which is then used to obtain the gust load factors.
2. The three typical flight speed intervals proposed in Section 3.1 (V_{ml}, V_{mm}, V_{mh}) are obtained in EAS and represented in the horizontal axis of the flight envelope.
3. The following step consists of the selection of V_C. As mentioned in Section 2.2, this is one of the matters in which both the AEP-4671 and CS-LUAS codes leave a higher degree of choice to the applicant, with both codes only stating that it must be selected based on RPA operating requirements. The process for the selection of this airspeed that is proposed here is based on both the recommendations given in previous research within the field of manned aircraft [14] and also on the concept of the typical flight speed ranges proposed earlier in this paper. Considering that the V_{mm} interval does not only represent average to moderate flight speeds of the RPA, but it is also defined according to the most typical missions of the aircraft, it is proposed here to select V_C as the upper bound of the V_{mm} range. Selecting V_C at the upper bound of V_{mm} constitutes a conservative approach, since it ensures that the RPA shall be able to withstand the most demanding gusts (those of intensity U_C) within all potential operational scenarios corresponding to the typical missions of the aircraft. This degree of conservatism may then be reduced at later stages once more detailed information on the aircraft is known and its operational scenarios become defined with a higher level of detail, enabling the designer to adjust in a more precise manner the V_C value for each weight and altitude condition.
4. The minimum value that V_D may take is estimated, which can be done at this point according to the regulatory stipulations discussed in Section 2.2.

$$V_{D_{min}} = 1.25\, V_C \tag{8}$$

5. It is proposed that the next stage in the envelope build-up process consist of the selection of a value for the never-exceed speed, V_{NE}, that is consistent with the available operational data and with the prescriptions established by the regulations.

As seen in Table 2, there is a mathematical relationship between V_{NE} with both the minimum value of V_D as well as with the selected value of V_D, which can be set at any value above its minimum. On the one hand, selecting V_{NE} below the maximum value of the typical flight speed interval V_{mh} is not be fully compatible with all expected operations represented by V_{mh}, since some would not be able to be flown in operation, as they would fall above the never-exceed speed. Furthermore, this decision might not yield benefits in terms of the potential reduction in V_D, as this latter airspeed has a minimum value set by V_C as seen above. On the other hand, selecting a value of V_{NE}, which is significantly above the upper limit of V_{mh}, may give as a result remarkably high values of V_D, resulting in a heavier structure. Furthermore, selecting V_{NE} very much above the maximum of V_{mh}, is not consistent with the fact that the upper limit of V_{mh} is expected to represent the maximum level speed expected with the aircraft, thus V_{NE} might not even be achievable in level flight, thus not resulting in a practicable performance limitation. Thereby, it is proposed to select V_{NE} according to both considerations commented above. It is noted that the integration of V_{mh} in this step constitutes one of the novel additions of this work to the stipulations of the regulations. The above-mentioned considerations translate into the following mathematical expression, which is compatible with the requirements of Table 2:

$$V_{NE} = \max\left(\max(V_{mh}), 0.9\, V_{D_{min}}\right) = \max(\max(V_{mh}), 1.125\, V_C) \tag{9}$$

6. The following step consists of selecting a value of V_D that complies with the margins that this design airspeed must have with respect to V_{NE} while ensuring that it is also above its minimum value as obtained through V_C beforehand. According to the requirements included in Table 2, which translates into the expression indicated in Equation (10) found below, upon completing this step, the rightmost boundary of the envelope may be represented.

$$V_D = \max\left(V_{D_{min}}, \frac{V_{NE}}{0.9}\right) \tag{10}$$

7. Once the certification design airspeeds have been defined, the remaining boundaries of the flight envelope may be represented following the requirements of the regulations. Upon obtaining the stall limitations through Equation (5), their position with respect to the V_{ml} airspeed range may be analysed to study whether the results of the envelope are consistent with the envisioned operations at low-speed flight regimes. It is noted that some authors propose representing a vertical limitation at both the 1 g positive and negative stalling speeds [9,14,27], while others omit the representation of this constraint in the diagram, with the points between both stall parabola representing feasible flight conditions up until both converge at the coordinate origin [13,16]. In this work, following the example envelope provided in the NATO AEP-4671 [34], these vertical 1 g stall limitations are not represented in the envelopes depicted in this paper, but they could be added to the envelope build-up process if the designer prefers to do so.
8. The limit load manoeuvring factors n_{lim+m} and n_{lim-m} are both obtained according to CS-LUAS.337(a), USAR.337(a), CS-LUAS.337(b), and USAR.337(b). These represent the top and bottom boundaries of the manoeuvring envelope.
9. Finally, the gust envelope is represented following the model prescribed in the regulation and described in Section 2.1. The aeroplane mass ratio μ_g is first obtained attending to the weight and altitude conditions at which the envelope is being evaluated (Equation (4)), allowing to calculate the gust alleviation factor K_g (Equation (3)). This variable then enables obtaining the positive and negative gust lines for gust intensities U_C and U_D through Equation (2).

3.3. Results and Analysis of the Proposed Flight Envelope Build-Up Methodology Based on RPA Airworthiness Codes

This subsection contains the application of the proposed envelope build-up process to two different case studies. The purpose is not only to demonstrate the practical use of the methodology, but also to study the particularities of the gust behaviour of both RPA that will be analysed here based on the resulting flight envelope so as to answer the research questions laid out in the introduction throughout the application of this methodology.

As commented beforehand, the procedure can be used in different application cases (new RPA design and analysis of existing RPA based on the data commonly available in the literature) as well as in three potential scenarios related to data availability (scenarios A to C discussed in Section 3.1). Both examples found in this subsection have been carried out within the context of the second application case, where existing RPA concepts shall be studied. The scenario related to data availability in this case is scenario C, due to the information that can be readily found in the open literature on RPA designs being usually limited. The application case corresponding to the conceptual design of a new RPA shall be demonstrated along with a different data availability scenario in the methodology proposed in Section 4.

The RPA that have been selected for study in this subsection are the RQ-2 Pioneer and the Predator A. Both are among the RPA for which a larger amount of information is available in the open literature [16,17,50,52,58,59]. Nevertheless, certain data items have not been found in the consulted references, such as information on potential high-lift devices. Furthermore, it has been necessary to make certain assumptions starting from the available information to define all data required for to perform the calculations. The RQ-2 Pioneer is a tactical RPA mainly intended for short and medium range intelligence and surveillance operations [16,52], whereas the Predator A can be classified within the Medium Altitude Long Endurance (MALE) category of unmanned vehicles, with its main purpose being surveillance sorties while also showcasing a noteworthy adaptability to other types of missions [16,50,60].

The selection of both of these aircraft seeks to cover certain gaps in previous studies that have obtained the flight envelopes of RPA, which have mostly focused on either small or large aircraft, without an explicit comparison between the envelopes of RPA of differing categories being currently found. These kinds of comparative assessments provide valuable information on the differences in the manoeuvring and gusts conditions corresponding to each aircraft type. While a comparison between various envelopes of distinct manned aeroplanes can be found in the works of [13,14], such an analysis has yet to be conducted for RPA. Therefore, the comparison of the application cases conducted here constitutes a novel contribution of the present research. For each of these RPA, two different conditions of weight and altitude shall be analysed, so as to study the changes in the envelope between both scenarios for each aircraft, with this constituting an original addition with respect to previous works in the field of RPA, which have focused on the analysis of a single envelope for a particular operational case.

3.3.1. Tactical RPA: RQ-2 Pioneer

The information used to perform the estimation of the flight envelope of the RQ-2 Pioneer has been mainly obtained from references [52,58]. According to the envelope build-up process proposed in Section 3.2, information on the operational missions of the RPA is particularly relevant to set up the typical flight speeds, V_{ml}, V_{mm}, and V_{mh}. The data gathered from the literature results in the selection of the airspeeds and operational height band summarised in Table 5.

Table 5. Inputs for typical flight speed intervals for the RQ-2 Pioneer, derived from data obtained from [52,58].

Data Item	Value	Units
V_{mh} (TAS)	185	km/h
V_{mm} (TAS)	148	km/h
V_{ml} (TAS)	118–148	km/h
Operating height band	0.3–3.0	km

Certain hypotheses were required to derive the values contained in Table 5 from those found in the literature. It is noted that in Jane's datasheets, information was only found on "maximum level speed", with a value of 185 km/h, and on "cruising/loiter speed", with a value of 148 km/h. These data are not given along with information on the weight and altitude conditions corresponding to these airspeeds, which constitutes a challenge towards defining different typical airspeed intervals as a function of these conditions. Furthermore, the cruising and loiter speeds are given within the same data item in Jane's datasheets. This might be considered to be consistent with the fact that surveillance operations (which benefit from being carried out in flight conditions close to those of maximum endurance) are among the most typical missions of the RQ-2 Pioneer.

Seeking further information in the literature to complement that found in Jane's datasheets, in the research in [58] a series of estimated performance curves are given for the Pioneer based on wind tunnel data, where it is seen that flight conditions of higher range and endurance may be attainable at lower airspeeds than the cruising/loiter value given in Jane's datasheets. Based on those results, a value of 118 km/h is selected here to complement the aforementioned data given in Jane's datasheets and define a lower bound to the interval of V_{ml}, while also including the 148 km/h value from Jane's datasheets as an upper bound to cover the information given by both studies. The V_{mm} and V_{mh} values are then selected following the guidelines from Section 3.2 according to the cruising and maximum level speed data provided in Jane's datasheets, albeit in this case they are defined as single values instead of intervals, since no information on the variation in these airspeeds depending on weight and altitude conditions is given. Therefore, the approximate methodology for estimating conservative ranges of typical airspeeds in EAS that was proposed in Section 3.1 needs to be used here. As anticipated in this paper beforehand, the lack of more detailed performance data on RPA requires supplementation with additional hypotheses and estimations to enable reaching the information required to represent the flight envelope.

Before obtaining the airspeed intervals in EAS attending to the process proposed in Section 3.1, an overall height band that is expected to cover all envisioned operations of the RPA needs to be defined. The data from Jane's datasheets declares an interval in the range of 0.3–4.6 km [52]. However, the estimated performance in [58] results in an approximate ceiling of 3.2 km for the RPA. Thereby, the interval proposed here and included in Table 5 is set with its upper limit slightly below the ceiling given in the second reference, which in any case is also contained within the information provided in Jane's.

It is noted that the typical airspeeds, V_{ml} and V_{mm}, shall present an overlap due to the upper bound of the first one, coinciding with the single value declared for the second. It is considered that this can be substantiated based on the aforementioned fact regarding the typical missions of the RQ-2 Pioneer, which are precisely surveillance operations. This airspeed interval overlap is also consistent with the observations related to the definitions of these airspeeds as proposed in Section 3.1.

Once the typical flight speed intervals in EAS are derived, the envelope build-up process proposed in Section 3.2 can be applied. From the possible combinations of weight

and altitude for the Pioneer, two envelopes have been represented in Figure 6: one with the maximum mass and low altitude and another with the minimum mass and higher altitude. This choice is intended to showcase the most contrasting shapes that the flight envelope can take for a given aircraft when considering the way in which these weight and altitude conditions impact the flight envelope as expounded in Section 2.3.

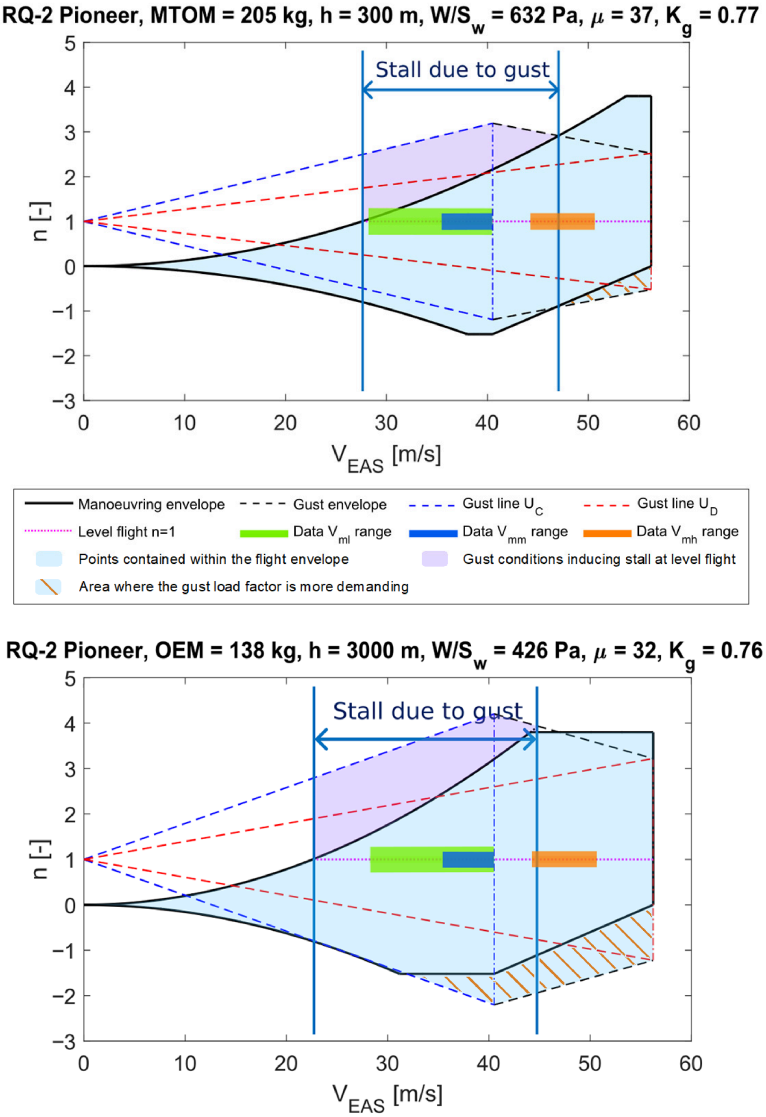


Figure 6. Flight envelopes obtained for two flight conditions of the RQ-2 Pioneer according to the procedure described in Section 3.2. V_{EAS}: equivalent airspeed, n: load factor, MTOM: Maximum Take-Off Mass, OEM: Operating Empty Mass, h: flight altitude, W/S_w: wing loading, μ: mass ratio of the aeroplane, K_g: gust alleviation factor.

With respect to the aforementioned choice of mass values at which the envelope will be evaluated, it is noted that the usual operating conditions of the aircraft shall present a certain variation when compared to these scenarios. In the case of the first envelope, this difference happens because the RPA will have consumed a certain quantity of its fuel before reaching the operating altitude, resulting in a mass lower than the MTOM at the altitude that is being considered here. In the case of the second envelope, the aircraft is expected to carry a certain quantity of reserve fuel in most operating cases and additional fuel is required for descent, approach, and landing. Thereby, the weight at the altitude considered in the second envelope would be higher than OEM. Thus, the scenarios that have been represented here have been selected to be illustrative of the most disparate envelopes

that could result from the available data. In contrast, the aforementioned considerations related to fuel mass shall be taken into account within the forthcoming mission-based gust analysis methodology proposed in Section 4, since it is focused to a greater extent on the modelisation of different segments of the operation itself.

The shapes of the envelopes are quite distinct to those typically found in manned aeroplanes, with some examples of such being found in [13,14] as well as in Appendix A. The different highlighted regions in the n = 1 line represent the typical airspeed ranges obtained beforehand. Since this aircraft is mainly intended for Intelligence, Surveillance, and Reconnaissance (ISR) operations, these speeds are generally low, and consequently quite close to stall in many cases. In the first envelope, the segments corresponding to n_{lim} are very short, and stall dominates most of the diagram in spite of the comparatively low wing loading. This is due to the cruise and maximum flight speed of the aircraft not being much higher than the 1 g stall speed of the RPA, resulting in a reduced value of V_D, and thus producing a compact envelope.

The observations discussed above are in contrast with many manned aeroplane envelopes as seen in the examples in Appendix A. The typical operating speeds of these aircraft, which would be located around V_C, show a much higher margin with respect to the 1 g stall airspeed, thus the values of V_D are also higher, and the envelope presents a much more expanded shape on the V_{EAS} axis. For these manned aircraft, the stall limitation takes a comparatively lower share of the full boundary of the envelope, while manoeuvring load limit conditions become more prevalent. Albeit it could be expected from the start that the envelopes and design airspeeds between both types of aircraft would be different due to their dissimilarities in terms of mission and design, this application case allows to assess these discrepancies in a more direct manner.

It is noted that there is a significant range of operational flight speeds where the gust load factors fall above the stall parabola. This means that those load conditions are not attainable since at those speeds encountering a gust as prescribed by the regulations would result in the aircraft stalling according to the model used in this research. This could compromise the operation and the integrity of the aircraft. This gust-induced stall interval covers approximately 70% of the range of level flight conditions, which is in stark contrast to the envelopes for manned aeroplanes seen in Appendix A, where this gust-induced stall interval is in the range of 15–30%. Thus, gust-induced stall conditions in RPA constitute a remarkably more significant issue than in typical manned aeroplanes. Further implications of this shall be discussed in Section 6.

The second envelope is notably different, which showcases the impact of the mission and weight condition on gust and stall behaviour. The stall curve moves to the left due to the reduced wing loading as discussed in Section 2.3, leaving more room for limit manoeuvring load conditions. This also results in a higher margin between stall and the range of V_{ml} airspeeds, which is beneficial in terms of operational safety. However, this decrease in W/S_w increases the gust load factors. Thus, in spite of the reduced stall speed, the increased slope of the gust curves leads to a similar overall length of the gust-induced stall interval, albeit shifted to the left and in this case covering approximately 65% of the level flight cases, which again quantitatively indicates the remarkable issue that gust-induced stall conditions represent for this RPA.

The prevalence of the stall limitation throughout both envelopes, which is particularly remarkable in the first case, greatly limits the set of load cases that the aircraft must be designed to withstand. Notwithstanding the above, and with respect to the interaction of manoeuvring and stall load conditions in structural sizing, in the first envelope it may be seen that manoeuvring load cases dominate most of the boundary of the envelope that is not defined by the stall limitation. Thus, manoeuvring conditions drive the structural

design of the aircraft in these regions. However, at the bottom-right corner, there is an area where the gust load factor is the most demanding. This predominance of gust loads with respect to the manoeuvring ones for downward gusts increases in the second envelope, with the share of the boundary covered by these cases becoming expanded. This is due to both the increment of gust load factor due to the smaller wing loading and also because of the change in atmospheric density, which affects the mass ratio of the aeroplane, μ. Further comments on the design implications of the shape of the envelope as well as on the comparison with those of manned aeroplanes shall be provided in the discussion section.

3.3.2. MALE RPA: Predator A

In the case of the Predator A, the information available in the open literature is more limited when compared to that from the previous case study. Here, the data has been mainly obtained from [50,60–62]. Before going forward, it is noted that the value of the MTOM of the Predator falls outside the range of applicability of the CS-LUAS regulation. However, this value is included within the applicability scope of the AEP-4671 code, which is the one that is used here. In any case, as seen in Section 2.2, the provisions of both codes with respect to the flight envelope are very similar, so there is no remarkable difference caused by only using the second document here.

The typical flights speeds, V_{ml}, V_{mm}, and V_{mh}, as well as the operational height band that has been derived from the source data, are summarised in Table 6.

Table 6. Inputs for typical flight speed intervals for the Predator A, derived from data obtained from [50,60–62].

Data Item	Value	Units
V_{mh} (TAS)	222	km/h
V_{mm} (TAS)	176	km/h
V_{ml} (TAS)	135	km/h
Operating height band	3.0–7.0	km

As in the previous case, various assumptions have been required to arrive at the airspeeds compiled in the aforementioned table. In the case of the Predator, Jane's datasheets only contained a single value for the maximum level speed and loiter speeds, without correspondence to weight or altitude conditions and with no data given for the cruising speed. Therefore, the aforementioned two data items have been selected as V_{mh} and V_{ml}, attending to the guidelines proposed in Section 3.1. To set the cruising speed, additional information was sought in the literature. The U.S. Air Force factsheet corresponding to reference [62] contains an interval for the cruising speed between 135 and 217 km/h, which is a broad range of values. Consulting the research work of [61], a representative airspeed of 176 km/h was selected for aerodynamic calculations of the Predator, which coincides with the average of the airspeed range given in the factsheet and is also close to the average between the maximum and loiter speeds given in Jane's datasheets. Therefore, this value has been selected here as V_{mm} in absence of more detailed information.

As in the case of the RQ-2 Pioneer, since no correspondence is provided in the literature between the aforementioned airspeeds and their weight and altitude conditions, the approximate method for the derivation of the EAS intervals proposed in Section 3.1 is also applied in this case study. The operating height band of the Predator is not given in Jane's datasheets, with the only related value being the ceiling of 7.6 km. In the research work [60], it is stated that the lower band of the typical operational missions of the Predator can be located around 3 km, and the investigation then analyses a mission carried out by this aircraft with a maximum altitude close to its ceiling. Considering the above, an interval

of 3–7 km is chosen here to leave a certain margin with respect to the maximum attainable altitude of this aircraft. As in the previous case, the conservative EAS intervals obtained through this approach shall be used in both envelopes to be analysed for this RPA.

Once the airspeed intervals in EAS have been derived, the envelope build-up process may be applied. Following the same rationale as in the previous case study, two envelopes are obtained, one for the MTOM and minimum altitude and the second corresponding to OEM and the maximum altitude. These are represented in Figure 7.

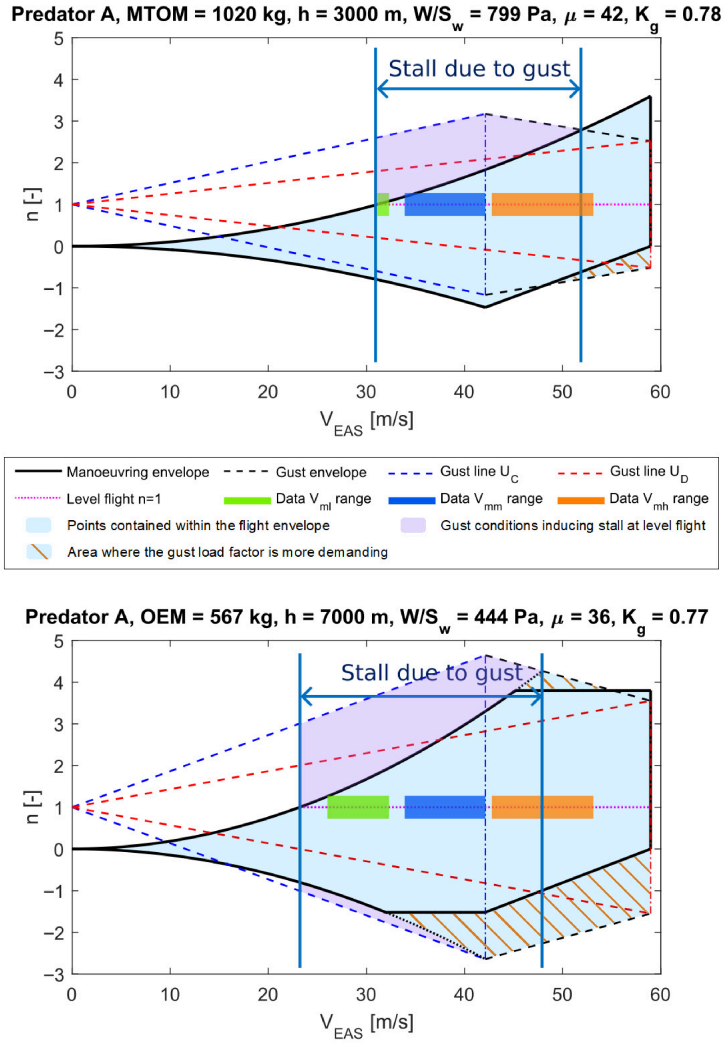


Figure 7. Flight envelopes obtained for two flight conditions of the Predator A according to the procedure described in Section 3.2. V_{EAS}: equivalent airspeed, n: load factor, MTOM: Maximum Take-Off Mass, OEM: Operating Empty Mass, h: flight altitude, W/S_w: wing loading, μ: mass ratio of the aeroplane, K_g: gust alleviation factor.

The differences between both envelopes corresponding to different flight conditions are even more remarkable in this case. In the first one, the n_{lim} values are not attained for any velocity due to the large impact of stall. This is caused by the combination of the higher maximum W/S_w of this aircraft in comparison with the RQ-2 Pioneer, but with similar maximum values of V_{EAS} in both RPA due to the effect of the different mission altitudes. This significant prevalence of stall results in the full range of speeds corresponding to the V_{ml} interval not being attainable for this flight condition, with the potential loiter speeds being very close to stall. It was mentioned beforehand that the comparison between the V_{ml} interval and the stall conditions may be used to check whether the envelope is consistent with the operational data. In the case of the envelope at the MTOM, this proximity between

V_{ml} and stall does not constitute a significant issue, since the RPA shall only usually fly in loiter conditions once it has first flown to the site where the surveillance operation is to be conducted after an ingress flight. Therefore, upon reaching the location where the mission is to be carried out, a certain quantity of fuel will have already been consumed, reducing the wing loading and also the stall speed. Thus, the conditions corresponding to missions conducted at the loiter speed are not expected to coincide with those of the MTOM, reducing the criticality of the proximity between both airspeeds in this case.

The envelope changes substantially in the second condition due to the high fuel mass of the Predator, resulting in a larger absolute variation in W/S_w between both envelopes once the fuel is depleted. Here, the n_{lim} values are no longer overpowered by stall and the load factors for downward gusts take a remarkable share of the bottom-right side of the envelope. Furthermore, in this case, the full range of potential airspeeds corresponding to loiter are attainable, which is due to the impact of wing loading on stall as discussed earlier. Therefore, it can be considered that the V_{ml} interval corresponding to the operational speed data is compatible with the resulting stall speeds.

It is also noted that, as in the case of the RQ-2 Pioneer, both envelopes also present a significant gust-induced region. In the first case, the relative percentage of level flight conditions where gust-induced stall may occur is of 76%, whereas in the second envelope it covers 72%. This allows to quantify the range of potential airspeeds where gust-induced stall constitutes a significant issue, which in this case is even more remarkable than for the RQ-2 Pioneer due to the way in which the wing loading influences the interaction between stall and gust conditions as expounded beforehand.

Both case studies presented in this section have not only allowed to assess various aspects of the gust behaviour of these RPA through their envelopes according to the regulations, but they have also served to show the challenges faced when tackling the estimation of the flight envelopes when accounting for the low volume of information available on RPA in the literature. It is also noted that, due to the assumptions required to manage the low volume of data available, these envelopes constitute approximations, with more detailed information being required to address certain estimations made here, such as the typical airspeed intervals being common for both altitudes. This matter has been addressed here by following a conservative approach when deriving the operational intervals in EAS and when selecting the certification design airspeeds. More detailed information would allow to obtain intervals specific to each weight and altitude condition. In any case, the impact of altitude has been accounted for in the envelope through the gust modelisation expounded in Section 2.1.

Further discussion on the significance of the results of these envelopes and their potential implications in design considerations shall be addressed in Section 6 along with an expanded comparison with the shapes of typical manned aeroplane envelopes.

3.4. Results and Analysis of the Flight Envelopes Obtained Through the Procedure of CS/Part-23 When Applied to RPA

The flight envelope construction process found in the manned aeroplane CS/Part-23 regulations [39,40] is significantly different from that of RPA airworthiness codes. This is an intuitive premise, since both types of aircraft present many differences in design and operation, among other aspects. However, the process of applying the CS/Part-23 envelope construction process to RPA can be expected to yield instructive results, as discussed at the start of the current section. These include findings regarding the way in which different airworthiness requirements impact the set of cases with which the same aircraft must comply, the shortcomings of certain CS/Part-23 stipulations with respect to their consistency of operational characteristics of RPA, and the way in which both types of envelopes compare in terms of target load conditions, with this latter point being relevant for the design of OPVs.

Some singularities in the construction of CS/Part-23 envelopes are discussed in Appendix A, where various example envelopes for manned aeroplanes are also provided. Further details may be found in the codes [39,40]. The data used for each of the RPA are the same as in Section 3.3. It is noted that the CS/Part-23 methodology does not use the typical flight speed intervals, V_{ml}, V_{mm}, and V_{mh}, proposed in this paper, since these are novel contributions of the method proposed here. However, they will still be represented for illustrative purposes in the envelopes obtained within this subsection to show how the resulting envelopes compare to the envisioned operations of the RPA.

3.4.1. Tactical RPA: RQ-2 Pioneer

The flight envelopes resulting from the application of the CS/Part-23 envelope build-up process for the RQ-2 Pioneer are shown in Figure 8.

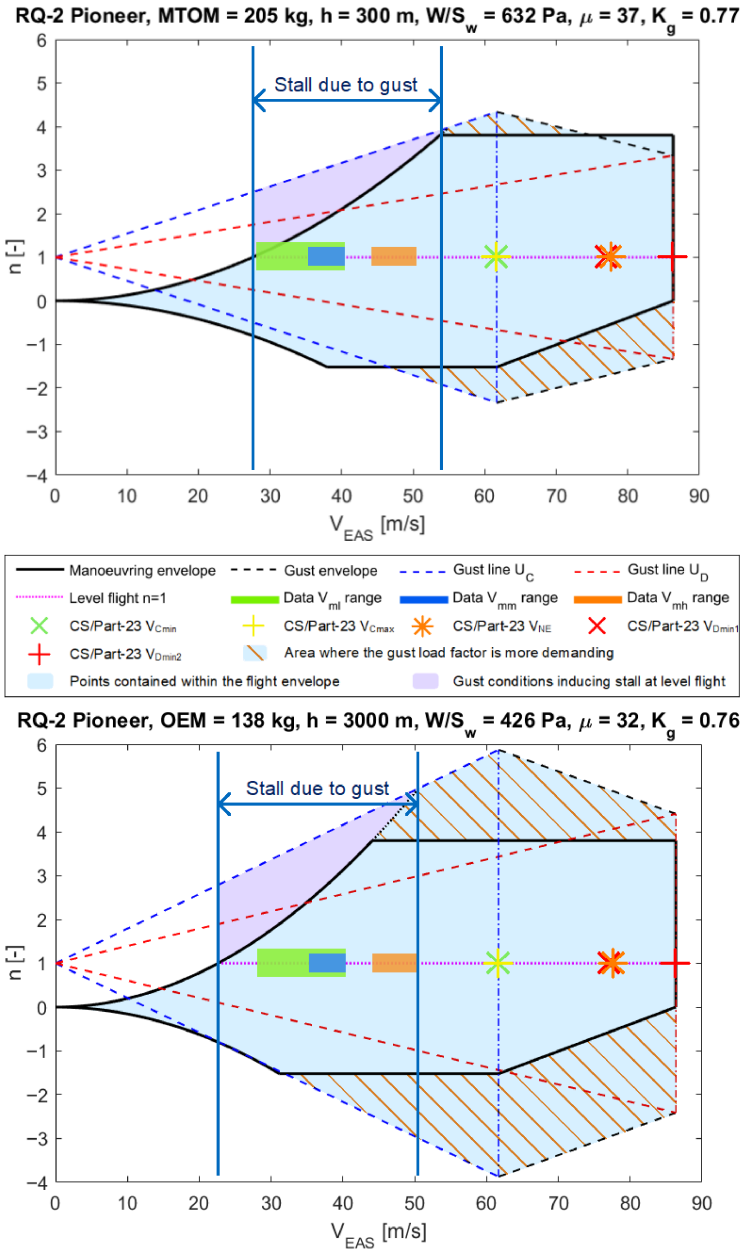


Figure 8. Flight envelopes for two flight conditions of the RQ-2 Pioneer as obtained from the application of the CS/Part-23 regulations [39,40]. V_{EAS}: equivalent airspeed, n: load factor, MTOM: Maximum Take-Off Mass, OEM: Operating Empty Mass, h: flight altitude, W/S_w: wing loading, μ: mass ratio of the aeroplane, K_g: gust alleviation factor.

The envelopes seen here show remarkable differences to those obtained through the methodology based on RPA regulations as seen in Section 3.3. Albeit this may be expected from the start due to the differences in the codes, the purpose here is to analyse and discuss the particular aspects that cause these discrepancies, as well as to discuss the potential design implications of applying the manned aviation code to RPA.

The first major difference that can be seen is that the horizontal space covered by the envelope is much wider, with the boundary of V_D being located at much higher airspeed values. The stall restriction is the same in both application cases (RPA and CS/Part-23), so the discrepancy is caused by the exceedingly high values of V_C and thus of V_D. The crucial insight to be provided here is that these certification airspeeds, which are obtained from the formulae and coefficients given in the codes, are not representative of the typical operating airspeeds of the RPA. As it can be seen, V_C is located at an airspeed value that is 50% higher than the maximum value of the typical operating airspeeds given by V_{mm} as obtained from the literature data. More significantly, V_C is 20% higher than the maximum mission speed expected during the aircraft's operation, which makes this value of the certification speed not aligned with the operating requirements of this RPA.

The main factor driving this large value of V_C is the lower boundary of V_{Cmin}. This value is obtained by applying the mathematical expressions found in CS/Part-23.335(a)(1) [39,40], which depend on the wing loading at maximum take-off weight, as discussed in Appendix A. Most likely, since the expression found in the regulations is tailored to manned aeroplanes, when applied to the typical values of W/S_w that are found in RPA, which are much lower than those of manned aeroplanes [16], it does not give representative results. V_{Cmax} coincides with V_{Cmin} since it must be higher or at least equal to the value of V_{Cmin}. V_{Cmax} is obtained by applying a factor to the maximum level speed of the aircraft, with this latter airspeed in the case of the RQ-2 Pioneer not being much higher than the typical cruising speed, giving as a result the low value of V_{Cmax}.

Therefore, owing to the high value of V_C, the resulting V_D also falls at a value of airspeed that is much higher than the expected operational speed of the aircraft. The same happens with V_{NE}, which is not representative of V_{mh}, with this latter interval being represented here to compare the resulting airspeeds with the high regime operations expected for the RQ-2 Pioneer.

Since gust load factors depend on the values of both the gust intensity, U, as well as on the airspeed, V, and owing to the fact that gust intensities with value U_C must be considered up until V_C, the values of gust load factors are also remarkably higher in both envelopes when compared to those of the case study in Section 3.3.1. Albeit the value of U_C is the same in both regulations, this intensity is maintained here up until much larger airspeeds due to the larger value of V_C. As a result, gust loading conditions take a much larger share of the boundary of the envelope, thus driving the criteria for structural design. In the case of the MTOM, positive gusts predominate over manoeuvring conditions through over half of the n_{lim+m} segment, albeit there is not a large difference between the load factors of both loading conditions. However, in the case of OEM, positive gust load factors become exacerbated due to the low wing loading, with manoeuvring loads not being the critical loading conditions at any point of the envelope, which is in contrast with the previous results. In the case of negative gusts, which already represented critical loading conditions in the case of RPA regulations, the load factors become even larger here. The observations discussed here also substantiate the reason for vertical positive gust load conditions not dominating the cases of the RQ-2 Pioneer for RPA regulations even for OEM as seen in Section 3.3.1, as the value of V_C was much lower in that case, and the gust intensity started decreasing shortly after stall in those case studies.

With respect to the prevalence of gust-induced stall, here the relative range of level flight conditions where it would occur is much lower compared to the full range of speeds covered by the envelope. However, this is an artificial result caused by the exacerbated design certification speeds, which are not representative of the real operating conditions of the aircraft. As it can be seen, the gust-induced stall interval covers practically the full range of intended operating airspeeds (indicated by the V_{ml}, V_{mm}, and V_{mh} intervals) at OEM, and it covers all of these intervals in the case of the MTOM. This is not due to any change in the gust model but is instead caused again by the position of V_C, which forces U_C intensities to be considered in a wider range of airspeeds of the envelope. Thus, in spite of gust-induced stall scenarios covering a lower percentage of the potential level flight speed conditions, the issue is much more significant when considering the practical flight conditions of the aircraft.

Therefore, if CS/Part-23 regulations were applied to the RQ-2 Pioneer, the gust load conditions would dominate the structural sizing and thus drive the design of the aircraft, which is a much different scenario than that from Section 3.3.1. Furthermore, the higher area covered by the envelope and larger load factors would result in a significantly heavier structure, hindering the design and efficiency of the RPA. However, the key consideration to be extracted from these results is that the envelope would not be representative of the operating conditions expected of this RPA due to the discrepancy between the certification and operational airspeeds.

3.4.2. MALE RPA: Predator A

The flight envelopes resulting from the application of the CS/Part-23 envelope build-up process for the Predator A are shown in Figure 9.

The differences in these envelopes with respect to those that were obtained using the RPA codes follow the same general pattern as the ones discussed in the case of the RQ-2 Pioneer. Once again, the main cause behind the different shapes of the envelopes is the value of V_{Cmin} obtained through the wing loading at the maximum take-off weight of the Predator A, which is much higher compared to that of the Pioneer. At the same time, the maximum level speed of the Predator A is not much higher when compared to the values of expected operation, causing V_{Cmax} to coincide with V_{Cmin}. This drives the values of V_C, V_{NE}, and V_D even further, resulting in an envelope covering a much higher range of airspeeds than the one seen in Section 3.3.2.

The high values of V_C result in a predominance of the gust load factors through most of the envelope in the case of the MTOM, with these load conditions dominating the complete boundary of the envelope not corresponding to stall in the case of OEM. This means that, again, the structural sizing is driven by gust load requirements. When compared to the envelopes obtained using RPA-specific codes in Section 3.3.2, for OEM, the gust conditions were also prevalent along the boundary of the envelope that was not limited by stall, whereas in the case of MTOM, both gust and stall loads took a similar share of the small part of the boundary where stall was not limiting. The largest difference in terms of load conditions here is seen in the extraordinarily high values that the gust load factors take, reaching in the case of OEM values of up to almost 7, which places extraordinary demands on the structural design requirements. Finally, and once again, the shape of the envelope results in a gust-induced stall interval that is proportionally lower to the full range of airspeeds, but it covers all the envisioned operational conditions, resulting in a more unfavourable scenario to that of the RPA-specific envelopes.

Further discussion on the implications of these results for RPA design and on the interaction between airworthiness codes and RPA sizing may be found in Section 6.

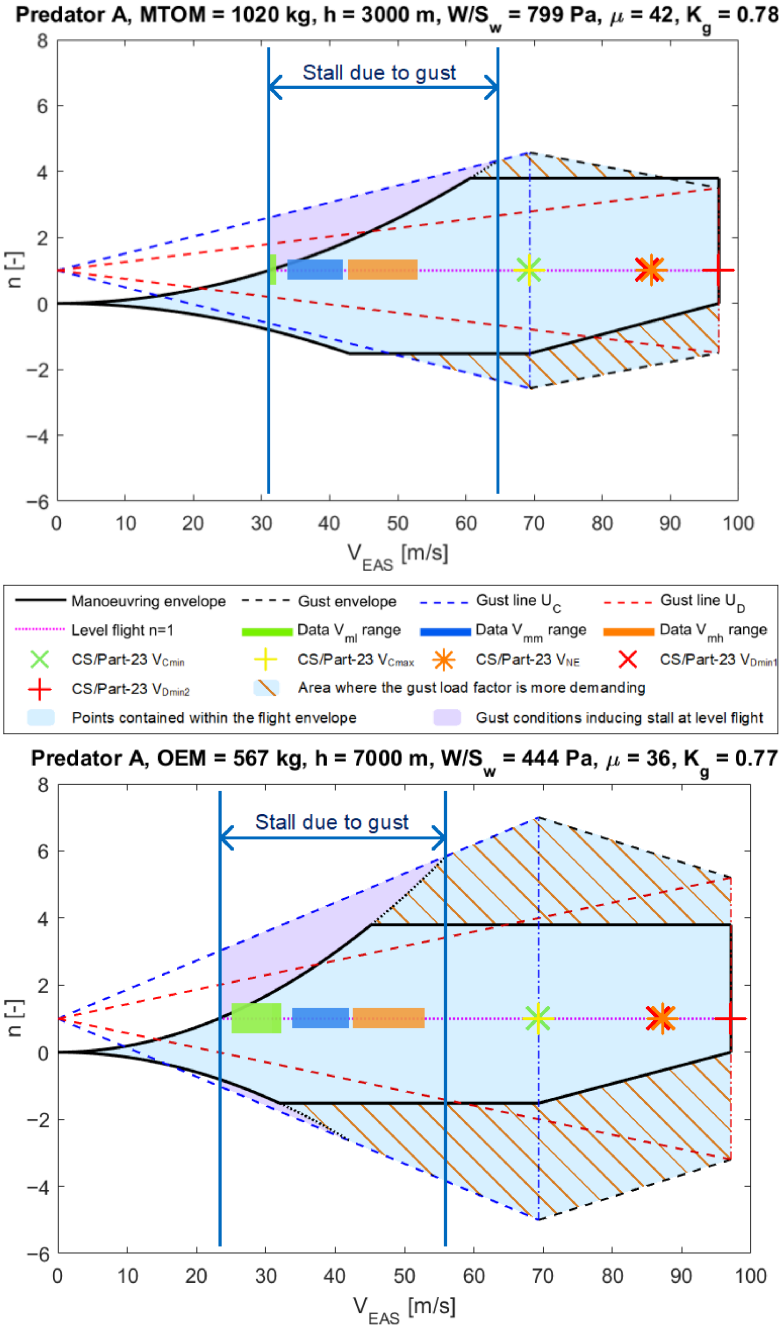


Figure 9. Flight envelopes for two flight conditions of the Predator A as obtained from the application of the CS/Part-23 regulations [39,40]. V_{EAS}: equivalent airspeed, n: load factor, MTOM: Maximum Take-Off Mass, OEM: Operating Empty Mass, h: flight altitude, W/S_w: wing loading, μ: mass ratio of the aeroplane, K_g: gust alleviation factor.

4. Methodology for Gust Load Factor Evolution Analysis Throughout the RPA Flight Profile

In spite of the insights provided by the flight envelopes of RPA, as seen in the previous section, there are certain aspects that are not as readily seen in this graphical representation, but which are nevertheless crucial in RPA operation. One of these is the evolution of the gust load factor throughout a particular mission. As commented in the introduction, RPA stand out for their marked multi-mission nature, with these air vehicles often conducting complex missions formed by various segments [17]. Each of these segments may potentially be flown with distinct cruise procedures (such as constant airspeed or constant angle of

attack) and in different flight conditions. As seen from the gust model formulation in Section 2, these are aspects that influence the gust behaviour of the RPA. Furthermore, since the gust load factor, n_g, also depends on the wing loading, the variation in mass of the RPA throughout the flight due to fuel consumption should also be taken into account. Therefore, there may be potentially relevant variations in gust behaviour throughout the flight of the RPA in different sorties that could benefit from a particular analysis conducted from a perspective based on the analysis of the mission itself. These aspects have yet to be analysed in more detail in the state-of-the-art within the context of RPA conceptual design and analysis approaches.

Considering the information presented above, this section presents a methodology for the gust behaviour of RPA within the context of RPA conceptual analysis and design that is complementary to the previous approach presented and Section 3. In this case, the procedure is focused on the study of the evolution of the gust load factor throughout the different phases of flight accounting for the effect of changing the flight conditions, cruise procedure, and RPA mass. This approach can be placed in the context of previous works within the research area on the impact of gusts in RPA operations, as identified in the introduction. Previous investigations on this topic have analysed the impact that gusts and turbulence may have on the operation of RPA [26,27], where it was seen that these atmospheric phenomena could potentially result in hazardous scenarios and noteworthy accelerations. These effects might not only affect the outcome of the operation, but also the flight safety of the aircraft. In contrast to the aforementioned works, the methodology proposed here presents the following novel contributions:

- It constitutes a rapid calculation approach that is compatible with a variety of mission profiles hat may be conducted by different RPA.
- The models used here are based on the regulatory requirements of RPA, which closes the current disconnection between operational and airworthiness aspects as discussed in the introduction. Thus, their results may also be used in airworthiness-driven design, being complementary to the approach from Section 3.
- The modelisation is compatible with multi-mission RPA and enables the identification of the most critical gust conditions based on their load factor (which is related to vertical acceleration) throughout the missions and their different segments.

The methodology proposed in this section shall be based, as in the case of the preceding envelope build-up approach, on the modelling assumptions expounded in 2.1, which are consistent with the applicable RPA regulatory requirements. According to the scope of this paper, it will also be based on approaches compatible with the needs and data availability typical of aircraft conceptual analysis and design methods. Furthermore, it will take into account both application cases discussed in Section 3, enabling its use both in new RPA design studies in their initial conceptualisation stages and also in the analysis of existing RPA, considering the information that is usually available in the open literature. However, in this case, certain additional data on the air vehicle are required for the mission modelisation. Therefore, when considering the three scenarios of data availability that were proposed in Section 3.1 and illustrated in Figure 4, the methodology proposed here is mostly intended for the use in scenario A, which requires a more detailed description of the missions with their different segments and defining parameters.

This section is organised according to the following schema. Firstly, in Section 4.1, the main equations describing the gust and stall conditions shall be formulated. These are based on the expressions expounded beforehand in Section 2, but, in this case, arranged in a different manner to adapt them to the mission-oriented approach used in this methodology. Then, Section 4.2 presents additional modelling assumptions to be added to those expounded in Section 2.1 and proposes a rapid calculation approach for performance

modelling to estimate the wing loading variation throughout the different segments of the flight. Section 4.3 then enumerates the proposed steps for the analysis of the gust load factor evolution throughout the flight of the RPA when accounting for various potential missions. This approach is then demonstrated in Section 4.4 where it is applied to the RQ-2 Pioneer, which has already been studied in the previous section.

4.1. Gust and Stall Load Factor Modelling

The main purpose of the methodology proposed in this section is to analyse the evolution of the gust load factor throughout the flight. Furthermore, considering the remarkable prevalence of gust-induced stall regions seen in the flight envelopes obtained in Section 3.3, the changes in the load factor corresponding to stall conditions, n_s, shall also be considered here. The equations expressing both of these load factors as a function of mass and flight conditions were already expounded in Section 2.1. These formulae were expressed in a way that made them more directly applicable to the representation of the flight envelope according to the airworthiness codes.

However, in the case of the methodology proposed in this section, the viewpoint shifts to one that is focused on mission and operational aspects. In particular, the equations should be expressed in a manner that makes them compatible with the different cruise procedures that shall be considered. For instance, if the RPA is flown at constant V_{TAS}, the equations should be expressed in terms of this variable, since it is the parameter used to set the flight conditions of the aircraft. In the case of flight at a constant angle of attack, the expressions may be formulated in terms of C_L to aid in their parametrisation according to the variable that is being used to determine the cruise procedure. Thereby, the original equations in terms of V_{EAS} are arranged here considering each of the two cruise procedures mentioned above to make them more directly applicable in the context of the proposed methodology.

The evolution of the gust and stall load factors in the case of the constant V_{TAS} cruise procedure may be expressed as follows. It is noted that in the gust load factor, the gust alleviation factor and aeroplane mass ratio have already been substituted according to their corresponding expressions.

$$n_g = 1 \pm \frac{0.88 U_{de} V_{TAS} \sqrt{\rho_0}}{MGC\ g \sqrt{\rho} \left(5.3 + \frac{2W/S_w}{\rho\ MGC\ a\ g}\right)} \tag{11}$$

$$n_s = \frac{\rho V_{TAS}^2 C_{Lmax}}{2W/S_w} \tag{12}$$

If these equations are expressed in terms of lift coefficient, C_L, towards their use in the constant angle of attack cruise procedure, the results are as follows:

$$n_g = 1 \pm \frac{0.88 U_{de} \sqrt{2\rho_0 W/S_w}}{MGC\ g\ \rho \sqrt{C_L} \left(5.3 + \frac{2W/S_w}{\rho\ MGC\ a\ g}\right)} \tag{13}$$

$$n_s = \frac{C_{Lmax}}{C_L} \tag{14}$$

The meaning of the different variables involved in these four equations is as discussed in Section 2. It is noted that the value of the gust intensity, U_{de}, may be selected attending to the regulatory requirements and depending on the airspeed and flight altitude, as expounded in Section 2, with the most demanding case being that of U_C.

Within the context of the methodology proposed in this section, the impact of W/S_w in the evolution of the load factors is particularly significant, since in this case it encapsulates the effect of the RPA's weight variation along the flight. Thereby, a perspective focused on operational aspects is used here instead of the design-oriented viewpoint that was prevalent throughout Section 3. The way in which the variables describing the cruise

procedure appear in the aforementioned equations, these being V_{TAS} and C_L, is also of particular relevance, since the analysis of the load factor evolution along the flight shall be parametrised according to them to represent different potential operational scenarios. The impact of the air density, ρ, in the expressions should also be observed.

It is noted that these equations have been expressed in terms of the lift force coefficient, C_L, instead of as a function of the normal force coefficient, C_N, which has been the form used in Sections 2 and 3 upon following the formulation of the regulatory requirements. In the context of the methodology proposed in this section, which is formulated from a mission-oriented perspective, the lift coefficient is much more widely used. In the initial stages of conceptual design, as long as moderate angles of attack are being considered and the aerodynamic efficiency is high, both coefficients take similar values, and they usually start departing once stall and post-stall conditions are reached.

4.2. Mission Fuel Consumption Modelling

The equations formulated in the previous subsection express the evolution of the load factors according to the change in aeroplane weight throughout the wing loading, W/S_w. However, to make the methodology compatible with a mission description considering the inputs available in scenario A, according to Section 3.1, the way in which the wing loading itself changes along the different flight segments of the RPA missions as fuel is consumed should also be modelled. RPA mission specifications are usually given in terms of the range or endurance, defining each of the segments of the mission. Therefore, expressing W/S_w in terms of these performance variables allows to more effectively cover the gap between the design requirements and mission analysis in the cases where the methodology is applied to the design of RPA, according to the research questions and gaps formulated in the introduction. The models and hypotheses presented here regarding the variation in wing loading throughout the flight complement the general modelling assumptions previously expounded in Section 2.1.

The way in which the fuel consumed by the aeroplane is related to its performance and flight parameters is usually expressed through integral performance modelisation. In the domain of conceptual design, approaches based on the analytical integration of simplified range and endurance equations are usually employed, such as those proposed in [12–14]. Similar performance models have been used by previous authors in the field of RPA conceptual design, such as in [17,19,46,54,55]. Therefore, this type of approach shall also be followed here.

The expressions used to obtain the variation in wing loading in this work are based on the integral performance expressions for range and endurance by Gudmundsson [14]. These have been obtained for both cruise procedures taken into account in this work. The assumptions employed for their derivation are the following:

- The flight altitude of the aeroplane remains constant throughout the mission segments.
- The drag coefficient of the aeroplane, C_D, may be represented in most typical flight conditions through an approximation that includes a constant and a quadratic term.
- The propeller efficiency is considered constant.
- The specific fuel consumption is considered constant.
- It is assumed that no atmospheric wind is present.

For flight at constant true airspeed, these expressions take the following forms:

$$R = \frac{\eta_p}{C_{pm} g \sqrt{C_{D0} K}} \left[\operatorname{atan}\left(\frac{m_i}{\sqrt{\frac{C_{D0}}{K}} \frac{\rho S_w V_{TAS}^2}{2g}} \right) - \operatorname{atan}\left(\frac{m_f}{\sqrt{\frac{C_{D0}}{K}} \frac{\rho S_w V_{TAS}^2}{2g}} \right) \right] \tag{15}$$

$$E = \frac{\eta_p}{V_{TAS} C_{pm} g \sqrt{C_{D0} K}} \left[\operatorname{atan}\left(\frac{m_i}{\sqrt{\frac{C_{D0}}{K}} \frac{\rho S_w V_{TAS}^2}{2g}} \right) - \operatorname{atan}\left(\frac{m_f}{\sqrt{\frac{C_{D0}}{K}} \frac{\rho S_w V_{TAS}^2}{2g}} \right) \right] \tag{16}$$

In the case of constant angle of attack cruise, the range and endurance equations be formulated in the following manner:

$$R = \frac{\eta_p \frac{C_L}{C_D}}{C_{pm}\, g} \ln \frac{m_i}{m_f} \tag{17}$$

$$E = \frac{\eta_p \sqrt{2\rho S_w}}{C_{pm} g^{3/2}} \frac{C_L^{3/2}}{C_D} \left[\frac{1}{\sqrt{m_f}} - \frac{1}{\sqrt{m_i}} \right] \tag{18}$$

where the meaning of the symbols not covered previously is as follows:

- C_D: overall drag coefficient given by the drag polar.
- C_{D0}: lift-independent coefficient of parabolic drag polar.
- C_L: selected lift coefficient.
- C_{pm}: power-specific fuel consumption expressed in terms of mass.
- K: quadratic term of parabolic drag polar.
- m_i: aircraft initial mass in the flight segment.
- m_f: aircraft final mass in the flight segment.
- η_p: propeller efficiency.

To make these expressions more directly compatible with those of the load factors derived in Section 4.1, they should be expressed in terms of the initial and final wing loading for each flight segment. Furthermore, since the definitions of the missions are expected to be given according to the requirements of scenario A, the range and endurance values for each segment are assumed to be inputs of the process included in the mission definition.

Arranging the previous integral performance equations according to the aforementioned considerations, the following formulae are obtained for the case of constant V_{TAS} cruise procedure:

$$\left(\frac{W}{S_w}\right)_f = \sqrt{\frac{C_{D0}}{K}} \frac{\rho V_{TAS}^2}{2} \tan\left[\operatorname{atan}\left(\frac{\left(\frac{W}{S_w}\right)_i}{\sqrt{\frac{C_{D0}}{K}} \frac{\rho V_{TAS}^2}{2}} \right) - \frac{R C_{pm} g \sqrt{C_{D0} K}}{\eta_p} \right] \tag{19}$$

$$\left(\frac{W}{S_w}\right)_f = \sqrt{\frac{C_{D0}}{K}} \frac{\rho V_{TAS}^2}{2} \tan\left[\operatorname{atan}\left(\frac{\left(\frac{W}{S_w}\right)_i}{\sqrt{\frac{C_{D0}}{K}} \frac{\rho V_{TAS}^2}{2}} \right) - \frac{E V_{TAS} C_{pm} g \sqrt{C_{D0} K}}{\eta_p} \right] \tag{20}$$

and in the case of the constant angle of attack cruise procedure:

$$\left(\frac{W}{S_w}\right)_f = \left(\frac{W}{S_w}\right)_i e^{-\frac{R\, C_{pm} g}{\eta_p C_L / C_D}} \tag{21}$$

$$\left(\frac{W}{S_w}\right)_f = \frac{g/S_w}{\left[\frac{1}{\sqrt{\frac{S_w}{g}\left(\frac{W}{S_w}\right)_i}} + \frac{E C_{pm} g^{3/2}}{\eta_p \frac{C_L^{3/2}}{C_D} \sqrt{2\rho S_w}} \right]^2} \tag{22}$$

where these equations have been expressed in terms of the initial wing loading (subscript i) and final wing loading (subscript f) in each flight segment, making them more directly applicable to the formulae of the preceding subsection. If the aeroplane wing loading at the start of a certain flight segment is known along with the parameters describing the mission phase, these expressions allow to obtain the wing loading at the end of the segment that is being analysed. This value can then in turn be used as the initial wing loading in the following mission segment.

It is noted that the aforementioned expressions are intended to capture the variation in fuel mass during the fuel-intensive mission segments, which are those corresponding to the main phases of the operation, covering the greatest portion of time and accounting for the majority of fuel expenditure. These are the ones that will be the main focus of the gust analysis methodology expounded here. However, the fuel consumption of other flight segments should also be considered. These flight phases, such as take-off, climb, descent, and landing, usually span a shorter duration of the mission, and in the early stages of aircraft analysis and design, they are usually modelled through typical mass quotients between the aircraft mass at their starting and final points. In the case of RPA, the typical values for these fractions may be found in [46], allowing to relate the wing loadings of the fuel-intensive phases to those at take-off and landing, completing the modelisation of the mission weight variation. In particular, the following hypotheses are employed to model fuel consumption in these mission segments:

- The fuel consumed during start-up, take-off, and climb are approximated by 5% of the RPA take-off mass, which is a conservative approach according to [46].
- The reserve fuel mass is assumed to be 7% of the RPA target landing mass, which is a value selected according to [46].
- As an initial approximation, the fuel consumed during descent and landing is considered to be negligible.

4.3. Procedure for the Analysis of Gust Load Factor Variation Throughout the RPA Missions

Once the equations used for load factor and integral performance modelling, the workflow of the procedure for the analysis of the evolution of gust behaviour throughout the mission may be proposed. The steps found below are formulated in a generic manner, with their application being demonstrated in detail in the following subsection.

1. Firstly, the information on the profiles of the missions that are analysed is compiled. This data is given in the form of the shape of the flight profile itself, its constituting segments, and the cruise procedure and parameters (altitude, range or endurance, value of the cruise procedure variable, etc.) describing each of these flight phases. Since the methodology is intended for use on multi-mission RPA, various operations may be analysed, which can also allow to study the differences in gust behaviour in each of them. This may aid in pinpointing the most critical gust condition among all RPA operating scenarios. These inputs should also include details on the RPA payload and fuel mass at the start of the operation to enable the calculation of the initial wing loading.
2. Considering the aforementioned information and the expected cruise procedures to be followed by the RPA along its different operations, Equations (11) and (13) allow to depict the curves representing the variation in n_g as a function of wing loading. These curves may be obtained for the expected range of wing loadings of the RPA, from the values corresponding to OEM conditions to those representing the MTOM scenarios, allowing to view the variation in n_g alongside the full range of expected RPA mass variations. The stall load factor curves, n_s, may also be represented in the same manner through the use of Equations (12) and (14).
3. The aforementioned n_g and n_s curves may be parametrised depending on the different values that the cruise procedure variable (V_{TAS} or C_L) may take in distinct flight segments. This enables a compact representation illustrating the way in which both mass and cruise procedure aspects influence the evolution of the load factor.
4. At this point, once the common curves for n_g and n_s have been obtained, the following process may be employed to analyse each of the envisioned RPA missions. For each of them, through the equations presented in Section 4.2, the values of wing loading at

the starting and final points of each mission segment are obtained. With these values, through the data available on each operating phase, the load factors may be obtained.

5. Once the wing loadings and load factors describing the initial and final points of each mission segment have been obtained, the evolution of the gust behaviour of the aircraft along the flight when accounting for the changes in mass and flight segment may be analysed. This includes the study of the stall load factor, which along with the one corresponding to gust, allows to study the difference between both to identify the flight phases and conditions where a gust-induced stall may occur.

4.4. Application Case: RQ-2 Pioneer

This subsection includes an application case of the methodology for analysing gust behaviour evolution of the RPA across the different segments of its missions following the steps proposed in the preceding subsection. The selected aircraft is the RQ-2 Pioneer, which was already studied in the flight envelope approach in Section 3. The use of this same aircraft allows to complement the results and insights derived from the application of the flight envelope approach with those of the methodology proposed here.

The data on the general characteristics of the RQ-2 Pioneer has been gathered from the references that were previously cited in Section 3.3 [52,58]. This information has been complemented with details on certain potential missions conducted by this aircraft from [59] and with the drag polar data of reference [58]. Typical values of parameters such as mass ratios and expected propeller efficiency have been obtained from references such as [17,46].

The RQ-2 Pioneer has been designed to perform mainly short- and medium-range intelligence and surveillance operations. The missions defined for the application case conducted here are proposed on the basis of the data from the aforementioned references as well as from the mission profiles proposed in [53,63]. The authors of the first referenced work performed the study of a surveillance mission for typical short- and medium-range RPA, whereas the second document contained various military mission profiles. Using these data sources, two representative missions that may be conducted by the RQ-2 Pioneer have been defined. Their flight profiles are depicted in Figure 10, which is complemented by Table 7, containing their main characteristics.

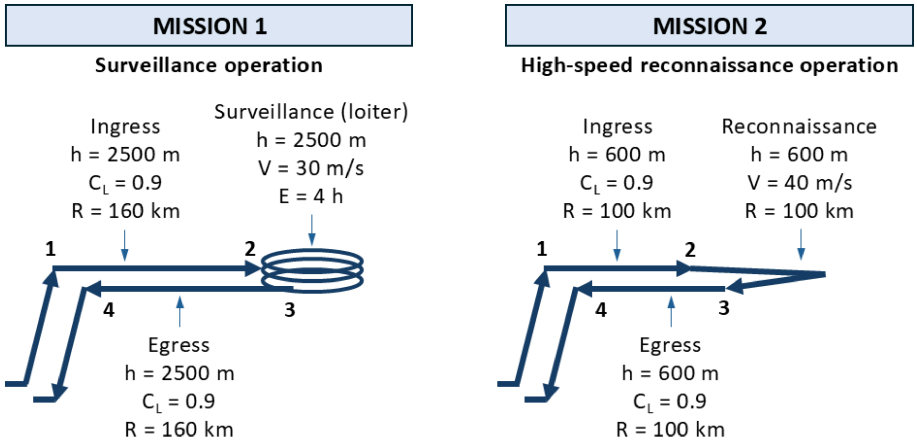


Figure 10. Missions to be studied in the application case. Their characteristics are compatible with the RQ-2 Pioneer and have been mainly derived from [53,59,63]. The lines represent the different mission segments, with the arrows indicating their progression. Each fuel-intensive segment is labelled in the figure attending to its purpose within the whole mission. The numbers represent the points of transition between mission segments. h: flight altitude, C_L: lift coefficient, R: range, V: true airspeed, E: endurance.

Table 7. Parameters describing the two missions to be studied in the application case, with characteristics mainly derived from [52,53,59,63].

Data Item	Mission 1	Mission 2
Payload (PL)	10 kg	30 kg
Trip fuel (TF)	25 kg	20 kg
Altitude	2500 m	600 m
Range of segments 1–2 and 3–4	160 km	100 km
Endurance/range of segment 2–3	4 h	100 km
Cruise procedure of segments 1–2 and 3–4	Constant C_L	Constant C_L
Cruise procedure of segment 2–3	Constant V_{TAS}	Constant V_{TAS}

Once the aforementioned details on the missions to be flown are available, the main steps of the procedure described in Section 4.3 may be followed. It is noted that the variations in wing loading during each mission are obtained through Equations (19)–(22) depending on the cruise procedure that is flown and whether the values of range or endurance are available. With respect to the variations in wing loading across missions, they are obtained through the data from Table 7. Considering that the OEM of the RQ-2 Pioneer takes a value of 138 kg, the initial mass values are obtained by adding those of PL, TF, and RF for each of the missions. The latter of these values is obtained through the approximation commented in Section 4.2.

Before obtaining the particular evolution of the wing loading for each of the missions, the overall $n_g = f(W/S_w)$ and $n_s = f(W/S_w)$ can be obtained for both cruise procedures through a parametrisation of the curves according to the variables corresponding to the constant V and constant C_L flight conditions. It is noted that the most demanding gust conditions, which are those corresponding to gust intensity U_C, have been selected for this analysis. The curves are represented in Figure 11, where they have been depicted covering the full range of wing loading values that may be expected in this RPA.

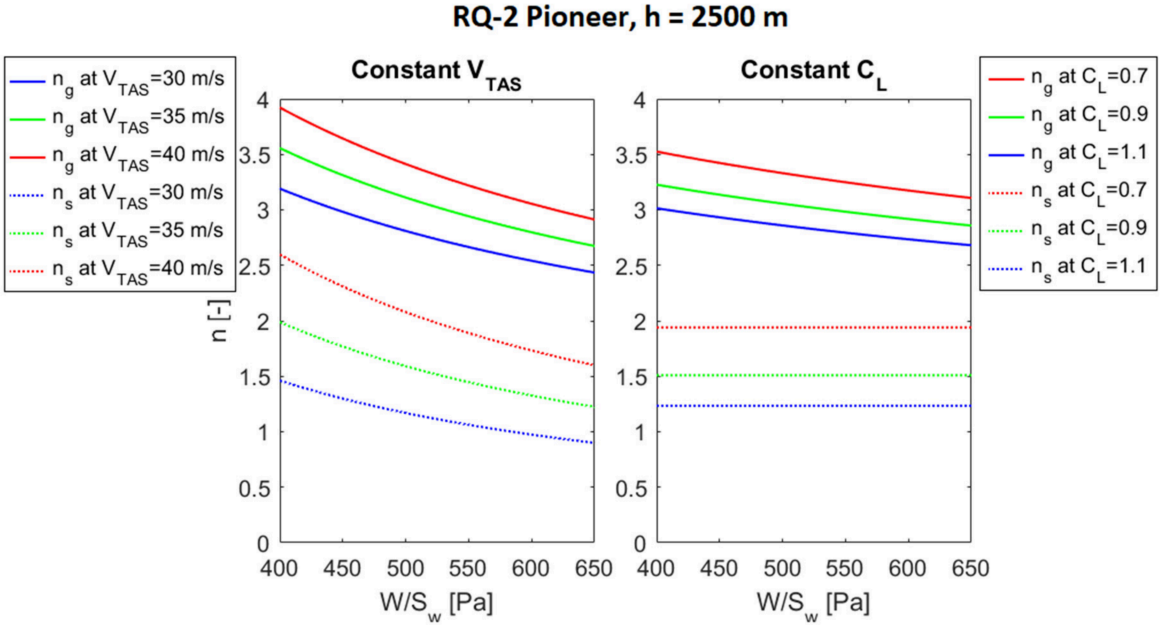


Figure 11. Evolution of RQ-2 Pioneer gust and stall load factors for an altitude of h = 2500 m. The curves are expressed as a function of wing loading for both cruise procedures. The gust load factors are represented in continuous curves and the stall load factors as dotted curves.

These curves contain much information describing the gust and stall behaviour of the studied RPA. It can be seen through the analysis of both cruise procedures that the value of

n_g increases as W/S_w becomes lower. This means that, as the aircraft becomes lighter due to fuel consumption, it becomes more susceptible to gusts, making the later segments of the operation the ones where the most demanding gust conditions in terms of acceleration may potentially appear. This does not only have an influence on the RPA loads, but also on its controllability, since the load factor is related to the acceleration of the aeroplane. This insight might point towards directing more attention to the later segments of flight in gust behaviour assessment, as it is possible that the most critical gust load factors shall occur there. Furthermore, it is also seen that the change in n_g per unit variation in wing loading becomes larger at lower values of W/S_w, since the slope of the curves increases as the wing loading is reduced. It is noted that, albeit significant variations in gust load factors may be seen when accounting for the full potential range of W/S_w values that the RQ-2 Pioneer may take, each sortie has its own W/S_w interval depending on the proportion between payload and fuel mass, which is a matter that will be studied further alongside this application case. Therefore, the effect of wing loading on gust load factor shall depend on the variations in the wing loading itself throughout the mission that is being considered.

Aside from the changes in n_g caused by the variations in wing loading, there are two additional aspects that also have a noteworthy effect in gust behaviour, with these being the selected cruise procedure and the set of values that the variable corresponding to the specific cruise procedure takes. In the case corresponding to constant V_{TAS}, the gust load factor increases as the airspeed becomes greater, which is expected in view of the equations derived in Section 4.1 and also from the gust envelope analysis conducted in Section 3. This means that the RPA becomes more susceptible to gusts when flying at faster airspeeds, which is an effect that is also accounted for in the airworthiness codes as discussed beforehand. This insight is also applicable to the constant C_L case, since larger values of C_L correspond to lower airspeeds attending to the vertical equilibrium equation. Due to the different ways in which either V and C_L appear in Equations (11) and (13), it can be seen through the space found between the parametric curves that the effect of V_{TAS} in gust load factor is linear, whereas in the case of constant lift coefficient cruise, the impact on n_g of reducing C_L is not uniform per unit change in the lift coefficient, but rather the change in n_g becomes more noticeable at lower values of C_L.

The stall load factor curves and their position at lower values of n when compared to the gust curves provide an insight that was already seen within the previous approach based on the flight envelope analysis. This insight corresponds to the prevalence of potential gust-induced stall scenarios across the different operational conditions. For all of studied values of wing loading and cruise procedures, the U_C gust intensity is expected to induce the stall of the aircraft, which is a noteworthy conclusion from both operational and safety viewpoints. If the aircraft encounters turbulent structures with lower gust intensity, this condition may not occur, since according to Equations (11) and (13), the value of n_g is lower if U_{de} decreases, thus for lower U_{de} values, n_g may fall below n_s, signifying the absence of gust-induced stall. The high prevalence of potential gust-induced stall issues under low and medium speed conditions for this RPA coincides with the conclusions extracted from the analysis conducted in Section 3.3.1.

Once the overall aspects of the evolution of gust and stall load factors have been analysed, each of the missions considered in this application case may be studied in more detail. Firstly, the surveillance operation will be analysed. Through the use of the mission fuel consumption models expounded in Section 4.2, considering the data corresponding to the payload, trip fuel, and segments of the mission, the evolution of W/S_w throughout the three fuel-intensive segments of the operation along with the specific variations in n_g seen along this mission may be obtained. The results of this analysis are illustrated in Figure 12, with the specific numerical values being listed in Table 8.

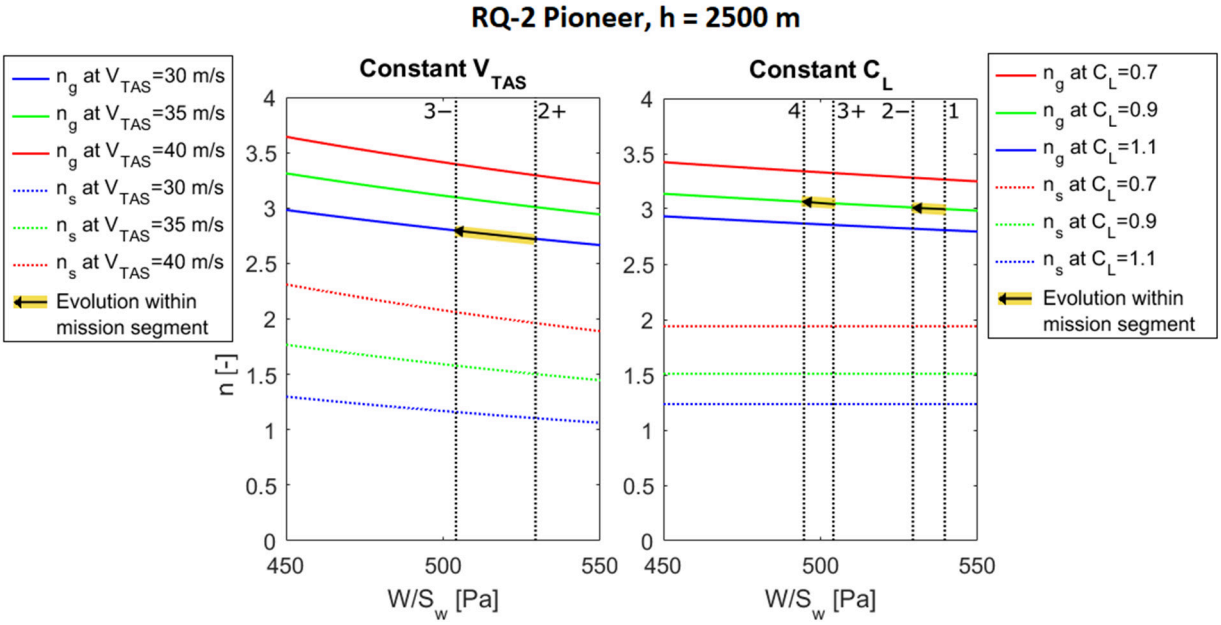


Figure 12. Evolution of RQ-2 Pioneer gust and stall load factors along the three fuel-intensive segments of mission 1. The vertical lines correspond to the values of the wing loading at each of the numbered points of the mission profile according to Figure 10, with the numbers appearing along each vertical line identifying each of the aforementioned points of the mission profile. The highlighted parts of the curves and the arrows indicate the regions corresponding to each of the mission segments and the way in which n_g varies.

Table 8. Values of the wing loading and gust load factor evolution throughout mission 1.

Mission Point	W/S_w [Pa]	n_g
1 (start of ingress)	539.5	2.998
2− (end of ingress)	529.4	3.012
2+ (start of surveillance)	529.4	2.722
3− (end of surveillance)	504.1	2.798
3+ (start of egress)	504.1	3.05
4 (end of egress)	494.7	3.064

The curves represented in Figure 12 share the same shape as those in Figure 11, since both cases have been calculated for the same flight altitude. However, here, the range of values on the x-axis is lower, since the focus is on a specific W/S_w interval corresponding to this sortie. The change in wing loading along the flight is relatively low when compared to aeroplanes intended for missions with a longer duration, since the RQ-2 Pioneer was designed for short and medium range operations. Therefore, the variations in gust load factor along each of the mission segments are low and fall in all cases below 3%. However, when moving from one segment to another, the changes in wing loading are more noticeable. In this case, lower load factors are seen in the surveillance phase, which is conducted at a very low airspeed when compared to those of the ingress and egress segments.

The values in Table 8 show that the highest gust load factor occurs at the final point of the egress segment, with a value of 3.064. The fact that the largest value of n_g happens here is consistent with the observations regarding the variation in gust load factor with W/S_w discussed beforehand. This value of n_g falls somewhat below the highest load factors seen in the second of the gust envelopes in Figure 6 in the analysis in Section 3. Two factors contribute to this result. The first is that the analysis conducted here is more representative of an actual RPA operation, with the RPA still having certain remaining fuel mass for

reserves and allowances after the end of the egress segment. Thus, the value of W/S_w at this point is noticeably higher than that corresponding to OEM. This latter value was used in the envelopes since the purpose there was to showcase the most contrasting shapes that they could take for a specific RPA. The second factor is related to the difference in the flight conditions assumed here when compared to those of the envelope at V_C, resulting in a lower gust susceptibility in this case.

Moving on to the second mission, this operation is conducted at a different altitude when compared to the previous one, thus modifying the shape of the load factor curves. The results of this case are illustrated in Figure 13, with the numerical values being listed in Table 9.

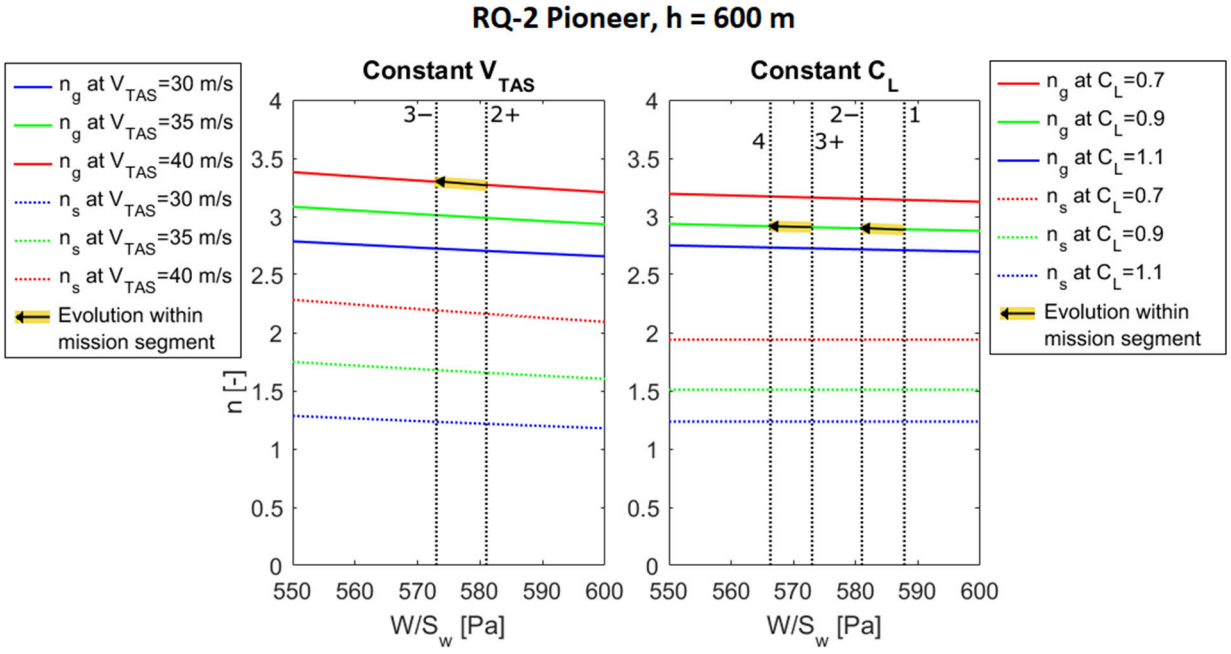


Figure 13. Evolution of RQ-2 Pioneer gust and stall load factors along the three fuel-intensive segments of mission 2. The vertical lines correspond to the values of the wing loading at each of the numbered points of the mission profile according to Figure 10, with the numbers appearing along each vertical line identifying each of the aforementioned points of the mission profile. The highlighted parts of the curves and the arrows indicate the regions corresponding to each of the mission segments and the way in which n_g varies.

Table 9. Values of the wing loading and gust load factor evolution throughout mission 2.

Mission Point	W/S_w [Pa]	n_g
1 (start of ingress)	587.8	2.889
2− (end of ingress)	581.0	2.898
2+ (start of reconnaissance)	581.0	3.271
3− (end of reconnaissance)	573.0	3.299
3+ (start of egress)	573.0	2.907
4 (end of egress)	566.3	2.915

In this case, since the fuel weight in the sortie is lower, the range of applicable W/S_w values is also narrower. This results in a lower effect of wing loading on the load factors, with the predominant effect being, in this case, the change in cruise procedure. Another factor contributing to the lower impact of wing loading is that the values of W/S_w corresponding to this case are located at the upper end of the overall range of potential wing loading values due to the larger payload being carried, with the curves having less slope in

the range of higher wing loadings. All these aspects, combined with the lower distance covered in the different mission segments in this operation when compared to the previous one, result in lower changes in n_g throughout each of the segments.

The greatest change in gust load factor comes from the variation in cruise procedure. In this case, the reconnaissance segment has higher values of n_g when compared to the ingress and egress phases. This is due to the high airspeed at which the former part of the mission is carried out, resulting in higher load factors that are in contrast with the lower load factors seen in the surveillance segment within the previous mission. As a consequence of the characteristics of the reconnaissance phase, in this case, this is the one in which the highest value of n_g is found, with a value of 3.299. This happens in spite of the slightly higher wing loading at this point when compared to the one at the end of the egress segment. Therefore, it is seen that the scenario of the highest gust susceptibility occurring at the end of the last segment when W/S_w is lower does not happen here. This highlights the relevance of considering the characteristics of each mission segment, and not only the variation in wing loading, since the variations in cruise procedure may result in the most demanding gust condition occurring at a point along the flight other than that corresponding to the end of the last mission segment.

With respect to the highest value of n_g seen throughout this mission, it falls below the highest load factors seen in the envelope corresponding to this aircraft in Section 3.3.2. Once again, the difference in wing loading when comparing the case study conducted here with that of the envelopes has an effect in this variation, since the RPA carries, in this case, reserve fuel that was not present in the previous analysis. However, in this mission, the airspeed of the reconnaissance segment is closer to the value of V_C seen in the envelope, which supports the fact that the maximum value of n_g is higher, in this case, compared to the surveillance operation studied above.

When considering the results of both types of sorties as part of the multi-mission analysis of this RPA, the conclusion is that the reconnaissance mission is more demanding from the perspective of gust behaviour when compared to the surveillance operation. One of the main benefits of the methodology proposed here is that it not only allows to determine the mission in which the most critical gust conditions occur but also the specific point along the flight profile where this happens. This constitutes a valuable feature particularly in the field of RPA in which complex multi-segment missions are more frequent than in the domain of conventional manned aircraft [17]. As seen in the case of the second mission, the cruise procedure may have a significant effect on where these the most demanding gust conditions happen, which substantiates the need to model the gust behaviour considering various potential ways in which the aircraft may be flown.

Overall, this case study demonstrates the insights that the methodology proposed in this section may reveal through an analysis of the gust behaviour of RPA along multi-segment mission profiles. This approach complements the previous one based on the flight envelope, since the present method is oriented towards the analysis of the mission itself, providing a higher level of detail on the evolution of the gust load factors through different mission segments described by potentially disparate flight conditions. In contrast, the procedure based on the flight envelope seeks to summarise within this type of graphical representation the gust and manoeuvring conditions with which the aircraft must comply according to the airworthiness codes, thereby being focused to a greater extent on the interaction between the regulatory requirements and the overall characteristics of the RPA.

It is noted that this case study has analysed two potential missions of a tactical RPA. However, different results may be obtained for distinct air vehicles to the one studied here, particularly if very different missions are flown. Further comments on the potential variations that may be expected are provided in Section 6.

5. Evaluation of Design Parameter Impact on Gust Behaviour

The two approaches proposed in the previous sections have provided insights into the gust behaviour of RPA through approaches based on flight envelope and mission modelling. However, the previous methodologies have mostly focused on the way in which changes in operational variables affect the gust and stall load factors, leaving some research questions formulated in the introduction, which are related to design considerations, yet unanswered.

Considering the information presented above, this section seeks to analyse how design parameters might impact the behaviour of the RPA when encountering gusts. In the conceptual design stage, the main variables taken into account are those referring to the overall aircraft size and mass. Some of these have a direct influence on the gust model used in this study as seen in the mathematical formulation expounded in Section 2.1. Despite the low number of variables involved, the study of their impact on gust behaviour provides additional insight into the linkage between aircraft design and gust physics and it also provides information that can guide designers through the modification of these design parameters to improve gust behaviour, allowing designers to mitigate potential undesirable effects such as high gust load factors, n_g, or gust-induced stall in this early stage of development.

As discussed in the introduction, current studies on RPA gust analysis have not considered the effect of overall aircraft design variables on their gust behaviour, and approaches towards modifying these variables within the context of the early design stages towards mitigating undesirable gust effects are not currently found in the open literature. The analysis conducted here seeks to fill this gap.

It has been seen through this investigation that high gust load factors and gust-induced stall constitute two undesirable effects that have an impact on RPA design and on their operational safety. Therefore, the absolute value of n_g as well as the difference between the stall and gust load factors, $n_s - n_g$, shall be used to quantify the magnitude of the aforementioned effects that the designer might seek to mitigate. The design variables that may be modified within the scope of the model according to Equations (2)–(5) are the wing loading W/S_w, the mean geometric chord, MGC, the aeroplane's normal force coefficient curve slope, a, and the maximum normal force coefficient, C_{Nmax}.

Firstly, a sensitivity analysis is conducted to study the variations that may appear in the aforementioned gust effects when modifying each of the four design parameters considered in this approach. This analysis is conducted using the RQ-2 Pioneer RPA, which has been studied through the previous two approaches, as a baseline. The four design parameters are modified in the range of positive and negative variations of 10% with respect to their baseline values.

A hypothesis used in this analysis is that the potential interactions appearing between each of these design parameters upon varying the others are neglected. These potential linkages might depend on various constraints depending on the design criteria used for each particular RPA and they might be quantified in different ways depending on the models used. Despite this, the aforementioned approximation may be considered acceptable for the purpose of this preliminary analysis within the scope of conceptual design, particularly when considering only small variations in each of the parameters. In any case, calculations considering combined changes in various design parameters among the ones considered above shall be presented later on in this section.

Figure 14 presents the results from the aforementioned sensitivity analysis for the V_C airspeed of the aircraft upon encountering a gust of intensity, U_C. The starting conditions have been selected to be those of minimum wing loading as seen in the second of the envelopes presented in Figure 6 found in Section 3.3.2.

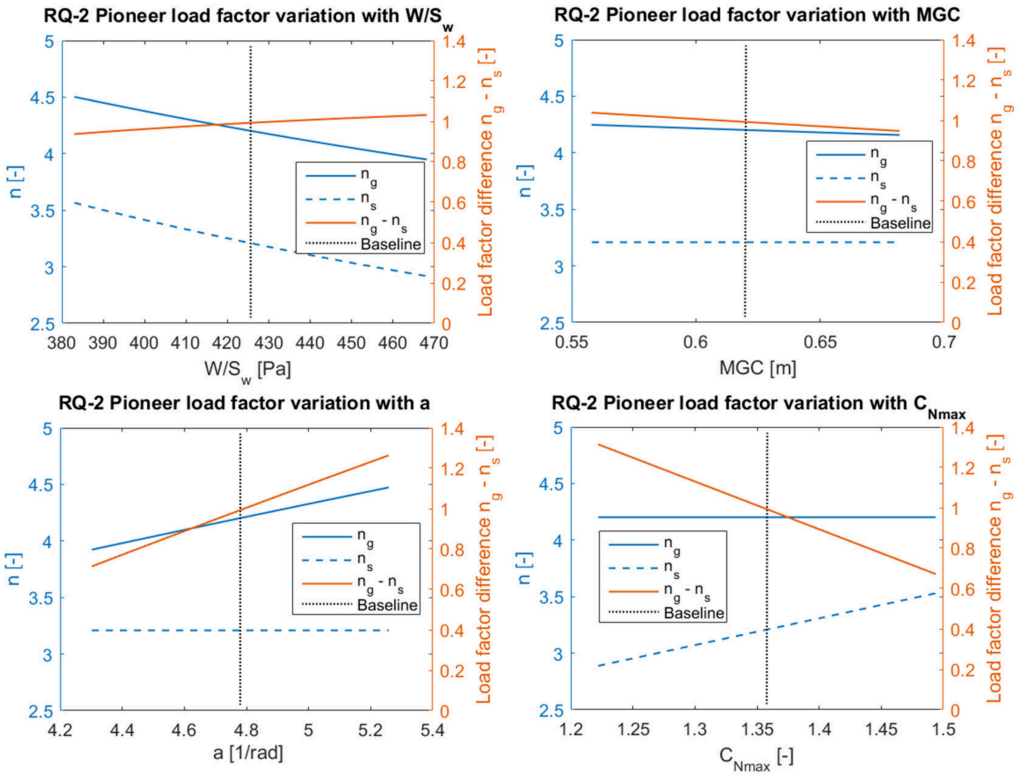


Figure 14. The results of the sensitivity analysis studying the influence of the four conceptual design parameters involved in the gust model from the regulations on the two gust effects considered in this section. n: load factor, n_g: gust load factor, n_s: stall load factor, W/S_w: wing loading, MGC: Mean Geometric Chord, a: slope of the aeroplane's normal force coefficient curve per radian, C_{Nmax}: maximum normal force coefficient.

The effect of each of the four variables along with its linkage with gust physics within the scope of the model use in this research are discussed below:

- W/S_w: As seen in Section 2, increasing the wing loading has a detrimental effect on stall but a beneficial effect on gust behaviour. The first effect is due to the wing area being reduced with respect to the aeroplane weight, which requires higher normal force coefficients to generate the lift required in the vertical equilibrium of forces. Thus, for the same value of lift, the C_{Nmax} is reached earlier, which is reflected on the reduction in load factor until stall, n_s. With respect to gust, the beneficial effect on the reduction in load factor, n_g, is due to the reduced lift increment as the aircraft encounters the gust, since S_w is reduced with respect to the aircraft's inertia. In view of the graphs, reducing W/S_w mitigates gust-induced effects since the difference between both load factors is reduced since n_s increases more rapidly, but this comes at the cost of higher values of n_g, which give higher loads and thus higher structural design as a result when designing the aeroplane to meet the envelope requirements.
- MGC: An increase in mean geometric chord decreases the gust load factor with no appreciable effect in stall, which is beneficial regarding both undesirable gust-related effects. This effect is caused due to the influence of MGC in the μ parameter as seen in Section 2.1. The physical meaning of this parameter is related to the quotient between the aeroplane mass and the mass of a volume of atmospheric air adjacent to the wing, which is influenced by the gust [1,2]. Thus, increasing MGC augments the volume of air relative to the aircraft inertia, reducing μ and thus K_g, giving the decrease in n_g as result. However, the impact of this variable on the aeroplane gust behaviour is comparatively small.

- a: The normal force curve slope is related to the increase in aeroplane normal force per unit change in angle of attack. The gust load factor is increased upon augmenting a since the lift increment for the same change in angle of attack due to the gust is magnified if a is greater. However, decreasing a to improve gust performance would be detrimental for many other aeroplane performance characteristics.
- C_{Nmax}: This variable does not directly influence gust load factor, but upon increasing it, the margin of the aeroplane with respect to stall becomes greater, having a beneficial effect since gust-induced stall becomes mitigated. This variable is mainly related to the characteristics of the aerofoil and wing at high angles of attack, which may be modified to allow the aircraft to reach higher angles of attack before stall occurs.

Within the scope of the small variations in these parameters considered within the sensitivity analysis, it is not possible to fully mitigate gust-induced stall at this airspeed. Therefore, a combined approach by modifying various parameters at the same time might yield increased benefits. Furthermore, this can allow to mitigate some of the detrimental effects of changing certain variables through others. For example, the increase in n_g due to the reduction in W/S_w can be slightly compensated by making MGC larger.

In the following analysis where combined modifications in design parameters are considered, variations in the normal force curve slope shall not be taken into account, since reducing this value to improve gust behaviour would be detrimental to many other aircraft aerodynamic and performance aspects. Combined modifications in the other three variables shall be considered. These shall be changed from their original values to relative variations of 5% and 10%, with the results being presented in Table 10.

Table 10. Impact of design parameter changes on gust load factor and gust-induced stall for the case study considered in the current section. The lowest achievable value of n_g has been highlighted in bold text, as well as the lowest achievable gust-induced stall margin.

C_{Nmax} [-]	MGC [m]	W/S_w [Pa]		
		383	**404**	**426 (Baseline)**
1.358 (baseline)	0.62 (baseline)	n_g = 4.50 n_s = 3.57 n_g-n_s = 0.94	n_g = 4.35 n_s = 3.38 n_g-n_s = 0.97	n_g = 4.20 n_s = 3.21 n_g-n_s = 0.99
	0.65	n_g = 4.48 n_s = 3.57 n_g-n_s = 0.91	n_g = 4.32 n_s = 3.38 n_g-n_s = 0.94	n_g = 4.18 n_s = 3.21 n_g-n_s = 0.97
	0.68	n_g = 4.45 n_s = 3.57 n_g-n_s = 0.88	n_g = 4.30 n_s = 3.38 n_g-n_s = 0.92	**n_g = 4.16** n_s = 3.21 n_g-n_s = 0.95
1.426	0.62	n_g = 4.50 n_s = 3.74 n_g-n_s = 0.76	n_g = 4.35 n_s = 3.55 n_g-n_s = 0.80	n_g = 4.20 n_s = 3.37 n_g-n_s = 0.83
	0.65	n_g = 4.48 n_s = 3.74 n_g-n_s = 0.73	n_g = 4.32 n_s = 3.55 n_g-n_s = 0.77	n_g = 4.18 n_s = 3.37 n_g-n_s = 0.81
	0.68	n_g = 4.45 n_s = 3.74 n_g-n_s = 0.71	n_g = 4.30 n_s =3.55 n_g-n_s = 0.75	**n_g = 4.16** n_s = 3.37 n_g-n_s = 0.79

Table 10. *Cont.*

C_{Nmax} [-]	MGC [m]	W/S_w [Pa]		
		383	**404**	**426 (Baseline)**
1.494	0.62	n_g = 4.50 n_s = 3.92 n_g-n_s = 0.58	n_g = 4.35 n_s = 3.72 n_g-n_s = 0.63	n_g = 4.20 n_s = 3.53 n_g-n_s = 0.67
	0.65	n_g = 4.48 n_s = 3.92 n_g-n_s = 0.55	n_g = 4.32 n_s = 3.72 n_g-n_s = 0.61	n_g = 4.18 n_s = 3.53 n_g-n_s = 0.65
	0.68	n_g = 4.45 n_s = 3.92 **n_g-n_s = 0.53**	n_g = 4.30 n_s = 3.72 n_g-n_s = 0.58	**n_g = 4.16** n_s = 3.53 n_g-n_s = 0.63

The main insights obtained from the analysis of these results are presented below:

- The design modifications that achieve the higher improvements in n_g do not coincide with those that result in the lowest gust-induced stall margin. This is mainly due to the contrasting effect of W/S_w on gust and stall.
- The reductions in n_g achieved through the modification of the design parameters considered above is low, since they are mainly driven by MGC, which has a low impact per unit change in n_g. Therefore, there is limited capability of improving gust-related structural sizing implications through modifications in these variables.
- In contrast, reductions of up to approximately 50% in the gust-induced stall margin may be achieved, with these being mainly driven by the change in C_{Nmax}, which in combination with W/S_w allows a further mitigation of this issue at the cost of increasing n_g. Thus, these three design parameters provide an effective way of reducing the gust-induced stall margin.

As seen above, through design changes in the variables involved in this simplified gust model which may be used in the early design changes, the issue of gust-induced stall may be mitigated. In contrast, the reduction in n_g that may be achieved is low, making the modification of these design parameters a comparatively ineffective way of reducing gust loads and thus decreasing structural weight when encountering these phenomena. However, as seen in the envelopes represented in Figure 6 in the case of the RQ-2 Pioneer, the main issue at V_C and minimum wing loading is gust-induced stall, since only downward gusts dominate the structural design, and even then only by a relatively small margin with respect to manoeuvring load conditions. Thus, the benefits that may be achieved in structural design are not as significant here, and mitigating gust-induced stall constitutes a more relevant issue.

In spite of the information presented above, it is noted that the issue of gust-induced stall is still present since the difference between both load factors has not reached zero. Therefore, additional means may be required in combination to the design changes commented here to further decrease the gust-induced stall margin. Some additional discussion on this subject along with other observations on the feasibility of the aforementioned design changes are discussed in Section 6. Finally, it is noted that the calculations performed here have been made for the particular case of the RQ-2 Pioneer, and this same analysis is expected to yield different results for differing RPA, albeit with the same overall trends as long as the same model is used. Thus, the purpose here has mainly been to propose this approach and demonstrate it through an application case, and each RPA design should be individually studied considering its particular challenges as reflected by its flight envelopes.

6. Discussion

The analysis of the results obtained from the application of the methodologies proposed in this paper provides several insights into the particularities of RPA gust behaviour. This section contains further discussion on the results and initial analysis presented in the previous sections, with a particular focus on the main challenges faced by these air vehicles when bearing gusts, the singularities that they present in this regard with respect to manned aircraft, and the implications on RPA design derived from the analyses and findings presented beforehand.

With respect to the results of the methodology based on the analysis of the flight envelope, one of the main particularities of the envelopes obtained for both RPA when compared to those of conventional manned aircraft is that they are noticeably more compact in the horizontal axis (V_{EAS}) dimension, corresponding to a lower interval of feasible flight speeds for RPA. This is consistent with the fact that many RPA missions, such as those of the air vehicles used in this work, are conducted at low speeds. This is, for instance, the case of ISR tasks, which are very common in the realm of RPA [16,17], as low flight speeds typically result in flight conditions of higher endurance [49] and also enhance the data capture quality of many ISR sensors [22]. These advantages substantiate the interest of flying at low speeds during these kinds of operations, even if these are often close to stall. The choice of lower values for cruise and maximum level speed avoids oversizing the powerplant and results in lower values of V_D. The above-mentioned considerations lead to a lower interval of possible level flight speeds. This also results in a large portion of the manoeuvring envelope being limited in terms of load factor by stall instead of reaching the prescribed values of n_{lim}, which, depending on the flight conditions, may not even be achievable for any value of V_{EAS}, as seen for example in Figure 7, where the high wing loading at the MTOM results in very restrictive stall conditions.

As a consequence of the information presented above, the gusts prescribed by the regulation, particularly those of intensity U_C, could potentially cause the stall of the vehicle in a large portion of the feasible level flight speed interval, since the gust lines fall above the stall parabola in most of the envelopes, as seen in the case studies. Only at large values of V_{EAS} do the gust lines fall below stall or n_{lim}, but the V_{EAS} values where this happens in the case studies are significantly higher than those corresponding to typical RPA mission speeds as given by V_{mm}. This is in contrast to conventional manned aircraft, where the proportion of the gust-induced stall interval is much lower with respect to the whole range of feasible flight speeds, as seen in the CS/Part-23 envelopes illustrated in Appendix A [14].

There are various factors that lead to the aforementioned crucial difference between the envelopes of both aircraft. The first reason for this includes the higher values of typical mission speed and maximum level airspeed that are usually characteristic of manned aeroplanes. Even if the values of W/S_w of these latter aircraft are typically higher, resulting in higher stall speeds, the effect of the increase in the rightmost limit of the envelope overpowers the higher values of stall airspeed in most cases. This produces an envelope for manned aircraft that covers a larger range of level flight speeds. As an added consequence of this, the n_{lim} manoeuvring limitation becomes more predominant for these aircraft when compared to RPA, since the envelope covers a higher range of values of V_{EAS}, allowing the stall parabola to reach the value of n_{lim} at values of airspeed significantly below the rightmost horizontal limit of the envelope. Furthermore, the higher wing loading of these aircraft reduces the slope of the gust lines attending to Equation (2), which mitigates the gust load factors and facilitates that they fall below the stall boundary, which would prevent the gust-induced stall. This undesirable effect covers a much lower percentage of the range of potential level flight speeds in these aircraft when compared to RPA.

However, aside from comparing the percentage of feasible level flight airspeeds in which gust-induced stall may occur between both aircraft types, the criticality of this undesirable gust effect needs to be weighted with respect to the location that the gust-induced stall interval takes when compared to the typical operating airspeed range of the aircraft. Here, an additional challenge related to the susceptibility of RPA to gust-induced stall appears, which is the fact that the region of the flight envelope in which this issue is expected to happen falls within the typical airspeed values at which these aircraft usually fly, represented by the V_{ml} and V_{mm} intervals in the envelopes seen in Figures 6 and 7 in Section 3.3.1. This represents a significant drawback for RPA, since their exposure to this risk happens precisely in the most usual flight conditions for these aircraft, which exacerbates the impact of this issue. Only at higher airspeeds, usually at the medium to high end of the V_{mh} interval, do the gust load factors fall below the stall boundary. However, this airspeed interval does not represent the typical operating conditions for the RPA that have been studied here, since it is reserved for particular operational conditions where a flight regime close to maximum level speed is required. Flying at these higher airspeeds only to mitigate gust effects does not appear to be a feasible solution in the usual operations of RPA, as it is expected that this would greatly reduce the performance of the aircraft, such as its flight endurance. Furthermore, these high-airspeed flight conditions may not even be compatible with the correct operation of the sensors of the RPA in the case of some operations, potentially hindering their capability to conduct the mission. Despite the fact that gust-induced stall events have a negative effect in RPA operations is an intuitive premise, the main findings and contributions of the research presented here with respect to this topic are the quantification of the proportion of level flight speeds of RPA where this issue is present, the identification of the design and operational conditions that explain the predominance of gust-induced stall conditions, and the discussion on the particularities of RPA operations which exacerbate the impact of this issue as commented above.

An additional insight with respect to the topic of gust-induced stall may be observed upon comparing the envelopes of RPA with those of CS/Part-23 manned aeroplanes as seen in Appendix A. Since low-speed operations are not as widespread in manned aeroplanes as in RPA, the typical values at which manned aircraft fly shall be expected to happen at the medium to higher end of the envelope [14], which is in contrast to RPA operating closer to stall. As seen in the flight envelopes of RPA in Section 3.3, the gust-induced stall region is mainly located close to the stall boundary. Thereby, since the usual operating conditions of most manned aircraft are located at higher airspeed values, as deduced by the values of V_C seen in the illustrative envelopes of Figure A1, they are also further from the area where gust-induced stall scenarios may be more prevalent. Thus, the exposure of manned aeroplanes to gust-induced stall is lower than in the case of RPA, as the speeds at which the former aircraft fly during most of their operation are significantly above the interval where this issue might occur. This constitutes another crucial insight with respect to the relative impact that these undesirable events have on each of these aircraft types.

Aside from comparing the envelopes of RPA built using their specific codes to those of CS/Part-23 manned aeroplanes, an additional analysis was carried out in Section 3.4, which was based on the application of the latter codes to RPA to assess how their envelopes would change. As seen in the results obtained within Section 3.4, these envelopes present a crucial issue, which is that their shape and certification airspeeds are not representative of operating conditions of RPA, falling at much higher V_{EAS} values. The higher certification airspeeds and load factors resulting from their shape would place much higher structural design demands on RPA. These would be excessively prescriptive, particularly since they would be based on flight conditions that are impracticable for them.

From the information presented above, it can be deduced that the emphasis of the RPA codes regarding the need of V_C being based on RPA operational conditions, as seen in Table 2, is strongly substantiated, since the formulae of the CS/Part-23 that are used to obtain the values of the certification airspeeds do not seem to be compatible with the design characteristics of RPA as they do not give representative certification airspeeds when applied to them. The fact that these different codes give strongly dissimilar envelopes as a result could be expected from the start. The main insights gained through the research conducted here are mainly related to the quantification and assessment of the deviations that appear between the target mission airspeeds of RPA and the certification airspeeds resulting from the regulation as seen in Figures 8 and 9, as well as the discussion on the design implications that applying these manned aviation codes give as a result.

Albeit the second scenario mentioned above would seem impractical due to the current availability of RPA-specific codes, it is noted that, when carrying out the design of an OPV, the aircraft would possibly be expected to comply with both manned and unmanned aviation codes. If compliance with both codes is sought, it may be expected from the results in Section 3 that the much more restrictive loading conditions corresponding to the CS/Part-23 would be the ones to drive the structural design of the aircraft, mainly through the high gust loads appearing in the set of flight conditions demanded by these manned aviation codes. However, this depends on the particular design being studied, as well as on its mission and design characteristics, which may be analysed with the methodologies proposed in this research.

Aside from the issues related to potential gust-induced stall conditions, there are other ways in which gusts may hinder the operation of RPA. The high accelerations associated with the high gust load factor values seen in these aircraft may result in difficulties controlling the flight and they might also cause issues in sensor pointing [16], which are both key aspects when conducting the mission and particularly in those flight phases where the sensors are being used. A detailed analysis of the response and controllability of the RPA when withstanding gusts fall outside the scope of this research, which is focused on rapid calculation approaches applicable to both the analysis of the RPA when it is still in the early stages of design and also to the study of existing RPA accounting for the low volume of data usually found in the literature. Nevertheless, these matters connect with previous investigations on RPA controllability when encountering gusts and in turbulent environments such as those of [22,26].

There are further aspects that may be discussed with respect to the significance of the results obtained in this paper regarding the evolution of the gust load factor along the mission, particularly when considering the way in which it varies between different mission segments as analysed with the approach proposed in Section 4. As discussed beforehand, the accelerations caused due to gusts can be expected to have a negative effect when attempting to capture information on the environment through the sensors of the RPA. These sensors are mostly employed in the segments of the operation in which the main purpose of the mission is being carried out. For example, in a surveillance sortie, the sensors are expected to be used mainly when the aircraft is already located at the site that is to be observed, and not in the ingress and egress segments, whose main purpose is to fly the aircraft from the base to the surveillance area. Therefore, albeit the full range of values of n_g in the different segments of the operation need to be considered for aircraft sizing, those that occur during the phases where the sensors are used may require particular attention, since they might have an influence not only on aircraft sizing but also on sensor pointing and operation. Thus, even in cases such as the surveillance mission studied in the application case in Section 4.1, in which the highest gust load factors happened at the end of the egress segment, the load factors occurring in the surveillance phase, which were

lower in this case, should also be taken into account for further study regarding these additional aspects related to air vehicle controllability and sensor operation, which may be more critical for the outcome of the mission itself.

Continuing with the results corresponding to the mission-based analysis methodology proposed in Section 4, various trends on the gust behaviour of RPA have been identified following the application of this method to the case study of the RQ-2 Pioneer through two different missions. These trends include the increase in gust susceptibility as fuel is depleted, as well as the high impact that changing the cruise procedure can have if the associated flight variable (V_{TAS} or C_L) presents significant changes between different mission segments. Albeit these overall trends are expected to be present in different RPA other than the one analysed in the case study presented here, the impact that each of them might have in the evolution of the gust load factor, n_g, throughout the mission and in the resulting critical load factor condition. In the case of the RQ-2 Pioneer, which can carry a comparatively low quantity of fuel relative to its overall mass, it was seen that the variations in n_g due to the first effect mentioned above are much lower than those caused when moving from one mission segment to another and modifying the cruise procedure, which is the main factor driving the changes in n_g.

Therefore, even if the overall trends, which are given by the mathematical formulation expounded in Sections 4.1 and 4.2, are expected to be present in different RPA, the impact of each would have to be evaluated in each case. For example, for long endurance RPA carrying out high-persistence operations that may span tens of hours of surveillance, the effect of wing loading changes due to fuel depletion may be expected to be the predominant one. On the other hand, for RPA equipped with electric powerplants, there would be no effect of fuel consumption, thus here it is crucial to focus on the impact of the cruise procedure variations in the gust load factor evolution. There are other potential mission characteristics that may impact the change in n_g along the flight which fall outside of the scope of the model proposed here, such as the potential change in altitude when mission segments are conducted in cruise–climb conditions, which would impact gust behaviour through the μ parameter. The interaction of this effect with that of fuel consumption would have to be studied in detail in these cases. Overall, the methodology proposed in Section 4 seeks to provide a rapid calculation approach that may then be applied to particular RPA mission cases to study the specific ways in which their operations impact the gust behaviour of the air vehicle.

Moving on to the insights in terms of RPA design that may be derived from the results obtained through the application of the methodologies proposed in this paper, these are mainly related to the set of load cases attending to which the aircraft must be sized, as defined in the flight envelope. These load cases have a direct effect in the structural design and thus in the OEM of the RPA. However, aside from the impact of the interaction of gust and manoeuvring conditions in structural sizing through the values that the load factor takes, the matter of gust-induced stall should also be considered at the design stages due to its impact in the safety of the flight of the RPA, particularly considering the prevalence of this issue under the most usual operating conditions of the RPA.

In terms of the set of loading conditions attending to which RPA must be sized, and as seen in the envelopes of both study cases, at higher values of wing loading, there is a great prevalence of the stall limitation, and the remainder of the envelope boundary tends to see a slight predominance of manoeuvring conditions. However, when estimating the envelope at lower values of W/S_w, gust load conditions are the most demanding ones along the boundary of the envelope, which is not limited by stall. This correlates with the high impact of gusts in the envelope of normal category manned aeroplanes with low wing loading as seen in Appendix A, the envelopes of which are nonetheless less influenced by

stall when compared to RPA, as discussed above. In such a way, and in the case of RPA, it is noted that the high gust load factors are not reached for positive gusts in many cases due to stall occurring beforehand. However, there is a large area at the bottom right of the flight envelope, corresponding to downward gusts, where gust load factors are significantly more demanding than manoeuvring ones.

Large load factors are expected to result in a heavier airframe attending to typical semi-empirical weight estimation models, in which usually the weight of the wing may be related to the load factors in the form of $W_{wing} \propto n^x$ [13,14], with x being a constant which takes different values depending on the model. Thus, it can be expected that gust effects shall drive to a larger extent the structural design of RPA, particularly when compared to many categories of manned general aviation aircraft as seen in Appendix A. Structural design is a task usually carried out in further design stages to the ones that are within the scope of the present research, since the flight envelope itself is usually required to conduct these types of analyses, which constitute a potential area of future research.

Large gust load factors have many undesirable effects on RPA, as discussed in detail above. These range from a heavier structural airframe; moving to higher accelerations during flight which could potentially disrupt the operation in terms of stability, control, and sensor pointing; and also covering the issue of gust-induced stall when the gust load factors overpowers that of stall. Thus, Section 5 analysed potential ways in which the design of the RPA might be changed in the conceptual stage to mitigate these issues. This matter is not straightforward, since the design changes that drive the largest reductions in the magnitude of n_g do not coincide with the decisions that would produce the most significant mitigation of gust-induced stall, as seen in Table 10. In fact, it is noted that the main driver behind the mitigation of this latter issue, which is the reduction in W/S_w, has the negative effect of increasing n_g substantially. Therefore, depending on the characteristics of the particular design that is being assessed in each case and on the criteria of the designer, the way in which the design might be changed depends on whether structural or stall considerations are given the largest priority.

A key finding from the evaluation of the impact of the design on gust behaviour as seen from the results of Section 5 is that, even when changing the considered design parameters up to 10%, the issue of gust-induced stall for the RPA considered in the case study was not fully mitigated. This scenario might call to a combined use of design modifications such as those analysed here with other means for gust alleviation. Such measures might include, among others, passive twist wingtips, or active flight control systems that modify the positions of the RPA flight controls to reduce the loads when a gust event is identified [11]. Combining these measures with the modifications in overall design parameters might allow to achieve the desired result of preventing gust-induced stall for the reference flight conditions while also reducing the absolute value of n_g, thus reducing the negative impact of potential reductions in W/S_w in structural sizing.

With respect to the above-mentioned means of mitigating undesirable gust effects through design changes, it is noted that changing the aforementioned conceptual design variables would imply modifying certain aspects of the aerofoil and wing design, which would be extraordinarily costly for an existing RPA. Albeit the RQ-2 Pioneer has been used for the case study, if the approach is used for a new RPA design, assessing such design modifications in the early stages is a feasible task. This highlights the advantages of considering gust-related aspects in RPA design from the initial phases of development, enabling the application of measures to mitigate the issues related to gust behaviour which would not be applicable later on. In the case of the aforementioned active flight control approaches, these could still constitute a reasonable option for RPA which have already

been developed. The combined use of these approaches with the one proposed in this paper would constitute an area of future research.

Many RPA that are nowadays in operation have not been designed attending to current codes such as those used in this study. Therefore, if it is sought to certify these already existing designs according to these regulations to enhance their integration in non-segregated airspace and achieve larger operation flexibility, it is possible that the airframe might have to be reinforced to withstand these gust loads, resulting in a potentially costly endeavour. This was already suggested in previous research when studying the required structural weight for gust loads at the cruise speed of various RPA [28] and is further supported with the results obtained in this investigation for the whole flight envelope with present regulations. New RPA projects can choose to implement these structural sizing criteria from the initial phases of the design process through rapid methodologies such as the one used in this research, laying the groundwork for a code-compliant structure.

7. Conclusions

This section expounds the main conclusions derived from the results and findings of the research presented in this paper. Furthermore, the main novel contributions of the work are summarised, and some final remarks on the limitations of the models and scope of this research are discussed along with their implications in terms of future potential lines of research.

With respect to the main conclusions and findings of the work in relation to the research questions that they seek to answer, these may be summarised as expounded bellow. These conclusions are given in relation to the starting premises of the work, so as to highlight in a more precise manner which are the findings that constitute new scientific knowledge of the research presented here:

- Assessment of undesirable gust-related effects of RPA: The fact that gusts have a negative influence on RPA design and operation and that they may cause stall and increase structural sizing demands are intuitive premises. However, current research has not performed a dedicated study to assess the prevalence and impact of these effects on RPA using their dedicated airworthiness codes. The methodology used to arrive at the desired results was the estimation of the V—n diagram since it encapsulates much information related to the flight conditions of the RPA and the interactions between gust, manoeuvring, and gust effects. This has allowed to assess that stall limitations have the most significant effect on the set of flight conditions of the studied RPA and that the region where gusts prescribed by the regulations could cause the stall of the vehicle can cover more than 70% of the attainable level flight conditions, thus quantifying the magnitude of this issue. More importantly, this region of gust-induced stall overlaps with the expected usual mission speeds of RPA, supporting the noticeable risk due to the increased exposure of the vehicle. In terms of load conditions, those related to gust tend to predominate the boundary of the envelope at low weights, particularly when considering downward gusts at high airspeeds as seen in the shapes of the envelopes in Figures 6 and 7, signifying that gust loads are expected to drive the structural design of the aircraft. The high-load factors result in increased accelerations in flight and in higher structural weight.
- Differences in RPA flight envelopes with respect to those of manned aeroplanes: Albeit it could be expected that these envelopes would be different due to the dissimilarities in these types of aircraft and in their codes, it is nonetheless informative to quantify in what measures they change to assess the differences in the set of flight conditions that must be attained and in the structural design criteria that prevail in each case, which is essential for aircraft sizing. As seen through the results of Section 3 and

as discussed in Section 6, the main differences are that RPA envelopes are much more compact, that they present lower values of V_D, and that stall is much more prevalent in RPA relative to the overall envelope boundary. The main factors that drive these differences are the much lower typical operating missions of RPA along with the low wing loading values of these aircraft. Even when compared to normal category manned aeroplanes with low wing loading, where gust loads are greater, the differences in stall and horizontal range of the envelopes can still be seen. The main effect on design is that structural sizing of most typical CS/Part-23 manned aeroplanes is mainly driven by manoeuvring loads, while in RPA gust loads tend to prevail in view of the case studies carried out in this research. Furthermore, the issue of gust-induced stall is much greater in RPA than in manned aeroplanes, as these latter ones have wider ranges of operating airspeeds and tend to fly outside of the gust-induced stall region, substantiating the higher risk of this effect on RPA.

- Observations regarding the use of CS/Part-23 envelopes in RPA: The main issue seen when applying the manned aeroplane regulations in RPA is that the envelopes are not representative of the typical operations of these aircraft. Albeit this could be assumed to be an intuitive statement, the main findings here come from the quantification of these differences. The values of V_C increase around 50% with respect to the values given by RPA regulations and the typical airspeeds of RPA missions, giving much higher load factors than in the previous case, up to a factor of 1.5. Thus, structural sizing attending to these codes is much more prescriptive and the dominance of gust effects in the structural design is exacerbated. This does not only serve to quantify the differences in the demands placed by both codes and to substantiate the changes that were made in the ones of RPA, but also may serve in the design of OPV when accounting for both codes to identify the set of the most prescriptive loading conditions when considering the combination of both regulations.
- Influence of mission parameters in RPA gust behaviour: The fact that the gust load factor will vary throughout different segments of the mission of the RPA due to changes in variables such as airspeed or flight height constitutes a starting premise of the work and could be expected. The main contribution of the work presented here is in providing a rapid calculation approach compatible with the needs of RPA conceptual design to quantify the variations in load factor across various missions of the same RPA with each presenting different segments and cruise procedures as a function of V_{TAS} and C_L. One of the major findings is that, for the studied RPA, the variations due to fuel consumption are much lower than those due to cruise procedure, which are the ones that drive the variations in n_g throughout the mission. This conclusion may be extended to tactical RPA with similar missions, but other RPA types with distinct sortie types would have to be analysed to assess which of the effects prevail.
- Potential conceptual design changes to mitigate undesirable gust effects: Upon identifying the negative structural implications of the high values of n_g and the risk caused by gust-induced stall, a study was conducted within the scope of the design variables included in the model to identify potential modifications in conceptual design parameters to mitigate these issues. This has allowed to quantify that there is not much margin to improve n_g through these variables, while gust-induced stall may be mitigated with small variations up to 50%. However, the variables that must be changed in each case are different, with W/S_w being the one mainly driving improvements in gust-induced stall behaviour, albeit at the cost of higher structural weight. This feedback may be used by the designer to change these variables in the early design stages when this

is feasible, and also to consider other potential strategies to alleviate gust effects in combination with these design changes.

The novel contributions that have been implemented within the proposed methodologies as well as the original insights related to RPA gust behaviour that have been derived through their application to the case studies are summarised below.

- The step-by-step approach proposed in Sections 3.1 and 3.2 to derive the certification airspeeds required by the regulatory codes based on data describing the typical operating conditions expected from the aircraft. This process presents various challenges due to the potential variety in the operating conditions of multi-mission RPA, the low volume of available data in the literature and in the initial design stages, and the scarce guidelines given by the regulations at certain points. Thus, the approach allows to effectively connect operational and design aspects within the context of the flight envelope estimation, which is one of the main current gaps in the stipulations given by the regulations and previous scientific research.
- The combined modelling of mission and gust load factor in the methodology for the evaluation of load factor variation throughout the flight, with the approach being compatible with both constant V_{TAS} and angle of attack cruise procedures, enabling the rapid calculation of the evolution of gust effects through different segments of the flight profile of RPA missions when accounting for fuel consumption and cruise procedure variation. This also enables us to quantify the relative impact that each type of operational effect has on gust behaviour and to identify the most critical gusts loading condition along the missions.
- The assessment of the substantial differences seen when comparing the certification flight envelopes of RPA with the classic shapes seen in conventional manned aeroplanes, including an analysis on the operational and design reasons that substantiate these disparities. This analysis is complemented with the comparison of the flight envelopes resulting from the direct application of CS/Part-23 codes to RPA, which highlights the challenges resulting from the use of these regulations when applied to these aircraft.
- The identification and quantification of the prevalence of a hazardous aspect affecting RPA flight safety which is their susceptibility to gust-induced stall scenarios when considering the gust intensities prescribed by the regulations. The methodologies enable us to identify the interval of the envelope where this happens and the way in which the margin between both gust and stall load factors changes along the envelope and the different segments of the mission.
- The discussion of the implications that the aforementioned aspects have on RPA design and operation, including the evaluation of different impacts that the high gust load factors may have depending on the mission segment where they occur and the way in which the distinct shapes of the envelopes may impact the design of these aircraft.
- The identification of potential changes in conceptual design parameters of RPA that may be applied in the early design stages to mitigate the undesirable effects of gusts. Significant reductions in gust-induced stall may be attained by reducing W/S_w at the cost of higher values of n_g, which may themselves be slightly mitigated through a combined increase in C_{Nmax} and MGC.

The models used in this research have been based on the discrete gust model prescribed by current RPA codes, and the methodologies that have been derived are focused on vertical gusts and their effect on aircraft load factor and its implications in design and operation. However, there are many other issues related to gust effects on RPA that have not been accounted for within the scope of the current research. Among these, the response of the RPA when facing more complex gust and turbulent structures than the

discrete gust considered here should be highlighted. In particular, if the gust intensity is not homogeneous across the wingspan, the induced roll moment may cause the RPA to overturn, resulting in a hazardous flight attitude which could potentially result in the loss of control of the aircraft. This scenario could be caused by the encounter of the RPA with a squall wind and would warrant further analysis due to its impact in RPA flight safety. The analysis of the gust response of RPA when encountering other turbulent structures such as composite gusts could also constitute a line of future research towards studying RPA gust behaviour in a more comprehensive way.

Furthermore, albeit the models in this work have been based on those included in the RPA airworthiness codes, and as highlighted when delimiting the research scope, the purpose of this research is not to serve as an aid in certifying RPA. The process of airworthiness certification is a complex endeavour within which gust behaviour evaluation only covers a small part of the process, which involves negotiations with the authority, certification basis definition, and flight testing, among other aspects. The focus of this research is instead on the design implications resulting from accounting for the requirements laid out in the codes, which is also advantageous from the perspective of design–airworthiness integration as it contributes from the early stages towards achieving a design that may be compliant with the regulatory stipulations within the scope of the model.

Author Contributions: Conceptualization, C.C.-R.; methodology, Á.G.-R. and C.-J.V.-C.; software, Á.G.-R. and C.-J.V.-C.; validation, Á.G.-R., C.-J.V.-C. and C.C.-R.; formal analysis, Á.G.-R. and C.-J.V.-C.; investigation, Á.G.-R. and C.-J.V.-C.; resources, C.C.-R.; data curation, Á.G.-R.; writing—original draft preparation, Á.G.-R. and C.-J.V.-C.; writing—review and editing, C.C.-R.; visualisation, C.-J.V.-C.; supervision, C.C.-R. All authors have read and agreed to the published version of the manuscript.

Funding: This research received no external funding.

Data Availability Statement: The sources of information used in this work have been cited throughout the paper and the original contributions presented in this study are included in the article materials. Any further inquiries can be directed to the corresponding author.

Conflicts of Interest: The authors declare no conflicts of interest.

Abbreviations

The following abbreviations are used in this manuscript:

AEP	Allied Engineering Publications
AGL	Above Ground Level
AMC	Acceptable Means of Compliance
CS	Certification Specifications
EAS	Equivalent Airspeed
EASA	European Union Aviation Safety Agency
EASN	European Aerospace Science Network
FAA	Federal Aviation Administration
GM	Guidance Material
ISA	International Standard Atmosphere
ISR	Intelligence, Surveillance, and Reconnaissance
JARUS	Joint Authorities for Rulemaking on Unmanned Systems
LUAS	Light Unmanned Aeroplane System
MALE	Medium Altitude Long Endurance
MTOM	Maximum Take-Off Mass
NATO	North Atlantic Treaty Organization
OEM	Operating Empty Mass

PL	payload
RPA	Remotely Piloted Aircraft
SAR	Search and Rescue
TAS	true airspeed
TF	trip fuel
UAS	Unmanned Aircraft System
UAV	Unmanned Aerial Vehicle
VLA	Very Light Aeroplanes
VTOL	Vertical Take-Off and Landing

Appendix A. Typical Shapes of CS/Part-23 Manned Aeroplanes for Comparison with Those of Unmanned Aircraft

This appendix contains the manned aeroplane flight envelopes used for comparison with those of RPA.

CS/Part-23 [39,40] covers various aircraft certification categories that differ greatly in terms of design and operational characteristics. Thus, they can be expected to have very distinct flight envelopes. Thus, Figure A1, reproduced from Gudmundsson [14], presents expected shapes of the flight envelopes for different aircraft within these categories. It is noted that three different wing loading cases are illustrated for the normal category.

For the utility, aerobatic, and commuter categories, it can be seen that the loading cases dominating the structural sizing of the aircraft are mainly given by manoeuvring conditions, with gust cases only predominating at airspeeds close to V_C where the gust load factors are higher due to the combination of higher airspeeds with the gust intensity, U_C. Gust cases are also more demanding in a small portion of the bottom-right corner, where manoeuvring conditions are less restrictive since the corresponding load factors are linearly reduced up until V_D. It is noted that, for commuter category aeroplanes, the codes define an additional certification airspeed, which is the design airspeed for maximum gust intensity, V_B, as seen in the representative flight envelope for this aircraft type.

In the normal category, the scenarios depending on the wing loading of the aircraft are remarkably dissimilar. In the case of high wing loading, the influence of gust conditions on structural sizing is nearly negligible, whereas for average values of W/S_w, a similar scenario to that of utility aircraft is found. The greatest differences are seen in normal category aeroplanes with low values of W/S_w. These are also the ones that are the most similar in design characteristics to RPA, since these latter aircraft also tend to present very low values of W/S_w compared to the norm in manned aeroplanes. Thus, gust load conditions predominate here through nearly all of the envelopes, with extraordinarily high-load factors that have a significant effect on structural sizing.

However, when compared with the envelopes of RPA presented in Section 3.3 and as also discussed in Section 6, it is seen that, in the case of manned aeroplanes, stall does not predominate as much. This can be seen in the fact that the interval of level flight speeds where gust-induced stall may occur is much lower than in the case of RPA. This occurs despite the similar wing loadings in both cases. This happens due to the very different operational conditions of both aircraft types, since the RPA used in the calculations in Section 3.3 are mainly intended for low-speed loiter missions that are conducted quite close to 1 g stall conditions. Thus, low values of V_C and thus of V_D are selected, giving as a result a compact envelope in the case of RPA. However, general aviation aircraft such as the ones seen in this appendix usually cover a wider range of operational airspeeds and fly at speeds with a higher margin with respect to stall [14]. This is more relevant in terms of safety for this type of aircraft since they carry people on board.

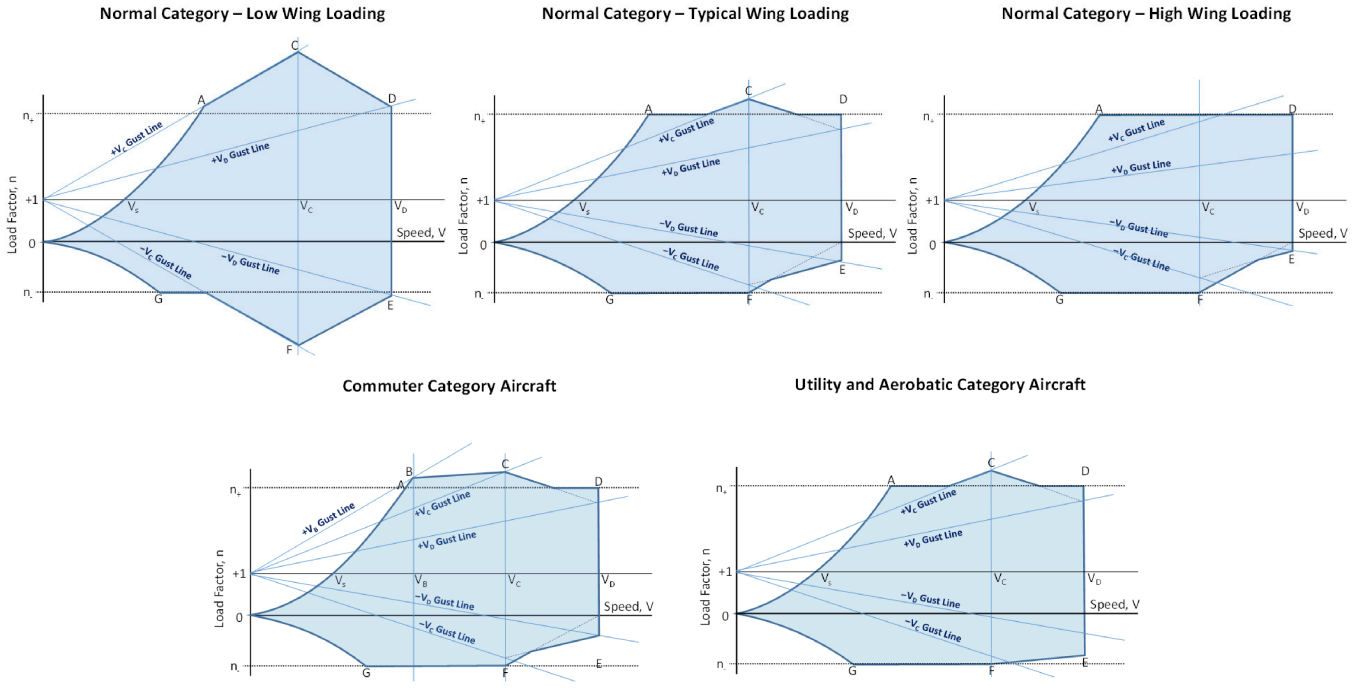


Figure A1. Representative envelopes for different categories of manned general aviation aeroplanes according to the stipulations of CS/Part-23 [39,40].

As the case of normal category with low wing loading is the one that is the most comparable to RPA, an envelope for a sample aircraft of this type has been estimated following the requirements given in CS/Part-23 [39,40]. The additional guidance for envelope construction provided in reference [14] has also been followed. The data from the sample aircraft has been taken from [14], with the resulting envelope matching the one given in the aforementioned reference. The flight envelope is presented in Figure A2.

This flight envelope has been obtained through the process defined in CS/Part-23. Thus, it presents various differences with the envelopes obtained in this work based on RPA regulations, shown in Section 3.3, since those are not only based on the regulations for RPA but also on the additional guidance and novel steps proposed in this paper.

The full considerations for building the envelopes according to CS/Part-23 can be consulted in the codes [39,40]. Here, an overview is provided on their singular aspects, particularly when compared to the method proposed and used in Section 3 of this paper.

- V_C: here, a lower bound, V_{Cmin}, is defined by the regulations, with its value depending on the wing loading at maximum take-off weight. Furthermore, a lower bound, V_{Cmax}, is also defined, which depends on the maximum level flight speed at sea level. V_C may not be lower than V_{Cmin} and need not be higher than V_{Cmax}, with reference [14] recommending its selection at or near the upper bound.
- V_D: two minimum values are prescribed by the codes. The one labelled in Figure A2 as V_{Dmin1} depends on the selected value of V_C, and it is obtained by multiplying it by a coefficient of 1.25. V_{Dmin2} is instead given as a function of V_{Cmin}, and in the case of normal aeroplanes it is obtained by multiplying the aforementioned speed by a coefficient of 1.4. In this paper, V_D is selected at the maximum of these two values to comply with both requirements, but no higher to avoid increasing structural weight.
- V_{NE}: the stipulations are comparable to those of RPA as seen in Table 2.

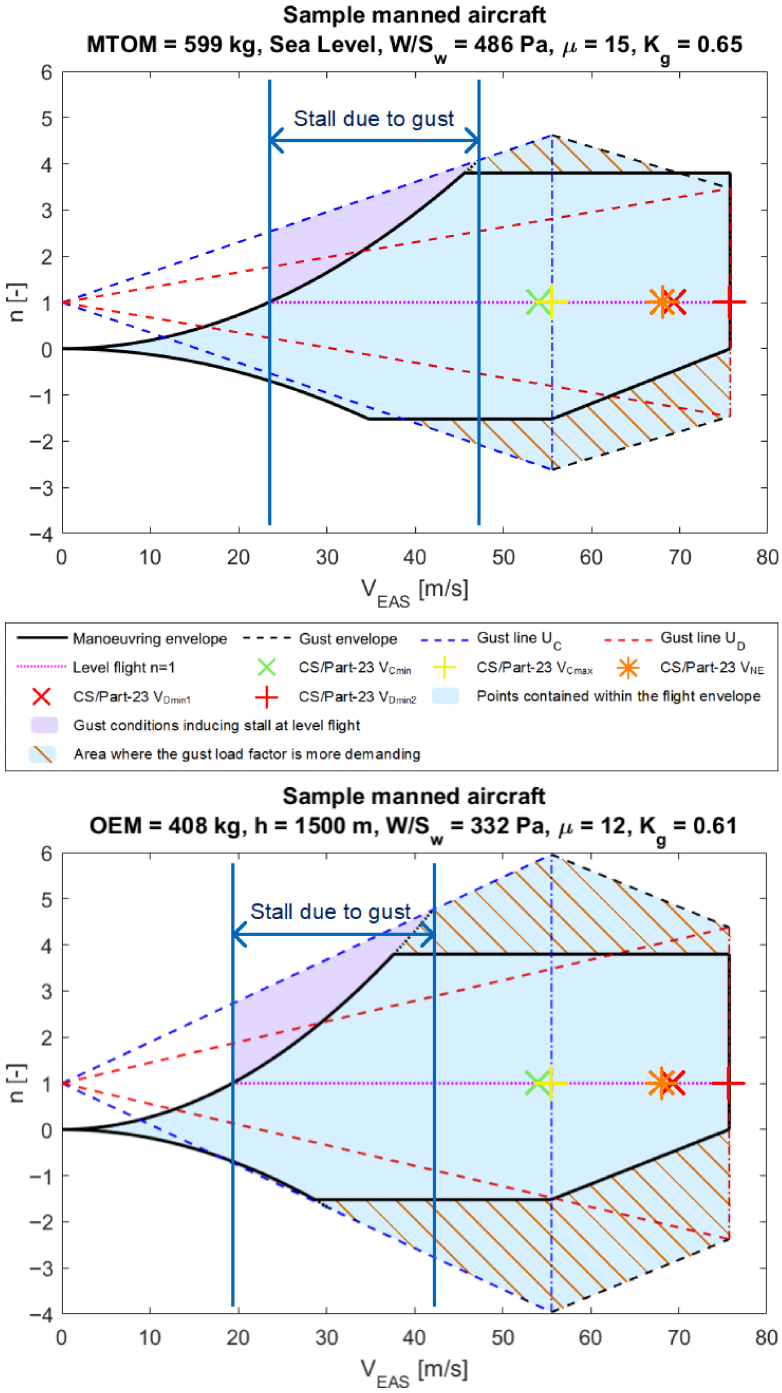


Figure A2. Flight envelopes for two flight conditions of the sample normal category manned aircraft with low wing loading provided in reference [14] as obtained from the application of CS/Part-23 regulations [39,40]. V_{EAS}: equivalent airspeed, n: load factor, MTOM: Maximum Take-Off Mass, OEM: Operating Empty Mass, h: flight altitude, W/S_W: wing loading, μ: mass ratio of the aeroplane, K_g: gust alleviation factor.

References

1. Pratt, K.G. A Revised Formula for the Calculation of Gust Loads. NACA TN-2964. 1953. Available online: https://ntrs.nasa.gov/citations/19930084025 (accessed on 10 February 2026).
2. Pratt, K.G.; Walker, W.G. A Revised Gust-Load Formula and a Re-Evaluation of V-g Data Taken on Civil Transport Airplanes from 1933 to 1950. NACA-TR-1206. 1954. Available online: https://ntrs.nasa.gov/citations/19930090988 (accessed on 10 February 2026).

3. Noback, R. Comparison of discrete and continuous gust methods for airplane design loads determination. *J. Aircr.* **1986**, *23*, 226–231. [CrossRef]
4. Saucray, J.M.; Artigues, C.; Squeglia, G.; Guillot, J. International Standardisation of Regulations for Gust Loading Calculations. *Aeronaut. J.* **1991**, *95*, 370–378. [CrossRef]
5. Fuller, J. Evolution and future development of airplane gust loads design requirements. In Proceedings of the 1997 World Aviation Congress, Anaheim, CA, USA, 13–16 October 1997. [CrossRef]
6. Thomas, C.; Nietzel, K.; Bouskela, A.; Dybskiy, P.; Shkarayev, S.V. Time Variations of Aerodynamic Forces in a Wing Encountering a Wind Gust. In Proceedings of the AIAA Aviation Forum and ASCEND 2025, Las Vegas, NV, USA, 21–25 July 2025. [CrossRef]
7. Avoni, L.; Bronz, M.; Condomines, J.-P.; Moschetta, J.-M. Enhancing ASWING Flight Dynamics Simulations with Closed-Loop Control for Flexible Aircraft. In Proceedings of the AIAA Aviation Forum and ASCEND 2025, Las Negas, NV, USA, 21–25 July 2025. [CrossRef]
8. Mohamed, A.; Marino, M.; Watkins, S.; Jaworski, J.; Jones, A. Gusts Encountered by Flying Vehicles in Proximity to Buildings. *Drones* **2023**, *7*, 22. [CrossRef]
9. Pensado, E.A.; López, F.V.; Jorge, H.G.; Pinto, A.M. UAV Shore-to-Ship Parcel Delivery: Gust-Aware Trajectory Planning. *IEEE Trans. Aerosp. Electron. Syst.* **2024**, *60*, 6213–6223. [CrossRef]
10. Della Vecchia, P.; Cusati, V.; Mirabella, C. Flight Loads Evaluation and Airworthiness Compliance for the V-Tail of a Medium-Altitude Long-Endurance Unmanned Platform. *Drones* **2025**, *9*, 835. [CrossRef]
11. Wu, Z.; Cao, Y.; Ismail, M. Gust loads on aircraft. *Aeronaut. J.* **2019**, *123*, 1216–1274. [CrossRef]
12. Torenbeek, E. *Synthesis of Subsonic Airplane Design*, 1st ed.; Kluwer Academic Publishers: Dordrecht, The Netherlands, 1982. [CrossRef]
13. Roskam, J. *Aircraft Design*; Design, Analysis and Research Corporation (DARcorporation): Lawrence, KS, USA, 1985.
14. Gudmundsson, S. *General Aviation Aircraft Design*, 2nd ed.; Butterworth-Heinemann: Oxford, UK, 2022. [CrossRef]
15. Karali, H.; Inalhan, G.; Tsourdos, A. AI-Driven Multidisciplinary Conceptual Design of Unmanned Aerial Vehicles. In Proceedings of the AIAA SciTech 2024 Forum, Orlando, FL, USA, 8–12 January 2024. [CrossRef]
16. Austin, R. *Unmanned Aircraft Systems: UAVS Design, Development and Deployment*; John Wiley & Sons, Ltd.: Hoboken, NJ, USA, 2010. [CrossRef]
17. Gundlach, J. *Designing Unmanned Aircraft Systems*, 1st ed.; American Institute of Aeronautics and Astronautics (AIAA): Reston, VA, USA, 2012. [CrossRef]
18. Palmer, J.L. Assembly and Initial Analysis of a Database of the Characteristics of Fixed-Wing Unmanned Aircraft Systems. *Australian Government Department of Defence*. 2014. Available online: https://apps.dtic.mil/sti/tr/pdf/ADA623605.pdf (accessed on 27 February 2026).
19. Clothier, R.A.; Palmer, J.L.; Walker, R.A.; Fulton, N.L. Definition of an airworthiness certification framework for civil unmanned aircraft systems. *Saf. Sci.* **2011**, *49*, 871–885. [CrossRef]
20. Watkins, S.; Milbank, J.; Loxton, B.J.; Melbourne, W.H. Atmospheric Winds and Their Implications for Microair Vehicles. *AIAA J.* **2006**, *44*, 2591–2600. [CrossRef]
21. Thompson, M. The Small Scales of Turbulence in Atmospheric Winds at Heights Relevant to MAVs. Ph.D. Thesis, RMIT University, Melbourne, Australia, 2012.
22. Abdulghani, M.; Massey, K.; Watkins, S.; Clothier, R. The attitude control of fixed-wing MAVS in turbulent environments. *Prog. Aerosp. Sci.* **2014**, *66*, 37–48. [CrossRef]
23. Stutz, C.; Bohl, D.G.; Hrynuk, J.T. Investigation of Lift Forces During Long Gust Interactions at Low Reynolds Number. In Proceedings of the AIAA SciTech 2022 Forum, San Diego, CA, USA, Virtual. 3–7 January 2022. [CrossRef]
24. Galinski, C.; Mieloszyk, J. Results of the gust resistant MAV programme. In Proceedings of the 28th Congress of the International Council of the Aeronautical Sciences 2012, Brisbane, Australia, 23–28 September 2012.
25. Rodzewicz, M.; Goraj, Z.; Tomaszewski, A. Design and testing of three tailless unmanned aerial vehicle configurations built for surveillance in Antarctic environment. *Proc. Inst. Mech. Eng. Part G J. Aerosp. Eng.* **2018**, *232*, 2598–2614. [CrossRef]
26. Bhandari, N.; Bhandari, P.; Poudel, N.; Karki, A.; Bhattrai, S. Near-Terrain Flight Operations and Performance of Unmanned Aerial Vehicles. *J. Aircr.* **2026**, *63*, 631–643. [CrossRef]
27. Kuliberda, J.; Kwiek, A. Determination of UAV loads based on flight simulation results. *Aircr. Eng. Aerosp. Technol.* **2025**, *97*, 824–832. [CrossRef]
28. Cuerno-Rejado, C.; Martínez-Val, R. Unmanned Aircraft Systems in the Civil Airworthiness Regulatory Frame: A case study. *J. Aircr.* **2011**, *48*, 1351–1359. [CrossRef]
29. Kontogiannis, S.G.; Ekaterinaris, J.A. Design, performance evaluation and optimization of a UAV. *Aerosp. Sci. Technol.* **2013**, *29*, 339–350. [CrossRef]
30. El Adawy, M.; Abdelhalim, E.H.; Mahmoud, M.; Ahmed Abo zeid, M.; Mohamed, I.H.; Othman, M.M.; ElGamal, G.S.; ElShabasy, Y.H. Design and fabrication of a fixed-wing Unmanned Aerial Vehicle (UAV). *Ain Shams Eng. J.* **2023**, *14*, 102094. [CrossRef]

31. Aribowo, A.; Adhynugraha, M.I.; Megawanto, F.C.; Hidayat, A.; Muttaqie, T.; Wandono, F.A.; Nurrohmad, A.; Chairunnisa; Saraswati, S.O.; Wiranto, I.B.; et al. Finite element method on topology optimization applied to laminate composite of fuselage structure. *Curved Layer. Struct.* **2023**, *10*, 20220191. [CrossRef]
32. Joint Authorities for Rulemaking on Unmanned Systems (JARUS). CS-LUAS. Document Identifier: Jar_del_wg3_d.04, JARUS. 2017. Available online: http://jarus-rpas.org/wp-content/uploads/2023/06/jar_07_doc_CS_LUAS.pdf (accessed on 15 February 2026).
33. Joint Authorities for Rulemaking on Unmanned Systems (JARUS). CS-UAS. Document Identifier: Jarus-del-wg3-cs-uas-d.04, JARUS. 2019. Available online: https://web.archive.org/web/20231025162716/http://67.217.59.217/jarus/wp-content/uploads/2023/06/jar_13_doc_CS_UAS-1.pdf (accessed on 28 April 2026).
34. *NATO Standard AEP-4671*; Unmanned Aircraft Systems Airworthiness Requirements (USAR). Edition B Version 1. NATO: Brussels, Belgium, 2019.
35. *NATO Standard AEP-83*; Light Unmanned Aircraft Systems Airworthiness Requirements. Edition B Version 1. NATO: Brussels, Belgium, 2016.
36. Gómez-Rodríguez, Á.; Turkoglu, C.; Cuerno-Rejado, C. A Systematic Approach towards the Integration of Initial Airworthiness Regulatory Requirements in Remotely Piloted Aircraft System Conceptual Design Methodologies. *Aerospace* **2024**, *11*, 735. [CrossRef]
37. European Union Aviation Safety Agency (EASA). Certification Specifications and Acceptable Means of Compliance for Large Aeroplanes (CS-25). Amendment 28 (with Correction). 2025. Available online: https://www.easa.europa.eu/en/document-library/certification-specifications/cs-25-amendment-28 (accessed on 23 April 2026).
38. Federal Aviation Administration (FAA); Department of Transportation (DOT). Part 25-Airworthiness Standards: Transport Category Airplanes. 29 FR 18291, Federal Register, USA. 2024. Available online: https://www.ecfr.gov/current/title-14/part-25 (accessed on 23 April 2026).
39. European Union Aviation Safety Agency (EASA). Certification Specifications and Acceptable Means of Compliance for Normal, Utility, Aerobatic and Commuter Category Aeroplanes (CS-23). Amendment 4. 2015. Available online: https://www.easa.europa.eu/en/document-library/certification-specifications/cs-23-amendment-4 (accessed on 23 April 2026).
40. Federal Aviation Administration (FAA); Department of Transportation (DOT). *Part 23-Airworthiness Standards: Normal, Utility, Acrobatic and Commuter Category Airplanes*; Federal Register: Washington, DC, USA, 2017.
41. European Union Aviation Safety Agency (EASA). Certification Specifications for Normal Category Aeroplanes (CS-23) and Acceptable Means of Compliance and Guidance Material to the Certification Specifications for Normal Category Aeroplanes (AMC & GM to CS-23). Amendment 6, Issue 5. 2026. Available online: https://www.easa.europa.eu/en/document-library/certification-specifications/cs-23-amendment-6-and-amc-gm-cs-23-issue-5 (accessed on 24 April 2026).
42. Federal Aviation Administration (FAA); Department of Transportation (DOT). Part 23-Airworthiness Standards: Normal Category Airplanes. 81 FR 96689, Federal Register, USA. 2022. Available online: https://www.ecfr.gov/current/title-14/part-23 (accessed on 24 April 2026).
43. European Union Aviation Safety Agency (EASA). Certification Specifications for Very Light Aeroplanes (CS-VLA). Amendment 1. 2009. Available online: https://www.easa.europa.eu/en/document-library/certification-specifications/cs-vla-amendment-1 (accessed on 24 April 2026).
44. Federal Aviation Administration (FAA); Department of Transportation (DOT). Revision of Airworthiness Standards for Normal, Utility, Acrobatic, and Commuter Category Airplanes. 81 FR 96572, Federal Register, USA. 2016. Available online: https://www.federalregister.gov/d/2016-30246 (accessed on 27 February 2026).
45. Yang, Y.; Chao, Y.; Zhigang, W. Aeroelastic dynamic response of elastic aircraft with consideration of two-dimensional discrete gust excitation. *Chin. J. Aeronaut.* **2020**, *33*, 1228–1241. [CrossRef]
46. Sadraey, M.H. *Unmanned Aircraft Design*, 2nd ed.; Springer: Cham, Switzerland, 2025. [CrossRef]
47. Sóbester, A.; Keane, A.; Scanlan, J.; Bressloff, N. Conceptual Design of UAV Airframes Using a Generic Geometry Service. In Proceedings of the Infotech@Aerospace, Arlington, VA, USA, 26–29 September 2005. [CrossRef]
48. Gómez-Rodríguez, A.; Cuerno-Rejado, C. Underlying Design Trend Evaluation of Fixed-Wing Remotely Piloted Aircraft (RPA) Through Factor Analysis. In Proceedings of the AIAA Aviation Forum and ASCEND 2025, Las Vegas, NV, USA, 21–25 July 2025. [CrossRef]
49. Gómez-Tierno, M.Á.; Pérez-Cortés, M.; Puentes-Márquez, C. *Mecánica del Vuelo*, 2nd ed.; Garceta Grupo Editorial: Madrid, Spain, 2012.
50. Daly, M.; Streetly, M. *Jane's Unmanned Aerial Vehicles and Targets; Issue Thirty-Seven*; IHS Jane's: Surrey, UK, 2011.
51. Parakala, A.; Kalra, A.; Wise, S. *Janes All the World's Aircraft Unmanned 2023–2024*; JANES: Surrey, UK, 2023.
52. Jane's. *Jane's Datasets: Products, Defence Equipment & Technology, Air & Space, Unmanned*; Janes: Croydon, UK.
53. Department of Defense (United States of America). *Department of Defense Standard Practice MIL-STD-3013A*; Department of Defense: Arlington, VA, USA, 2008.

54. Panagiotou, P.; Giannakis, E.; Savaidis, G.; Yakinthos, K. Aerodynamic and structural design for the development of a MALE UAV. *Aircr. Eng. Aerosp. Technol.* **2018**, *90*, 1077–1087. [CrossRef]
55. Bravo-Mosquera, P.D.; Botero-Bolivar, L.; Acevedo-Giraldo, D.; Cerón-Muñoz, H.D. Aerodynamic design analysis of a UAV for superficial research of volcanic environments. *Aerosp. Sci. Technol.* **2017**, *70*, 600–614. [CrossRef]
56. Chowdhury, S.; Maldonado, V.; Tong, W.; Messac, A. Comprehensive Product Platform Planning (CP3) for a Modular Family of Unmanned Aerial Vehicles. In Proceedings of the 39th Design Automation Conference, Portland, OR, USA, 4–7 August 2013. [CrossRef]
57. Cox, T.H.; Nagy, C.J.; Skoog, M.A.; Somers, I.A. *UAV Mission Capabilities Assessment*; NASA: Washington, DC, USA, 2004.
58. Bray, R.M. A Wind Tunnel Study of the Pioneer Remotely Piloted Vehicle. Master's Thesis, Naval Postgraduate School, Monterey, CA, USA, 1991.
59. Reid, S. Operational use of the Pioneer unmanned aerial vehicle (UAV) system. In Proceedings of the SPIE's 1996 International Symposium on Optical Science, Engineering, and Instrumentation, Denver, CO, USA, 5–9 August 1996. [CrossRef]
60. Dinc, A.; Otkur, M. Emissions prediction of an aero-piston gasoline engine during surveillance flight of an unmanned aerial vehicle. *Aircr. Eng. Aerosp. Technol.* **2021**, *3*, 462–472. [CrossRef]
61. Bagul, P.; Rana, Z.A.; Jenkins, K.W.; Könözsy, L. Computational engineering analysis of external geometrical modifications on MQ-1 unmanned combat air vehicle. *Chin. J. Aeronaut.* **2020**, *33*, 1154–1165. [CrossRef]
62. U.S. Air Force, Fact Sheet MQ-1B Predator Fact Sheet. 2016. Available online: https://www.govinfo.gov/content/pkg/GOVPUB-D301-PURL-LPS98704/pdf/GOVPUB-D301-PURL-LPS98704.pdf (accessed on 27 February 2026).
63. Götten, F.; Finger, D.F.; Havermann, M.; Braun, C.; Marino, M.; Bil, C. Full configuration drag estimation of short-to-medium range fixed-wing UAVs and its impact on initial sizing optimization. *CEAS Aeronaut. J.* **2021**, *12*, 589–603. [CrossRef]

Disclaimer/Publisher's Note: The statements, opinions and data contained in all publications are solely those of the individual author(s) and contributor(s) and not of MDPI and/or the editor(s). MDPI and/or the editor(s) disclaim responsibility for any injury to people or property resulting from any ideas, methods, instructions or products referred to in the content.